THESIS

RESOLVING NATURAL LOSSES OF LNAPL USING CO_2 TRAPS

Submitted by

Kevin M. McCoy

Department of Civil and Environmental Engineering

In partial fulfillment of the requirements

For the Degree of Master of Science

Colorado State University

Fort Collins, Colorado

Fall 2012

Master's Committee:

Advisor: Thomas C. Sale
Co-Advisor: Julio A. Zimbron

Charles D. Shackelford
Michael Ronayne

ABSTRACT

RESOLVING NATURAL LOSSES OF LNAPL USING CO_2 TRAPS

Pools of light non-aqueous phase liquids (LNAPLs) are a legacy of past practices at petroleum facilities. Traditional LNAPL remedies (e.g. hydraulic LNAPL recovery) are often costly and have limited effectiveness. Recent studies have indicated that natural losses of LNAPL can help to stabilize and even shrink subsurface LNAPL bodies once the LNAPL source is removed. Developing an effective understanding of natural losses of LNAPL is an important step in establishing LNAPL management strategies. Estimated rates of natural losses of LNAPL can be used to demonstrate LNAPL stability, form a basis for initiating or discontinuing hydraulic recovery, estimate longevity of LNAPL bodies, and as a benchmark to compare relative effectiveness of different remedial alternatives. Additionally, an understanding of underlying processes gained through field studies can guide development of new, more sustainable LNAPL remediation technologies.

A novel integral CO_2 Trap was created to measure soil CO_2 efflux at grade. This addresses a need for an efficient tool to quantify natural losses of LNAPL. The hypothesis of this thesis is that CO_2 Traps can be used to quantify natural losses of LNAPL at field sites. Laboratory and field tests were performed to test the CO_2 Traps and demonstrate their utility.

First, laboratory experiments were undertaken to demonstrate the ability of the traps to quantitatively capture CO_2 and effectively estimate CO_2 fluxes. Closed system column testing showed that the selected sorbent media is capable of quantitatively recovering CO_2. This testing also verified that the sorption capacity of the media (~30% CO_2 by mass) was in the range indicated by the manufacturer. This information is useful when planning maximum field deployment times, and as a means of quality checking field sampling results. Next, an open system column test showed that the CO_2 Traps are capable of quantitatively measuring CO_2 flux through porous media. The traps were field tested. Results of a single round of CO_2 Trap deployment at one field site showed that the traps could distinguish zones of elevated CO_2 flux over the LNAPL body, relative to naturally occurring CO_2 flux at background locations. Background subtracted LNAPL loss rates ranging from 800 to 12,000 gallons per acre per year (gal/acre/yr) were observed. Carbon isotope analysis was performed on one travel blank sample, two background samples, and one LNAPL area sample. Radiocarbon (^{14}C) results provided an independent means to estimate naturally occurring CO_2 flux. Results of the ^{14}C correction agreed well with the background subtraction method for that location.

CO_2 traps have been deployed at a total of 117 locations at 6 field sties. Seasonal resampling of selected locations has yielded a total of 194 CO_2 flux readings. Calculated background corrected LNAPL loss rates for ranged from 400 – 18,000 gal/acre/yr with a mean of 3,500 gal/acre/yr. A detailed analysis of the influence of site and LNAPL characteristics on calculated LNAPL loss rates was performed for one of

the six sites. Results indicated that natural losses of LNAPL are largely independent of in-well LNAPL thickness, depth to smear zone, smear zone thickness, or LNAPL type. However, temperature related seasonal trends were observed. Furthermore, natural losses of LNAPL appear to result in self heating of LNAPL zones with a potential benefit of enhancing natural losses. Additional data analysis suggests a link between temperature and natural LNAPL loss rate that may be useful in developing new, more sustainable, LNAPL management technologies.

ACKNOWLEDGEMENTS

I would like to recognize and thank the many individuals who provided support, aid, and guidance during the research and writing of this thesis.

- First and foremost, I would like to thank Dr. Tom Sale and Dr. Julio Zimbron for their guidance and patience throughout the development of this thesis, and for providing me an opportunity to grow.
- Dr. Charles Shackelford and Dr. Michael Ronayne for serving on the advisory committee.
- Mitchell Olson and Natalie Zeman for collaborative input and technical support.
- Dr. Ulrich Mayer and Natasha Sihota at the University of British Columbia for collaborative field studies.
- Gary Dick, Sonja Koldewyn, Sarah Breidt, Rebecca Bradley, Adam Byrne, Calista Campbell, and Ellen Daugherty for all of their support assembling field equipment and long hours analyzing samples in the laboratory.
- Bart Rust and Janice Barman for help procuring materials and developing CO_2 Trap hardware.
- Ben McAlexander, Paul Michalski, and Alysha Anderson of TriHydro Corp.; Andy Pennington of Arcadis; Rochelle Shang and Marisa Toma of URS Corp.; Becky Rewey of CH2M Hill; Elliot Trzcinski of AECOM, and Dianne Burnia and Joe Shoulders of Stantec for field support.
- Dr. Arthur Corey for his scholarship and input.

- Mark Lyverse from Chevron and Greg Fletcher from Suncor Energy for their knowledge and field site coordination.
- Jennifer Gelmini, Jim and Linda McCoy, and Russell and Muriel Jacobs, for all of their support and encouragement.
- MWH Americas, Inc. for support during my first semester at CSU.

Funding for this work was provided by:

- Chevron
- Suncor Energy
- Union Pacific Railroad
- University Consortium for Field-Focused Groundwater Contamination Research.

TABLE OF CONTENTS

LIST OF FIGURES

LIST OF TABLES

1 INTRODUCTION

Petroleum, and petroleum based products are an integral part of contemporary society. Historical practices have led to the accumulation of light non-aqueous phase liquids (LNAPLs) beneath many petroleum facilities. Traditional LNAPL remedies (e.g. hydraulic LNAPL recovery) are often costly and have limited effectiveness (ITRC, 2009a). Recent studies suggest that natural losses of LNAPL can help to stabilize and even shrink subsurface LNAPL bodies, once the LNAPL source is removed (Mahler et al., 2011; Mahler et al., 2012).

Recent studies by several investigators (Amos et al., 2005; Johnson et al., 2006; Lundegard and Johnson, 2006; ITRC, 2009b; Molins et al., 2010; Mahler et al., 2011; Sihota et al., 2011) have highlighted the large magnitude of natural losses of LNAPL occurring in the field. For instance, natural hydrocarbon loss rates ranging from 0.1 to 1 kilograms petroleum per square meter per year ($kg/m^2/year$) were estimated for the Guadalupe Oil Field site in California (Lundegard and Johnson, 2006) and losses of 3.3 grams petroleum per square meter per day ($g/m^2/d$) were estimated for a historical crude oil spill in Bemidji, Minnesota (Sihota et al., 2011). Assuming an LNAPL density of 0.8 g/cm^3, these rates are equivalent to 130 – 1,300 and 1,600 gal/acre/yr, respectively. These reported rates rival those of common engineered solutions (e.g. hydraulic LNAPL recovery; EPA, 2005). Based on these observations, it is clear that the ability to estimate natural LNAPL loss rates at these sites is an important step in establishing effective LNAPL management strategies.

Natural LNAPL loss rates can be used to demonstrate LNAPL stability, to form a basis for initiating or discontinuing hydraulic recovery, and as a benchmark to compare relative effectiveness of different remedial alternatives (ITRC, 2009b). Further, an understanding of underlying processes gained through field studies can guide development of new, more sustainable LNAPL remediation technologies. Finally, estimates of natural loss rates can facilitate calculating longevity of LNAPL bodies.

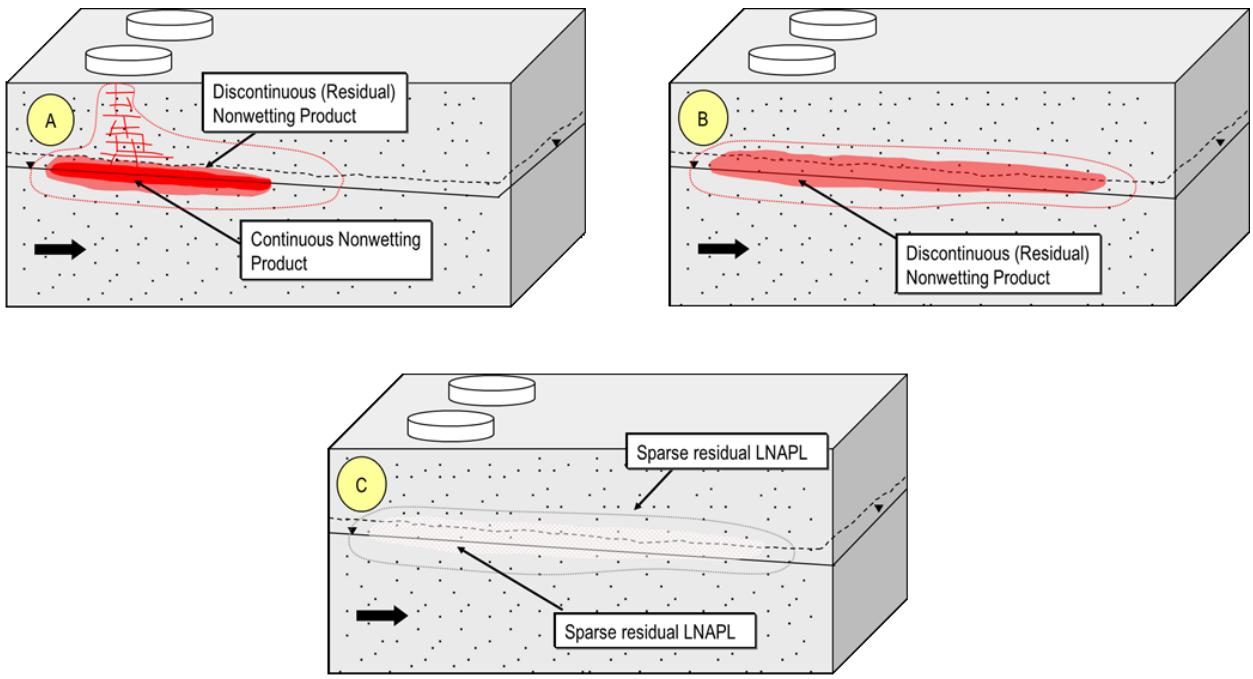

Figure 1.1. Conceptual evolution of an LNAPL release. A) Early stage. During or shortly after a release the LNAPL body expands and/or migrates. B) Middle stage. The release has been stopped. Natural losses lead to dynamic equilibrium. Overall LNAPL movement is primarily internal redistribution resulting in a stable LNAPL body. C) Late stage. Sparse residual LNAPL is immobile. Natural losses reduce extent of (i.e. shrink) LNAPL body.

Figure 1.1 shows a conceptual model of evolution of an LNAPL release. At early stages, during or immediately after a release, LNAPL can expand or migrate. As the LNAPL body expands total losses of LNAPL increase. Natural loss rates begin to

approach LNAPL inflow rates and the rate of expansion of the LNAPL body slows (Mahler et al., 2012). At the middle stage, LNAPL inflow and losses are nearly equal. During this stage, LNAPL bodies are largely stable or shrinking (Mahler et al., 2012). Field observations suggest that many historical LNAPL releases have reached this state. At a late stage, natural losses have removed the majority of the LNAPL. Hydraulic LNAPL recovery is best suited to early stage sites. A critical question at middle stage sites is when to transition from active hydraulic recovery to depletion of remaining LNAPL via natural losses.

Researchers have developed four methods of evaluating natural losses of LNAPL:

- Aqueous Electron Acceptors and Byproducts method – natural losses of LNAPL can be calculated using concentrations of aqueous phase hydrocarbon compounds, electron acceptors, and electron donors measured along an LNAPL body (Johnson et al., 2006; Lundegard and Johnson, 2006; ITRC, 2009b).
- Gradient method – natural losses of LNAPL can be calculated using Fick's first law, concentration gradients of gas phase constituents in the vadose zone, and estimated soil gas diffusion coefficients (Amos et al., 2005; Johnson et al., 2006; Lundegard and Johnson, 2006; ITRC, 2009b).
- Flux Chamber method – natural losses of LNAPL can be calculated by monitoring gas phase fluxes of CO_2 at grade (Sihota et al., 2011).

- Mass Balance method – Given a stable LNAPL body with known internal LNAPL fluxes, natural losses of LNAPL can be estimated from a simple mass balance (Mahler et al., 2011; Mahler et al., 2012; Smith et al., 2012).

Each of these methods has advantages and limitations. Concerns with existing methods include necessary inputs, need for invasive field investigation, accuracy, and cost. To overcome limitations of existing methods, Zimbron et al., 2011 advance a novel approach involving deployment of CO_2 adsorbing traps at grade.

CO_2 is the final end product of petroleum mineralization. CO_2 is directly produced by petroleum mineralization under aerobic conditions. Under conditions where all electron acceptors are depleted, methanogenesis is the primary degradation pathway. In many instances, outwardly migrating CH_4 converts to CO_2 upon encountering inward migrating O_2 in the vadose zone (Amos et al., 2005; Molins et al., 2010; Sihota et al., 2011; Ma et al., 2012). Molins et al., 2010 indicates that as much as 98% of total carbon released through petroleum mineralization exits the ground surface as CO_2. As such, CO_2 is a useful indicator of natural losses.

The principal hypothesis of this thesis is that CO_2 Traps can be used to calculate natural losses of LNAPL at field sites. Two chapters are presented. Both are written in a journal article format. The first article has been prepared for submittal to the Journal of Contaminant Hydrology. A journal has not been selected for the second article. The first article describes laboratory experiments undertaken to demonstrate the ability of

the traps to quantitatively capture CO_2 and effectively estimate CO_2 fluxes. A demonstration application of the traps to a single field site is discussed. The second article discusses results from deployment of CO_2 Traps at six LNAPL sites. Detailed analysis of the effects of site characteristics, LNAPL properties, and seasonal influences on calculated losses of LNAPL is explored. The final sections of this thesis provide a summation of the information presented and recommendations for further work.

2 MEASUREMENT OF NATURAL LNAPL LOSS RATES USING CO_2 TRAPS

2.1 Summary

This paper introduces a novel approach to quantifying CO_2 flux above light non-aqueous phase liquid (LNAPL) bodies, and correspondingly estimating natural losses of LNAPL. The method employs CO_2 adsorbing canisters placed at grade above LNAPL bodies. Total adsorbed CO_2 for a given trap cross-sectional area provides an integral time-averaged CO_2 flux. CO_2 fluxes are used to calculate natural LNAPL loss rates. The CO_2 Traps have been tested in the laboratory and in the field. A CO_2 Trap survey at a decommissioned petroleum refinery showed estimated equivalent natural LNAPL loss rates ranging from 800 to 12,000 gallons per acre per year (gal/acre/yr). These rates are of similar order of magnitude to estimates made by other investigators, and are supported by multiple lines of evidence including CO_2 isotopic signatures, groundwater thermal trends, and vadose zone gas profiles. These loss rates rival the capabilities of common engineered remedies to stabilize and/or shrink LNAPL bodies.

2.2 Introduction

Petroleum products are an integral part of modern living. Past industrial practices have led to accumulation of LNAPL pools beneath many petroleum refining, distribution, and storage facilities. A key factor driving remediation decisions at many of these sites is LNAPL stability (i.e. potential for an LNAPL body to expand or translate laterally) (ITRC, 2009a; Smith et al., 2012). Recent studies suggest that natural losses of LNAPL (e.g. dissolution, volatilization, biodegradation) can control LNAPL stability (Mahler et al., 2011; Mahler et al., 2012). Natural loss rates can be used to

demonstrate LNAPL stability, form a basis for initiating or discontinuing hydraulic recovery, and estimate longevity of LNAPL bodies. Additionally, with an understanding of underlying processes gained through field studies, new methods can be developed to sustainably accelerate natural losses.

In recent years, various studies have highlighted the large magnitude of natural losses of LNAPL (Amos et al., 2005; Johnson et al., 2006; Lundegard and Johnson, 2006; ITRC, 2009b; Molins et al., 2010; Mahler et al., 2011; Sihota et al., 2011). For instance, natural hydrocarbon loss rates ranging from 0.1 to 1 kilograms petroleum per square meter per year ($kg/m^2/year$) were estimated for the Guadalupe Oil Field site (Lundegard and Johnson, 2006) and losses of 3.3 grams petroleum per square meter per day ($g/m^2/d$) were estimated for the Bemidji site (Sihota et al., 2011). Assuming an LNAPL density of 0.8 g/cm^3, these rates are equivalent to 130 – 1,300 and 1,600 gal/acre/yr respectively. These reported ranges rival efficiencies of common engineered solutions (e.g. hydraulic LNAPL recovery) (EPA, 2005). Based on these observations, it is clear that knowledge of natural LNAPL loss rates at these sites could significantly influence remediation decisions.

Figure 2.1 presents a conceptual model of processes associated with natural losses of LNAPL. Building on Figure 2.1, researchers have developed four methods of evaluating natural losses of LNAPL:

- Aqueous Electron Acceptors and Byproducts method – natural losses of LNAPL can be calculated using concentrations of aqueous phase

hydrocarbon compounds, electron acceptors, and electron donors measured along an LNAPL body (Johnson et al., 2006; Lundegard and Johnson, 2006; ITRC, 2009b).

- Gradient method – natural losses of LNAPL can be calculated using Fick's first law, concentration gradients of gas phase compounds in the vadose zone, and estimated soil gas diffusion coefficients (Amos et al., 2005; Johnson et al., 2006; Lundegard and Johnson, 2006; ITRC, 2009b).
- Flux Chamber method – natural losses of LNAPL can be calculated by monitoring CO_2 effluxes at grade (Sihota et al., 2011).
- Mass Balance method – Given a stable LNAPL body with known internal LNAPL fluxes, natural losses of LNAPL can be estimated from a simple mass balance (Mahler et al., 2011; Mahler et al., 2012; Smith et al., 2012).

CO_2 is the final end product of petroleum mineralization. CO_2 is directly produced by petroleum mineralization under aerobic conditions. Under conditions where all electron acceptors are depleted, methanogenesis is the primary degradation pathway. In many instances, outwardly migrating CH_4 converts to CO_2 upon encountering inward migrating O_2 in the vadose zone (Amos et al., 2005; Molins et al., 2010; Sihota et al., 2011; Ma et al., 2012). Molins et al., 2010 conclude that as much as 98% of total carbon released through petroleum mineralization exits the ground surface as CO_2. As such, measuring soil-atmosphere exchange of CO_2 can be a useful indicator of natural losses.

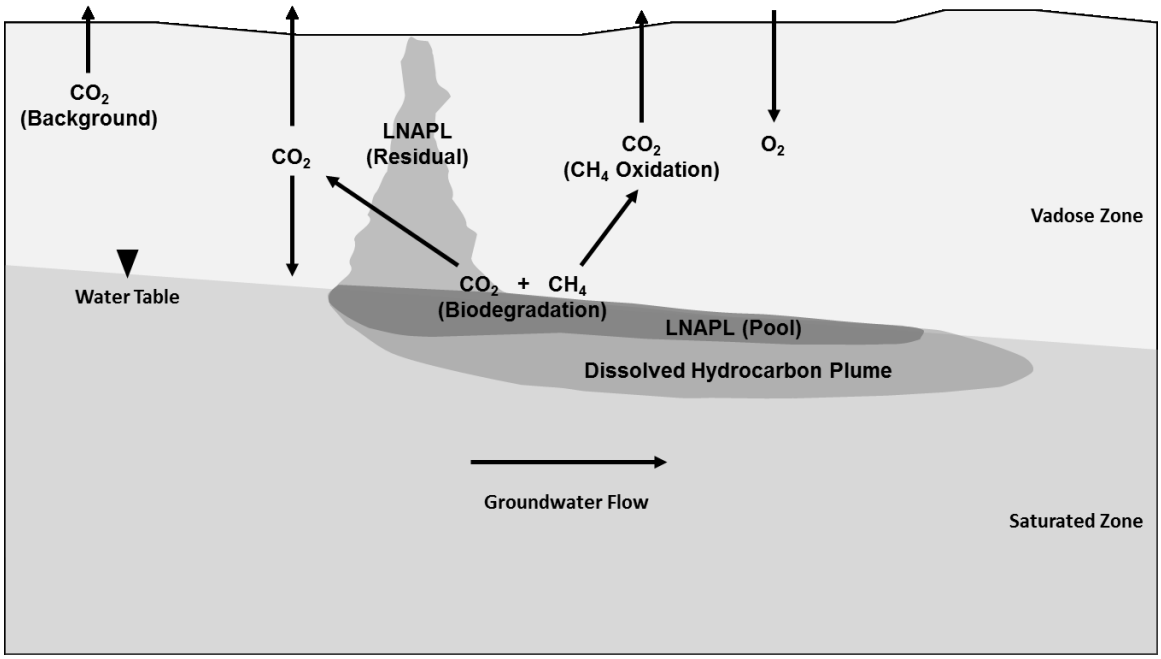

Figure 2.1. Conceptualization of processes governing natural losses of LNAPL (After Sihota et al., 2011).

The two most common approaches to quantify soil-atmosphere exchange rates are the Gradient method (i.e. calculation from diffusion theory), and the Flux Chamber method (Dane et al., 2002). Both methods have been used to estimate gas fluxes associated with LNAPL degradation. The gradient method relies on gas concentrations and estimated effective diffusion coefficients through the vadose zone (Johnson et al., 2006). Fick's first law is employed to estimate fluxes. The chamber method consists of measuring gas concentrations in a closed chamber over the soil. Fluxes are estimated based on changes in gas concentration in the chamber with time due to diffusive inflow (Healy et al., 1996). In modern chamber based systems, the analysis is often based on infrared gas analysis (IRGA), although other methods for CO_2 analysis have been used (Jensen et al., 1996; Pongracic et al., 1997; Keith and Wong, 2006).

Limitations related to the Gradient method revolve around uncertainty in estimated input parameters (including effective diffusion coefficients, soil porosity, and moisture content) in spatially and temporally variable soil profiles (Johnson et al., 1998; Dane et al., 2002). Limitations of the Flux Chamber method involve potential for the sealed chamber to perturb the gas flux during measurement due to transient gas build up in the chamber (Dane et al., 2002). Both methodologies produce estimates of instantaneous gas flux.

Transient conditions that affect single time gas transport measurements include barometric pressure changes and ambient temperature fluctuations, both of which have significant variability over periods of a few hours (Massmann and Farrier, 1992; Wyatt et al., 1995; Auer et al., 1996). Changes in CO_2 flux on the order of 50% within 6-8 hours are not uncommon (Keith and Wong, 2006). This observation highlights the dynamic nature of gas transport in soils. The Flux Chamber method can be adapted to capture temporal data. However, equipment costs and data interpretation can impose limitations on the number of practical long term measurements.

Simple reliable tools to quantify natural losses of LNAPL are needed. In response to this need, Colorado State University (CSU) has developed a novel tool referred to as a CO_2 Trap (Zimbron et al., 2011). CO_2 Traps measure advective and diffusive integral time-averaged CO_2 fluxes at grade. This paper advances the hypothesis that CO_2 Traps can be used to estimate biodegradation related natural LNAPL loss rates at petroleum impacted sites. The paper provides a brief description of

the current approaches to estimate natural losses of LNAPL, introduces CO_2 Traps, presents data supporting the use of CO_2 Traps to quantify CO_2 fluxes, and demonstrates the use of CO_2 Traps at an LNAPL site. Inclusive to the field data are methods to resolve CO_2 fluxes associated with natural soil respiration and losses of LNAPL.

2.3 CO_2 Traps

The following describes methods employed in this paper to test CO_2 Traps. Section 2.3.1 describes the trap design and features. Section 2.3.2 describes laboratory methods for quantifying sorbed CO_2. Section 2.3.3 discusses calculation of CO_2 fluxes. Section 2.3.4 describes two laboratory experiments designed to test the ability of the CO_2 Traps to quantitatively estimate CO_2 fluxes.

2.3.1 CO_2 Trap Design

Figure 2.2 presents a schematic drawing of the CO_2 Traps. Bodies of the CO_2 Traps are constructed of 0.10-m internal diameter Schedule 40 polyvinyl chloride (PVC) pipe fitted with rubber O-rings to create air-tight seals between CO_2 Trap components. Each trap features two passive sorption elements (bottom and top, Figure 2.2). The sorbent media is a commercially available soda-lime material (Sodasorb® HP-6/12, W.R. Grace, Co., a mixture of calcium and sodium hydroxides). CO_2 is first captured as carbonic acid in a thin film at the sorbent surface. A neutralization reaction follows, resulting in the formation of carbonate solids ($CaCO_3$ and Na_2CO_3) in the sorbent media.

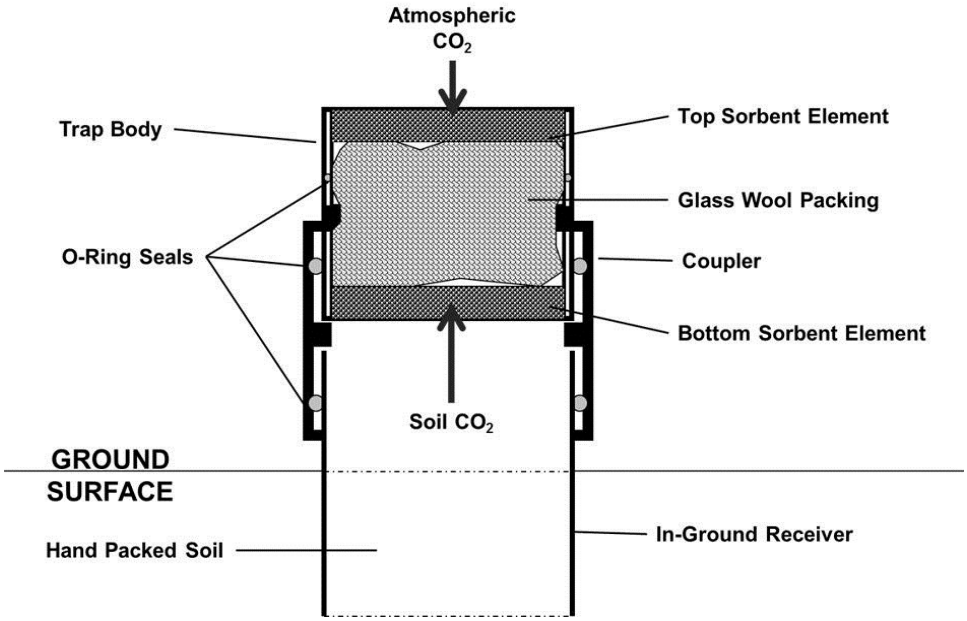

Figure 2.2. Schematic drawing of a CO_2 Trap. Each sorbent element consists of granular sorbent media sandwiched between two stainless steel screens packed into PVC grates; glass wool packing reduces dead space between trap elements and provides support to the screens. Trap elements are fit into a PVC cylinder (trap body) and connected to 4-inch diameter in-ground receivers using a PVC coupler. Components are sealed together with rubber O-rings. The bottom sorbent element captures CO_2 efflux from the soil; the top sorbent element intercepts atmospheric CO_2.

As a modification of the Flux Chamber method, measurement of CO_2 efflux using soda-lime has been studied in the agriculture and forestry fields over more than three decades (Edwards, 1982; Pongracic et al., 1997; Keith and Wong, 2006). Zimbron et al., 2011, add the novel features of unrestricted advective flow-through, and top and bottom trap elements. The bottom element captures CO_2 released from the soil surface while the top of the trap unit is open to the atmosphere. The novel open-top design addresses interferences due to concentration and/or pressure build up effects in sealed chambers that were identified by Dane et al., 2002. An upper trap element captures CO_2 driven into the trap, either due to diffusion or during periods when atmospheric pressure is greater than local soil gas pressure (Zimbron et al., 2011). The traps contain sufficient adsorbent to allow deployment for periods of two to four weeks. Traps

provide an integral time-averaged flux value. This helps overcome the limitations of collecting instantaneous flux estimates in a dynamic system.

2.3.2 CO_2 Trap Laboratory Analytical Methods

After field deployment, CO_2 Traps are returned to the lab and disassembled to recover the sorbent media. Prior to analysis, the sampled media is vacuum dried in a room temperature desiccator and homogenized. Total carbonate content of homogenized portions of dried samples is determined by gravimetric analysis (Bauer et al., 1972). Specifically, weight loss upon acidification of the sample in a system open to the atmosphere is used to determine the mass of sorbed CO_2. Samples are analyzed in triplicate. The average value is reported as CO_2 content by percent mass (CO_2/sorbent). Typical variations in replicate analyses are on the order of ± 10 – 15%. Generally, the variation in replicate analyses decreases as the concentration of sorbed CO_2 increases. The bottom trap elements are used to calculate efflux of CO_2 from soil. The top trap elements are analyzed as a quality control measure to evaluate the potential for cross-contamination of the bottom traps by atmospheric CO_2. CO_2 fluxes are generally not calculated for these elements. Trip blank samples are analyzed with each round of field samples, to correct for CO_2 present in the sorbent media prior to deployment and sorbed during sample handling.

2.3.3 Calculating CO_2 Fluxes

CO_2 fluxes are calculated by dividing the sorbed CO_2 mass by the cross-sectional area of the trap (8.1×10^{-3} m^2) and the period that the trap was deployed. Total CO_2 fluxes (J_{CO2_Total}) are reported in units of micromoles per square meter per second

(μmol/m^2/sec), consistent with soil science literature. Conversion of measured CO_2 fluxes to estimated natural LNAPL loss rates is discussed in Section 2.4.3.

2.3.4 Laboratory Studies

Laboratory studies were performed to demonstrate quantitative capture of CO_2. First, an experiment was conducted to test the ability of the sorbent material to quantitatively capture CO_2 in a closed system. Second, an experiment was conducted using a large sand column (open to atmosphere) to test ability of the CO_2 Traps to quantify flux in an open system.

2.3.4.1 Closed system experiment

A closed system experiment was performed using a small glass column packed with Sodasorb® to evaluate the ability of the sorbent to quantitatively recover CO_2. An additional goal of the experiment was to estimate the total sorption capacity of the Sodasorb®. Seven tests were performed using known masses of sorbent and variable masses of CO_2. Six tests were performed with ratios of CO_2 to sorbent (mass/mass) less than the manufacturers specified maximum sorption capacity of 30% to evaluate quantitative recovery of CO_2. The seventh test was performed with a ratio of CO_2 to sorbent of 60% to evaluate effects of exceeding the expected sorption capacity.

Figure 2.3 illustrates the experimental setup. Influent CO_2 was generated by reacting a solution composed of Na_2CO_3 (A.C.S. Grade) dissolved in deionized water, with 6N HCl in a closed flask. A syringe pump delivered a known mass of Na_2CO_3

solution at a steady rate to the HCl flask. Nitrogen gas carried the CO_2 from the flask through a column containing the soda-lime sorbent media. A minimum of 5 system volumes of carrier gas were passed through the system following completion of injection to avoid dead space losses.

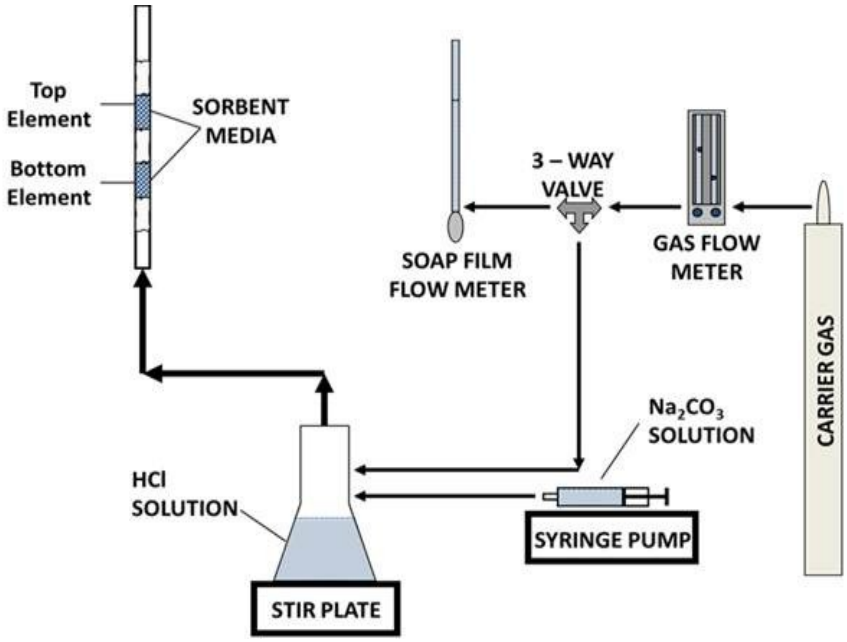

Figure 2.3. Closed system test setup. CO_2 gas is generated by reacting HCl and Na_2CO_3 in the sealed flask. The CO_2 is delivered to the sorbent media by N_2 carrier gas.

Total CO_2 delivered was calculated by change in weight of the syringe, based on measured fluid density and known mass of carbonates added to the solution. The sorbent media was analyzed using a gasometric analysis following (Dreimanis, 1962). Lab blanks were analyzed and CO_2 content of the blanks was subtracted prior to calculating recovery.

2.3.4.2 Open system experiment

An open system experiment was performed to test the ability to quantitatively measure known CO_2 fluxes through a soil column at field scale. A 1.82 m tall by 0.686 m diameter PVC column was filled with fine to medium sand from an onsite stockpile. Sand was placed in the column at field moisture content. Moisture content for 4 representative samples was analyzed by gravimetry. Gravimetric moisture content ranged from 1 – 3 %. The column was allowed to rest for approximately 6 months between filling and first use. It was assumed that the soil moisture distribution in the column equilibrated over that time. CO_2 gas (Bone Dry grade: Airgas, Inc., Fort Collins, Colorado) was metered with a pressure regulator (Marsh / Bellofram Type 40) and a rotameter style gas flow meter fitted with needle valve cartridge (Cole Parmer # 03217-92). The gas was delivered through nominal ¼ inch (0.006 m) diameter copper tubing. Swagelok™ connectors were used throughout the system. Gas was delivered to the base of the sand column through the 0.006 m diameter tubing fit to a pass-through Swagelok™ fitting in the bottom of the tank. A three way valve allowed for measurement of gas flow rates using a soap film flow-meter. The general experimental setup is shown in Figure 2.4.

Seven sample runs were performed. Gas flow rates were adjusted between each run and the flow was allowed to equilibrate for a period of several days prior to deployment of CO_2 Traps. Gas flow rates were measured at prior to deployment, and when the CO_2 Traps were collected. A minimum of 10 replicate gas flow measurements (soap film flow meter) were collected for each run. Variability of measured gas flow

rates (standard deviation/mean) did not exceed 2%. Ambient air pressure and temperature was monitored throughout each run using a barometric pressure logger (Solinst Canada, Ltd. Georgetown, Ontario). Molecular concentration of the influent CO_2 (μmol/ml) was calculated from measured ambient temperature and barometric pressure, using the ideal gas law. Variability of calculated gas concentrations did not exceed 0.4%. Molecular flow rates (μmol/sec) were calculated using the mean gas flow rate (ml/min) and the mean molecular concentration. Injected CO_2 flux rates (μmol/m^2/sec) were calculated from the injected gas flow rate and the cross-sectional area of the tank (0.369 m^2).

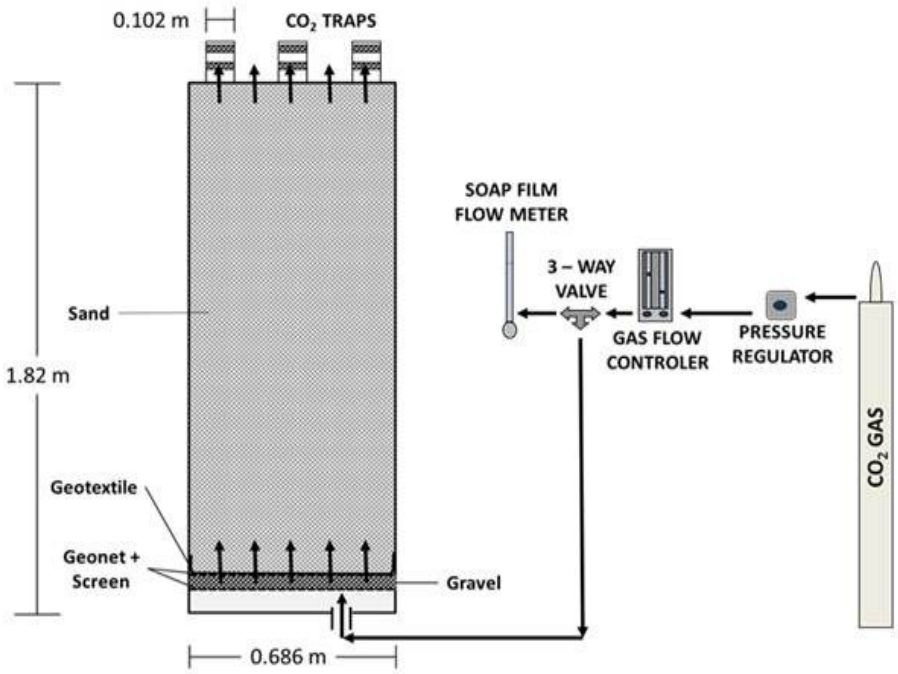

Figure 2.4. Open system test setup. Metered CO_2 gas flows into the bottom of the large PVC column. The gas passes through dead space, a layer of gravel, and a geotextile liner before entering the base of the sand column. The gas flows through the sand column and exits to the atmosphere. Three CO_2 Traps capture CO_2 flux at the top of the tank.

Three traps were deployed in a triangular pattern for each test round. Gas was delivered through a 0.006 m diameter hole, offset toward the edge of the column. An assumption that the gas flow was evenly distributed over the entire cross-sectional area of the tank was later confirmed by the trap replicates for 6 of the 7 sample runs. Results of the largest flux run suggest heterogeneous flow through the column at large injected gas flow rates (see Results section). A travel blank was analyzed for each sampling round. The CO_2 concentration from the blank was subtracted prior to calculating fluxes.

2.4 Field Study

A field study was performed at a decommissioned petroleum refinery to estimate CO_2 flux and LNAPL loss rates in the field. Section 2.4.1 briefly describes the field site and CO_2 Trap field deployment procedures. Section 2.4.2 describes methods to resolve CO_2 fluxes associated with natural soil respiration and losses of LNAPL. Section 2.4.2.1 discusses background correction methods. Section 2.4.2.2 describes carbon isotope methods. Section 2.4.3 discusses calculation of natural LNAPL loss rates from measured CO_2 fluxes.

2.4.1 Field Site Description and CO_2 Trap Deployment

Twenty three CO_2 Traps were deployed at a former petroleum refinery in Wyoming between September 29 and November 10, 2011. The site is underlain by braided stream deposits of sand with a typical depth to water of 3 m. Twenty CO_2 Traps were located above LNAPL impacted soils as delineated using historical laser induced fluorescence (LIF) data. Three traps were deployed above unimpacted (background)

soils (per LIF data). Additionally, three traps were deployed approximately 2 m apart at an impacted location where an earlier round of CO_2 Trap sampling indicated large LNAPL loss rates. The triplicate location provides a basis for estimating variability of measured CO_2 fluxes at a single location. Additional site information is provided in the results section.

For CO_2 Trap field deployment, a 0.10 m diameter x 0.31 m long PVC receiver is installed to approximately 0.2 m below grade and the hollow center is re-packed with site soil to minimize disturbance of natural soil gas flow. The receivers are installed at least one day prior to deployment of the CO_2 Traps, to allow the soil to recover from installation disturbance. A PVC cap with an approximately 0.03 m hole drilled in the center is placed on top of the CO_2 Traps during deployment. This feature allows advective air flow through the CO_2 Trap, while providing an approximately 94% reduction in cross-sectional area for diffusive flux of atmospheric CO_2 to the top sorbent element. Reducing diffusive flux to the top trap is important to ensure that that top sorbent element does not saturate and allow cross contamination of the lower element with atmospheric CO_2. Vented protective PVC covers are placed over the CO_2 Traps during deployment for protection from weather and for increased visibility.

2.4.2 Correction for Naturally Occurring CO_2

Total CO_2 captured by the traps results from a mixture of LNAPL degradation and natural soil respiration processes. Establishing the contribution of LNAPL degradation to the total CO_2 flux is critical to accurately estimating natural losses of LNAPL.

Background subtraction and carbon isotope analysis can be used to estimate the relative CO_2 contributions from LNAPL degradation and natural soil respiration (Sihota et al., 2011; Sihota and Mayer, 2012). The following sections describe each of these methods in turn.

2.4.2.1 Background Subtraction Method

Background subtraction (Sihota et al., 2011), is based on the principle that total CO_2 flux (J_{CO2_Total}) at LNAPL sites is the summation of the fluxes due to petroleum degradation (J_{CO2_LNAPL}) and natural soil respiration ($J_{CO2\_Background}$):

Equation 2.1. $$J_{CO2\_Total} = J_{CO2\_LNAPL} + J_{CO2\_Background}$$

or

Equation 2.2 $$J_{CO2\_LNAPL} = J_{CO2\_Total} - J_{CO2\_Background}$$

Using this method, CO_2 efflux measurements are collected at grade over the LNAPL body (LNAPL areas) and over areas presumed to be unaffected by LNAPL (background areas). It has been shown that background subtraction can be effective at identifying regions of large natural LNAPL loss rates, and effectively estimating the loss rates (Sihota et al., 2011; Sihota and Mayer, 2012).

This method is by far the simplest avenue for generating natural loss rate estimates from measured CO_2 fluxes. However, the background subtraction method is not appropriate at all sites. Spatial variability of background CO_2 effluxes at some sites leads to uncertainty in the calculated LNAPL loss values. Additionally, some sites have

shown LNAPL area CO_2 effluxes of similar order of magnitude to background area CO_2 fluxes. This leads to ambiguity as to whether or not natural losses of LNAPL are occurring. The problem is that natural losses of LNAPL may be occurring at rates that are undetectable using the background subtraction method. This phenomena has been studied at a site in Bemidji Minnesota (Sihota and Mayer, 2012). Finally, selecting appropriate background sample locations at many active or recently decommissioned industrial facilities can be challenging.

2.4.2.2 Carbon Isotope Sampling

The second method used to separate CO_2 contribution from soil respiration and natural losses of LNAPL is stable carbon (^{12}C and ^{13}C) and radiocarbon (^{14}C) isotope analysis (Sihota and Mayer, 2012). Stable carbon (^{12}C and ^{13}C) and radiocarbon (^{14}C) analyses of groundwater and soil gas have previously been used to evaluate natural attenuation at hydrocarbon and chlorinated solvent sites (Suchomel et al., 1990; Aggarwal and Hinchee, 1991; Conrad et al., 1997; Coffin et al., 2008). Carbon isotope analysis has also been used to study weathering of petroleum reservoirs (Stahl, 1980) and to differentiate anthropogenic and natural sources of atmospheric CO, CO_2 and CH_4 (Klouda and Connolly, 1995; Levin et al., 1995; Avery Jr et al., 2006). More recently, the technique has been suggested as a method of evaluating the source of CO_2 efflux at grade over petroleum impacted sites (Sihota et al., 2011).

Radiocarbon techniques rely on the analysis of radiocarbon (^{14}C). Radiocarbon is an unstable carbon isotope (with a half-life of approximately 5,600 years) generated

by cosmic rays in the atmosphere. Contemporary (modern) organic carbon is ^{14}C rich, while fossil fuel carbon is ^{14}C depleted. Furthermore, contemporary samples and atmospheric samples have the same characteristic amount of ^{14}C. The detection limit of ^{14}C by accelerator mass spectrometry enables dating of samples younger than 60,000 years, while older samples (such as those associated with fossil fuels) have non-detectable ^{14}C activity (Stuiver and Polach, 1977). By convention, radiocarbon isotope analysis results are reported as fraction modern (Fm) based on a 1950 NBS oxalic acid standard, synthesized when the ^{14}C atmospheric levels were less than at present.

For a sample that contains modern and fossil fuel carbon (e.g. CO_2 Traps measuring natural losses of LNAPL and soil respiration), measurement of ^{14}C enables quantitation contribution from both sources. The fossil fuel fraction of the sample, ff_{sample}, and the remaining non-fossil fuel or contemporary (1- ff_{sample}), are related by the two-component mass balance:

Equation 2.3. $$Fm_{sample} = (ff_{sample})(Fm_{ff}) + (1 - ff_{sample})(Fm_{atm})$$

In this formula, Fm_{sample} is the measured modern fraction of the sample, Fm_{ff} is the fraction of modern carbon in fossil fuel ($Fm_{ff} = 0$), and Fm_{atm} is the fraction of modern carbon in contemporary living material ($Fm_{atm} = 1.15$) (Avery Jr et al., 2006). As discussed previously, due to reporting conventions, Fm_{sample} is reported as if the analysis was performed in 1950. Current Fm_{atm} is larger than 1.

The fossil fuel fraction of a sample can be calculated by rearranging Equation 2.3:

Equation 2.4. $ff_{sample} = [1 - (Fm_{sample})/(Fm_{atm})]$

Equation 2.4 can be used to estimate the relative contribution from natural losses of LNAPL:

Equation 2.5. $J_{CO2\_LNAPL} = (J_{CO2\_Total})(ff)$

Stable carbon isotope techniques are based on measuring the ratios of the stable isotopes ^{12}C and ^{13}C in a sample. Stable carbon isotope results are reported as $\delta^{13}C$ in parts per mil (‰) (Craig, 1953):

Equation 2.6. $\delta^{13}C$ ‰ $= [(^{13}C_{sample}/^{12}C_{sample}) / (^{13}C_{std}/^{12}C_{std}) - 1] \times 1000$

Where $^{13}C_{std}$ and $^{13}C_{std}$ are the carbon isotope concentrations of a standard. Ratios are most commonly reported relative to Vienna PeeDee Belemnite (VPDB) standard (Conrad et al., 1997). Stable carbon isotopes are useful for comparing sources, and can provide evidence of biodegradation (Aggarwal and Hinchee, 1991).

Four subsamples of solid CO_2 Trap media remaining after analysis of the field trap elements were submitted to the Institute of Arctic and Alpine Research (INSTAAR, UC Boulder) for stable and radiocarbon isotope analysis. The sample set consisted of a travel blank, two background locations, and an LNAPL location with large CO_2 flux.

Additionally four diesel range hydrocarbon samples were submitted to CSU's Natural Resources and Ecology Lab (NREL) for stable carbon isotope analysis to compare with the CO_2 Trap results. The hydrocarbon samples were collected from sub samples of a soil core collected approximately 27 meters northwest of the LNAPL CO_2 Trap location. Hydrocarbon samples were extracted from the soil subcores with hexane. The hexane was allowed to evaporate for a period of several days in a fume hood until mass stabilized. The remaining fluid was retained and submitted for carbon isotope analysis.

2.4.3 Natural LNAPL Loss Rate Calculations

Stoichiometric production of CO_2 from LNAPL (based on J_{CO2_LNAPL}) can be transformed into a volumetric LNAPL loss (gal/acre/yr) based on the density and molecular weight of the LNAPL. Estimates of natural losses of LNAPL reported in this paper are calculated using an assumption of benzene (C_6H_6) as the characteristic stoichiometric composition of LNAPL, and an assumed LNAPL density of 0.8 g/ml. These assumptions result in a conversion factor of approximately 550 (gal/acre/yr) per 1 (μmol/m^2/sec). The advantage of quantifying natural losses in units of gal/acre/yr is that the results can readily be compared to common performance data for other remedial technologies (e.g. hydraulic LNAPL recovery). LNAPL loss rates for the field study described herein were calculated using the background subtraction method. A comparison of the background subtraction method to carbon isotope analysis methods for one sample is provided in Section 2.5.4.

2.5 Results

The following presents results from laboratory and field studies. Section 2.5.1 discusses closed system sampling results. Section 2.5.2 discusses open system sampling results. Section 2.5.3 discusses field sampling results. Section 2.5.4 presents carbon isotope sampling results and provides a brief comparison of natural loss rates calculated using both background subtraction and ^{14}C.

2.5.1 Closed System Experiment Results

Figure 2.5 presents captured CO_2 as a function of injected CO_2 for the closed system experiment (plotted as % - mass CO_2/mass sorbent) captured by the bottom trap elements. The data were plotted this way to facilitate analysis of sorption capacity for the SodaSorb® media. Data for top trap elements are not shown, although they remained similar to the unexposed sorbent material. An exception was an injection which exceeded the manufacturer's specified sorption capacity and therefore achieved breakthrough from the saturated bottom element. The solid line shows the least squares best fit curve (slope = 0.87, R^2 = 0.99). The best fit line has been projected past the manufacturer's reported sorption capacity of 30% by mass, but the seventh data point lies clearly below the line (near ~30%). A 95% confidence interval calculated for the slope and intercept of the best fit line indicate that the slope is not significantly different from 1 and the intercept is not significantly different from 0. The results indicate that the media is capable of quantitative CO_2 recoveries so long as sorbed CO_2 is less than the manufacturer's specified sorption capacity of 30% by mass.

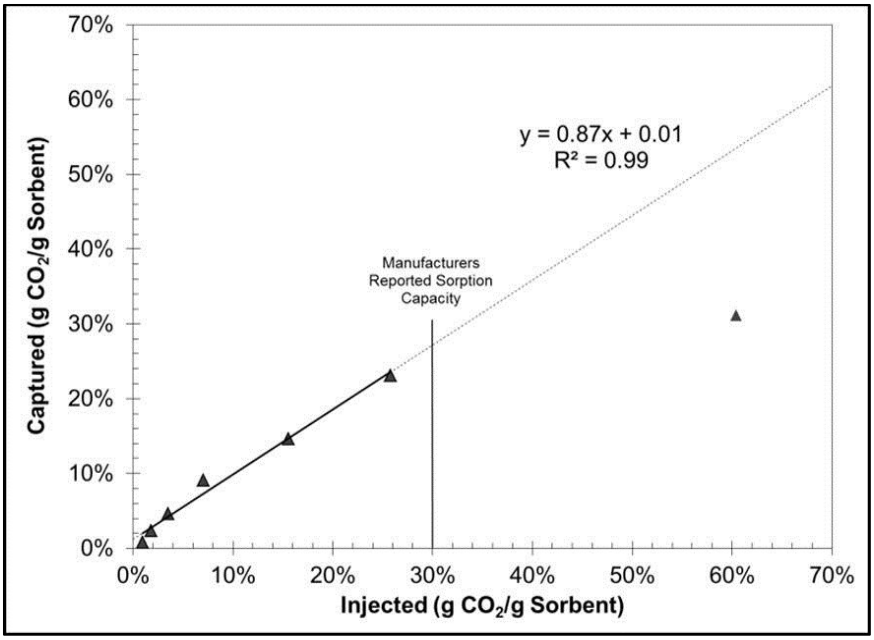

Figure 2.5. Closed system test results. Triangles show results of closed system tests. The solid line is the least squares best fit. The dashed line shows the projection of the least squares best fit beyond the manufacturers reported sorption capacity (30% by mass).

It should be noted that the estimated sorption capacity includes any CO_2 sorbed to the media prior to testing or field deployment. This CO_2 is subtracted based on lab and travel blanks prior to data reporting, however, it should be considered when planning for maximum field deployment times. Experience has shown that up to 2% CO_2 by mass is generally present in the media prior to sample deployment. Therefore, it is recommended that deployment times be planned to not exceed ~28% CO_2 by mass in the sorbent media.

2.5.2 Open System Experiment Results

Figure 2.6 presents measured CO_2 flux vs. injected CO_2 flux from open system testing plotted in units of (μmol/m^2/sec). Each individual point represents a single trap measurement. The colored symbols highlight individual trap locations. Location A is

approximately directly over the CO_2 inlet port. Locations B and C are further from the inlet port.

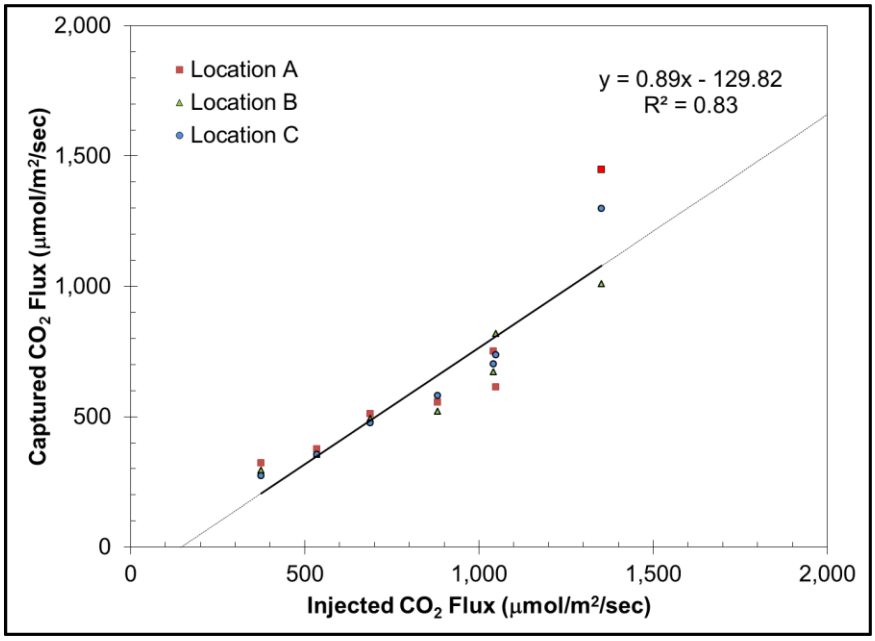

Figure 2.6. Open system test results. Three traps were deployed per test. Each individual point represents a single trap measurement. Location A is situated directly above the CO_2 inlet port. Locations B and C are further from the port. The solid line is the least squares fit. The light dashed line shows the projection of the least squares best fit beyond the range of measured fluxes.

The solid line shows the least squares best fit (slope = 0.89, R^2 = 0.83). The dashed line shows the projection of the modeled fit to beyond the measured flux interval. A 95% confidence interval calculated for the slope and intercept of the best fit line indicate that the slope is not significantly different from 1 and the intercept is not significantly different from 0, demonstrating that that CO_2 capture in an open system is quantitative.

It should be noted that the inlet port is offset from the center of the column. Additionally, gas flow rates are greater than would be expected at a field site. The

spread in measured fluxes at largest injected flux tested may result from non-uniform flow (i.e. channeling of CO_2) causing more localized flux over the inlet port and less local flux at the other traps. In most cases, Location A (directly over the inlet port) had the largest estimated CO_2 flux.

2.5.3 Field Sampling Results

Figure 2.7 presents site maps illustrating key site features and results. Symbol size on Figure 2.7a is proportional to measured CO_2 flux ($\mu mol/m^2/sec$). Symbol size on Figure 2.7b is proportional to calculated LNAPL loss rate (gal/acre/yr). The shaded area outlines the LNAPL body as defined from LIF data. General groundwater flow is toward the river. Groundwater at the site is controlled by pumping and a Waterloo™ sheet pile wall located along the river. J_{CO2_Total} values calculated for each location (Figure 2.7a) are shown on Table 2.1. Locations 1-3 are unimpacted background sampling. Measured background CO_2 fluxes ($J_{CO2\_Background}$) range from 1.7 to 3.6 $\mu mol/m^2/sec$. These values are consistent with expected background CO_2 fluxes in a grassland (Bremer and Ham, 2002).

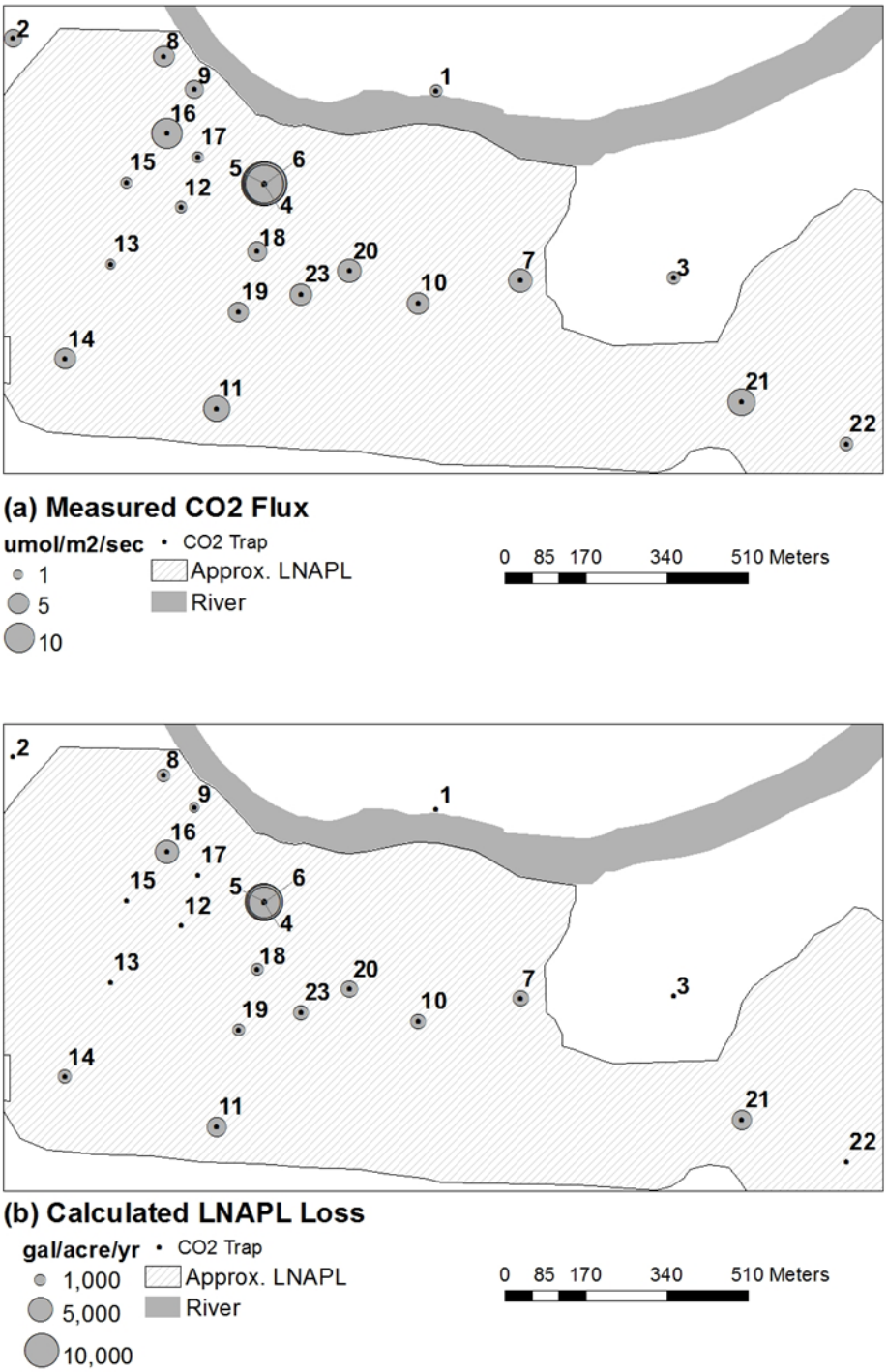

Figure 2.7. Field site map and CO_2 Trap survey results. Numbers correspond to the CO_2 Trap sample IDs in Table 2.1. (a) Measured CO_2 flux, size of gray circles is proportional to J_{CO2_Total} (μmol/m^2/sec). (b) Calculated LNAPL loss, size of gray circles is proportional to loss rate (gal/acre/yr). Locations without gray circles did not significantly exceed background CO_2 flux. The cross hatched areas show approximate extent of onsite LNAPL body as estimated by LIF survey. General groundwater flow is toward the river.

Table 2.1. CO_2 Trap Field Sampling Results Sampling Period 9/29 – 11/10, 2011.

Category	Sample ID	J_{CO2_Total} ($\mu mol/m^2/sec$)		Calculated LNAPL Loss (gal/acre/yr)		Comments
		Avg	Stdev	Avg	95% CI	
BG	1	1.7	0.3	- -	- -	
BG	2	3.6	0.9	- -	- -	
BG	3	1.9	0.5	- -	- -	
LNAPL	4	17	1.1	**8,100**	**6,900 - 9,300**	Triplicate Location
LNAPL	5	24	0.1	**12,000**	**11,000 - 12,000**	Triplicate Location
LNAPL	6	22	0.3	**11,000**	**10,000 - 11,000**	Triplicate Location
LNAPL	7	6.4	0.4	**2,200**	**1,700 - 2,700**	LNAPL to total depth
LNAPL	8	5.0	0.5	**1,400**	**880 - 2,000**	
LNAPL	9	3.9	0.1	**800**	**350 - 1,300**	
LNAPL	10	5.8	0.4	**1,900**	**1,300 - 2,400**	
LNAPL	11	8.3	0.1	**3,200**	**2,800 - 3,700**	
LNAPL	12	1.6	0.2	ns	ns	
LNAPL	13	1.1	0.2	ns	ns	
LNAPL	14	5.1	0.4	**1,500**	**950 - 2,100**	
LNAPL	15	1.5	0.4	ns	ns	
LNAPL	16	11	0.4	**4,700**	**4,200 - 5,200**	
LNAPL	17	1.5	0.1	ns	ns	
LNAPL	18	4.6	0.2	**1,200**	**730 - 1,700**	
LNAPL	19	4.8	0.6	**1,300**	**610 - 2,000**	
LNAPL	20	6.6	0.3	**2,300**	**1,800 - 2,800**	
LNAPL	21	8.4	0.1	**3,300**	**2,800 - 3,700**	
LNAPL	22	2.1	0.1	ns	ns	
LNAPL	23	5.8	0.2	**1,900**	**1,400 - 2,300**	

Notes:
See Figure 2.7 for sample locations. Samples 1-3 are unimpacted background locations.
Samples 4-6 are collocated ~2 m apart.
- - No data.
Avg - Average (mean) of replicate CO_2 trap laboratory analyses.
BG - Background CO_2 trap location.
Calc - Calculated LNAPL loss rate based on background CO_2 flux subtraction method.
gal/acre/yr - Gallons LNAPL per acre per year.
LNAPL- LNAPL loss rate measurement CO_2 Trap location.
$\mu mol/m^2/sec$ - 10^{-6} moles CO_2 per square meter per second.
ns - CO_2 flux not significantly greater than background based on 95% confidence interval. No LNAPL loss calculated.
Stdev - Standard deviation of replicate CO_2 trap laboratory analyses.
95% CI - 95% Confidence interval of the calculated LNAPL loss rate. Calculated as described in the text.

Means of each replicate analysis for each of the background locations were compared to those of individual LNAPL locations by a two sample T-test. J_{CO2_Total} was in general significantly greater than background over the LNAPL body with several exceptions (denoted as "ns" in Table 2.1). LNAPL loss rates were calculated using the background subtraction method and a conversion factor of 550 (gal/acre/year) per 1 ($\mu mol/m^2/sec$) for locations that significantly exceeded background (as determined by the two sample T-test). Estimated LNAPL loss rates range from 800 to 12,000 gal/acre/yr. These rates of natural losses of LNAPL are of similar magnitude to those

calculated by others at other petroleum-impacted sites (Lundegard and Johnson, 2006; Sihota et al., 2011).

2.5.4 Carbon Isotope Sampling Results

Figure 2.8 presents results of carbon isotope sampling for the analyzed subset of CO_2 Trap samples. The data bars along the horizontal axis represent total mass of trapped carbon as grams of CO_2. These are raw data (not blank corrected). The hatched areas are interpreted as non-fossil fuel (i.e. recent carbon). The white bars are interpreted as resulting from fossil fuels (i.e. biodegradation of LNAPL). The total CO_2 recovered from the travel blank and the two background locations (Locations 1 and 2 on Figure 2.7) is relatively small (< 5 g). Accordingly, the relative fossil fuel fraction is quite small (< 1 g). In contrast, the sample from above the LNAPL pool (Location 6 on Figure 2.7) contained more total carbon (> 27 g) and fossil fuel related carbon (~25 g). These data are a strong indication that the significantly elevated CO_2 flux over the LNAPL body results from degradation of LNAPL.

Estimated LNAPL loss rate for Location 6 (Figure 2.7) based on fossil fuel fraction correction of non-blank subtracted CO_2 flux is (23 μmol/m^2/sec x 0.89 x 550 [gal/acre/yr]/[μmol/m^2/sec] = <u>11,000 gal/acre/yr</u>). Alternatively, the background-corrected LNAPL loss rate is 11,000 gal/acre/yr (Table 2.1). These results indicate that the background subtraction method can be applied at sites with small variability in background CO_2 flux and sufficiently large LNAPL loss rates. However, experience shows that obtaining accurate background CO_2 fluxes is difficult at many sites due to

variability in soil and plant conditions, and concerns with finding unaffected soils. Thus, ^{14}C analysis provides a useful alternative to background subtraction. However, in some situations, analytical costs for ^{14}C analysis may limit its practical application.

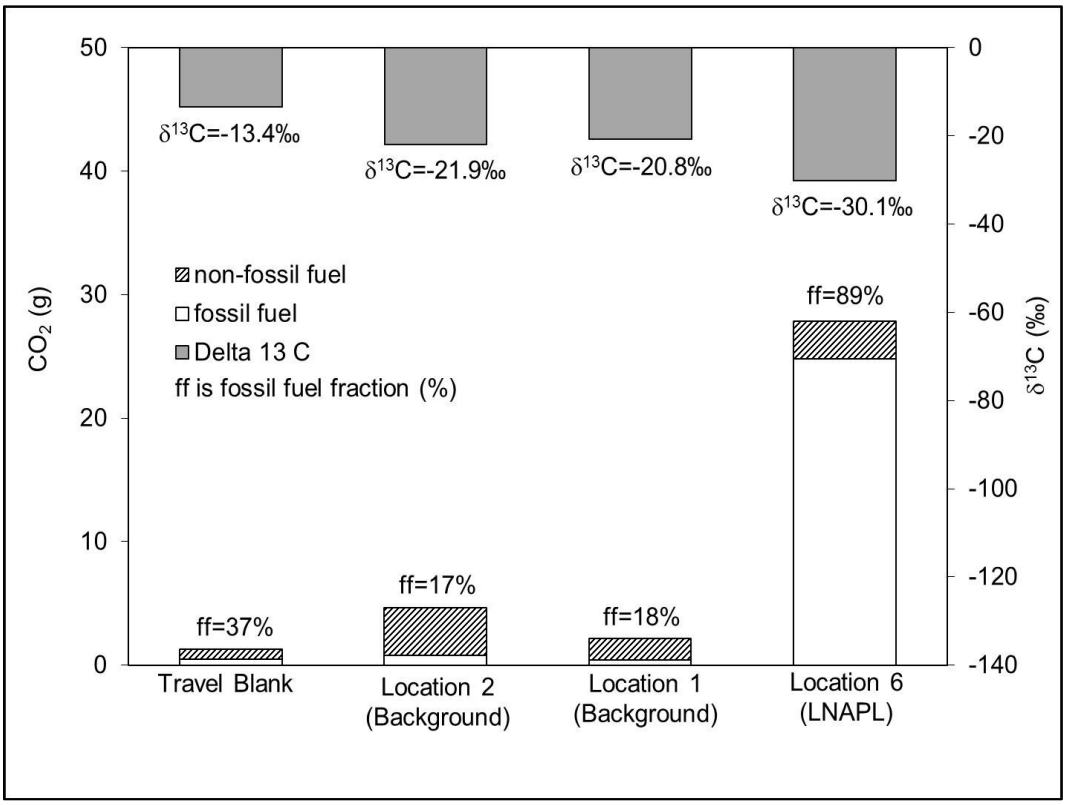

Figure 2.8. Carbon isotope sampling results. Bars along lower axis show total carbon (g CO_2) recovered from each trap element. Hatched areas represent contribution from recent carbon (i.e. natural soil respiration); white areas represent contribution from fossil fuel carbon. Bars along upper axis show $\delta^{13}C$ (‰) for the respective locations identified along the lower axis. The $\delta^{13}C$ values of the two background locations are similar to each other. The $\delta^{13}C$ value for the LNAPL location shows a distinct difference from the two background locations, and is closer to $\delta^{13}C$ values from nearby LNAPL samples (-26.5 to -27.3 ‰).

The gray shaded bars along the upper axis of Figure 2.8 show the results of stable carbon isotope sampling as $\delta^{13}C$ (‰). The $\delta^{13}C$ values of the background locations are similar to each other (-21.9 and -20.8 ‰) and are similar to those reported for natural plant respiration at other sites (Suchomel et al., 1990). The $\delta^{13}C$ value from

the LNAPL location is distinctly less (-30.1 ‰) than that of the background samples. The $\delta^{13}C$ value from the LNAPL area CO_2 trap is significantly closer to the $\delta^{13}C$ values of the four LNAPL samples (mean = -26.97, stdev = 0.395) than to either background sample or the travel blank. The observation that the $\delta^{13}C$ value from the CO_2 Trap at the LNAPL location is less than that of the LNAPL itself may be due to isotopic fractionation associated with degradation of the LNAPL. These data provide further evidence that the CO_2 captured by the traps was derived from biodegradation related natural losses of LNAPL at the site.

2.6 Conclusions

The ability to estimate natural losses of LNAPL is critical to developing effective remediation strategies at LNAPL sites. CO_2 Traps provide an alternative to current methods, that is simple to deploy and capable of providing quantitative estimates of CO_2 flux. Potential advantages over current methods include the ability to capture both advective and diffusive fluxes, and providing integral time-averaged flux estimates. Laboratory studies showed that CO_2 Traps are capable of quantitatively capturing CO_2 with experimental regression fits of 87 to 89% recovery efficiencies. A field study showed that CO_2 fluxes can be measured in the field using CO_2 Traps. Additionally, it was shown that CO_2 production at LNAPL locations can significantly exceed CO_2 production rates associated natural soil respiration. Carbon isotope sampling supports the interpretation that observed CO_2 fluxes in excess of natural background fluxes are due to biodegradation of LNAPL. Finally, field sampling indicates that natural losses of LNAPL ranging from 800 to 12,000 of gal/acre/yr are occurring beneath a former

petroleum refinery. These observations support the use of CO_2 Traps as a tool for resolving natural LNAPL loss rates: a parameter that is central to forming effective remediation strategies at LNAPL sites.

It should be noted that while the carbon isotope correction and background subtraction matched well for this particular site and sampling round, this may not always be the case. Experience gained by the researchers at this and other sites indicates that background CO_2 flux readings can vary widely across a site during one sampling event. Isotopic analysis provides a more accurate method of separating captured CO_2 related to natural losses of LNAPL from CO_2 related to other processes. However, current costs associated with ^{14}C sampling may limit its practical utility.

An ongoing series of field studies is underway at several field sites to evaluate natural losses of LNAPL under a range of conditions. The goal of the ongoing work is to better understand processes and drivers for natural losses at LNAPL sites.

2.7 Recognition

Funding for this work was provided by Chevron, Suncor Energy, ExxonMobil, and the University Consortium for Field-Focused Groundwater Contamination Research. The authors thank Gary Dick (lab technician) and undergraduate students Sonja Koldewyn, Sarah Breidt, Rebecca Bradley, Adam Byrne, and Calista Campbell for support during trap construction and analysis, and site consultants from TriHydro Corporation for site support.

3 ESTIMATING NATURAL LOSSES OF LNAPL AT SIX FIELD SITES USING CO_2 TRAPS

3.1 Summary

Extensive bodies of light non-aqueous phase liquids (LNAPLs) are commonly found beneath petroleum facilities. Hydraulic LNAPL recovery and other common remedial measures can be costly and often have limited effectiveness. Recent studies suggest that quantifying natural LNAPL loss rates can provide important information for developing effective LNAPL management strategies. CO_2 Traps located at grade have been shown to be an effective tool for quantifying natural losses of LNAPL at field sites. Over a 2-year period, CO_2 Traps were deployed at 117 sampling locations at 6 field sites. Calculated LNAPL loss rates from a single round of sampling at the six field sites ranged from 660 – 18,000 gal/acre/yr with a mean rate of 3,800 gal/acre/yr. The effects of in-well LNAPL thickness, depth to smear zone, smear zone thickness, LNAPL type, shallow groundwater temperature, and seasonal influences were explored at one of the 6 sites. Results indicated that LNAPL loss rates are largely independent of smear zone thickness, depth to smear zone, LNAPL type, and in-well LNAPL thickness. However, temperature related seasonal trends were observed. These observations provide important support for development of new sustainable LNAPL remediation technologies.

3.2 Introduction

Past industrial practices have led to the accumulation of extensive LNAPL bodies beneath many petroleum facilities. Traditional LNAPL remedies (e.g. hydraulic LNAPL recovery) are costly and often have limited effectiveness (ITRC, 2009a). Recent studies (Mahler et al., 2011; Mahler et al., 2012) suggest that natural losses of LNAPL (e.g.

dissolution, volatilization, biodegradation) can control LNAPL stability (i.e. potential for an LNAPL body to expand or translate laterally). LNAPL stability is a key factor driving remediation decisions at many sites (ITRC, 2009a; Smith et al., 2012). Achieving a sound understanding natural LNAPL loss rates may prove valuable in developing effective long-term strategies for LNAPL sites.

Rates of natural losses of LNAPL have multiple potential uses. These include demonstrating LNAPL stability, forming a basis for initiating or discontinuing hydraulic recovery, estimating longevity of LNAPL bodies, and developing a benchmark to compare relative effectiveness of different remedial alternatives. Furthermore, an understanding of processes governing natural losses of LNAPL, gained through field studies, can guide development of new, more sustainable LNAPL remediation technologies.

Recent studies have shown large natural LNAPL loss rates at field sites (Amos et al., 2005; Johnson et al., 2006; Lundegard and Johnson, 2006; ITRC, 2009b; Molins et al., 2010; Mahler et al., 2011; Sihota et al., 2011). Lundegard and Johnson estimated natural hydrocarbon loss rates ranging from 0.1 to 1 kilograms petroleum per square meter per year ($kg/m^2/year$) at the Guadalupe Oil Field site in California (Lundegard and Johnson, 2006). Sihota et al. estimated natural losses of 3.3 grams petroleum per square meter per day ($g/m^2/d$) at a historical crude oil spill site in Bemidji, Minnesota (Sihota et al., 2011). Assuming an LNAPL density of 0.8 g/cm^3, these rates are equivalent to 130 – 1,300 and 1,600 gal/acre/yr respectively. These reported natural

LNAPL loss rates are large when compared to recovery rates associated with common engineered solutions (e.g., EPA, 2005).

A conceptual model of key processes is shown on Figure 3.1. With this conceptual model as a reference, researchers have studied natural losses of LNAPL using: aqueous geochemistry (Aqueous Electron Acceptors and Byproducts method - Johnson et al., 2006; Lundegard and Johnson, 2006; ITRC, 2009b); soil gas profiles (Gradient method - Amos et al., 2005; Johnson et al., 2006; Lundegard and Johnson, 2006; ITRC, 2009b); efflux of CO_2 at grade (Flux Chamber method - Sihota et al., 2011); and direct measurements of LNAPL fluxes (Mass Balance method - Mahler et al., 2011; Mahler et al., 2012; Smith et al., 2012). Two of these approaches (Gradient method and Flux Chamber method) are based on estimation of gas fluxes, notably CO_2 either through the vadose zone or at grade.

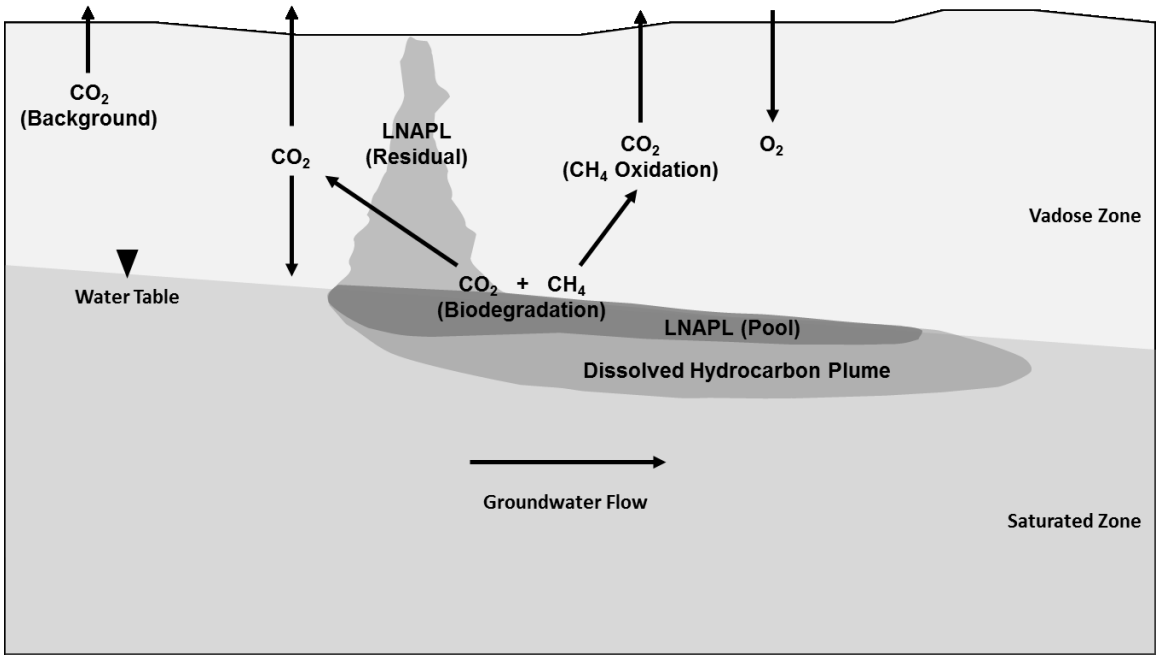

Figure 3.1. Conceptualization of processes governing natural losses of LNAPL (After Sihota et al., 2011).

CO_2 is the final end product of petroleum mineralization. CO_2 is directly produced by petroleum mineralization under aerobic conditions. Under conditions where all electron acceptors are depleted, methanogenesis is the primary degradation pathway. In many instances, outwardly migrating CH_4 converts to CO_2 upon encountering inward migrating O_2 in the vadose zone (Amos et al., 2005; Molins et al., 2010; Sihota et al., 2011; Ma et al., 2012). Molins et al., 2010 suggest that as much as 98% of total carbon released through petroleum mineralization exits the ground surface as CO_2. As such, measuring soil-atmosphere CO_2 exchange can provide a useful indicator of natural losses.

The two most common approaches to quantify soil-atmosphere exchange rates are the Gradient method and the Flux Chamber method (Dane et al., 2002). The Gradient method utilizes Fick's first law to estimate fluxes. The method relies on measured gas concentrations and estimated effective diffusion coefficients through the vadose zone, e.g. (Johnson et al., 2006). The Flux Chamber method consists of measuring gas concentrations in a closed chamber over the soil. Fluxes are estimated based on changes in gas concentration in the chamber with time due to diffusive inflow (Healy et al., 1996). In modern chamber based systems, the analysis is often based on infrared gas analysis (IRGA), although other methods for CO_2 analysis have been used (Jensen et al., 1996; Pongracic et al., 1997; Keith and Wong, 2006).

Limitations related to the Gradient method revolve around uncertainty in estimated input parameters (including effective diffusion coefficients, soil porosity, and

moisture content) in spatially and temporally variable soil profiles (Johnson et al., 1998; Dane et al., 2002). Limitations of the Flux Chamber method involve potential for the sealed chamber to perturb the gas flux during measurement due to transient gas build up in the chamber (Dane et al., 2002). These methodologies commonly ignore transient conditions (e.g. barometric pressure changes and ambient temperature fluctuations), which cause measurable variability over a period of hours (Massmann and Farrier, 1992; Wyatt et al., 1995; Auer et al., 1996). Changes in CO_2 flux on the order of 50% within 6-8 hours are not uncommon (Keith and Wong, 2006). This observation highlights the dynamic nature of gas transport in soils. The Flux Chamber method can be adapted to capture transient data. However, equipment costs and data interpretation can impose limitations on the number of practical long term measurements.

In response to a need for a reliable tool to quantify natural losses of LNAPL, Colorado State University (CSU) has developed a novel tool referred to as a CO_2 Trap (Zimbron et al., 2011 and McCoy et al., 2012). CO_2 Traps measure integral time-averaged CO_2 fluxes at grade. CO_2 fluxes are used to calculate natural LNAPL loss rates. CO_2 Traps have been tested in the laboratory and in the field. The primary purpose of this paper is to present LNAPL loss rates estimated from CO_2 Trap surveys conducted at six LNAPL sites. First, field methods, CO_2 Trap design, and laboratory analytical methods are discussed. Next, results of one round of sampling at each of the six sites are presented. Then, the effect of site characteristics, LNAPL characteristics, and seasonal factors are explored for one of the six sites. Finally, insights gained from these studies are presented.

3.3 Methods

The following sections describe methods used to estimate natural LNAPL loss rates six field sites. CO_2 traps have been deployed at a total of 117 locations. At one site, three sampling rounds were completed over a 1-year period. First, the field sites are described. Second, field methods for CO_2 Trap surveys are presented. Finally, procedures for analyzing CO_2 Trap data and calculating natural LNAPL loss rates from measured CO_2 fluxes are discussed. Field data were acquired through collaborative efforts between Colorado State University and parties identified in the acknowledgements section of this article.

3.3.1 Field Sites

Field surveys were performed at a total of six sites labeled A to F. Maps showing approximate LNAPL extent, CO_2 Trap survey locations, surface water bodies, and generalized groundwater flow directions are presented on Figure 3.2. LNAPL encountered at the six sites ranges from light end hydrocarbons including gasoline and diesel to heavy end hydrocarbons including fuel oils and lubricants. The extent of LNAPL at sites A, C, D, and E were estimated based on soil core and monitoring well data. Direct push Laser-Induced Fluorescence (LIF) data were used to refine the extent of LNAPL at sites A and D. The extent of LNAPL at sites B and F were estimated based solely on limited monitoring well data. This yields a more generalized (blob shape) characterization of LNAPL bodies. Depths to water and LNAPL at the sites range from 1.5 to 7.6 meters (m) below ground surface (bgs). The groundwater flow

directions shown on Figure 3.2 are based on historical groundwater gauging data. No efforts were made to resolve temporal variation in groundwater flow directions.

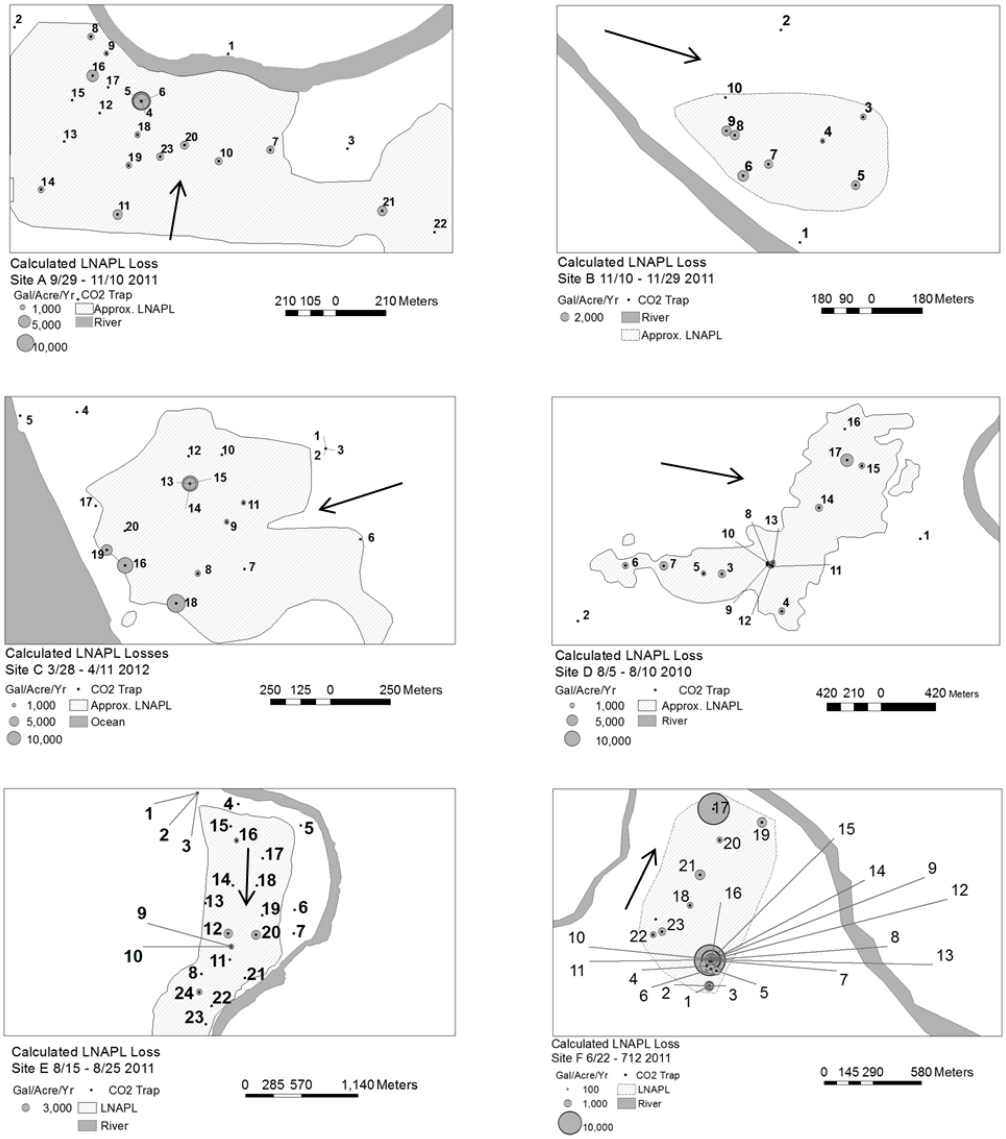

Figure 3.2. Maps of field sites with estimated rates of natural losses of LNAPL. Numbers correspond to the CO_2 Trap "Location" in Table 3.1. Sizes of gray circles for Sites A-E are proportional to background subtracted LNAPL loss (gal/acre/yr). No background locations were available for Site F. Sizes of gray circles for Site F represent uncorrected equivalent losses of LNAPL. Locations without gray circles did not significantly exceed background CO_2 flux. The cross hatched areas show approximate extent of LNAPL bodies. Arrows show general groundwater flow direction.

In general, LNAPL impacted media at each site occur in fluvial sand aquifers. At most of the sites, relatively fine sediments consisting of clay, silt, and fine sand (overbank deposits) are present in the vadose zone. Where present, overbank deposits may affect gas transport processes and therefore affect surface measurements of gas flux. The potential impact of fine grained overbank deposits is complicated by the effect of soil moisture content on gas transport. Wherever possible, CO_2 Traps were placed adjacent to pre-existing monitoring wells and/or soil boring locations to facilitate analysis of the effects of local hydrogeologic conditions on measured CO_2 fluxes.

Characterizing vadose zone conditions and site specific attributes for all six field sites is beyond the scope of this study. However, a detailed review of soil boring logs and direct push cone penetrometer test (CPT) logs was performed at Site A. CO_2 Trap survey locations were selected to estimate natural LNAPL loss rates over a variety of field conditions. Field conditions considered include: LNAPL type, smear zone depth, smear zone thickness, in-well LNAPL thickness, and groundwater temperature. Clusters of CO_2 Traps were deployed within 1 to 3 m of each other at sites A, C, D, E, and F to evaluate local measurement variability. Three rounds of measurements were collected at Site A, and four rounds of measurements were collected at Site D to assess seasonal trends. Discussion of the effects of site characteristics and seasonal influences on natural LNAPL loss rates at Site A is provided in the Section 3.4.2.

3.3.2 CO_2 Traps

Figure 3.3 presents a schematic drawing of the CO_2 Traps. Bodies of the CO_2 Traps are constructed of 0.10-m internal diameter Schedule 40 polyvinyl chloride (PVC) pipe fitted with rubber O-rings to create air-tight seals between CO_2 Trap components. Each trap features two passive sorption elements (bottom and top, Figure 3.3). The sorbent media is a commercially available soda-lime material (Sodasorb® HP-6/12, W.R. Grace, Co., a mixture of calcium and sodium hydroxides). CO_2 is first captured as carbonic acid in a thin film at the sorbent surface. A neutralization reaction follows, resulting in the formation of carbonate solids ($CaCO_3$ and Na_2CO_3) in the sorbent media.

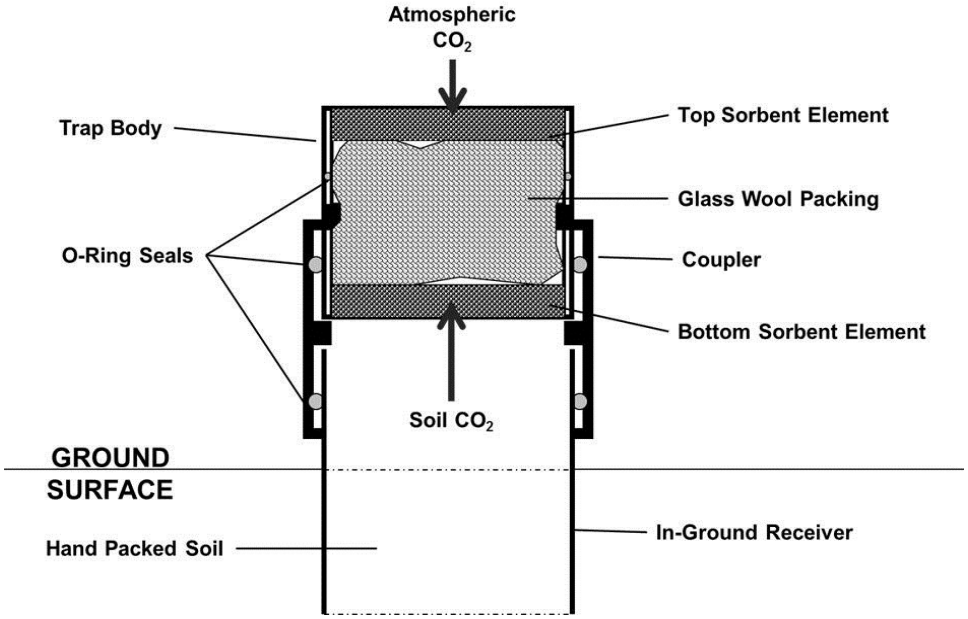

Figure 3.3. Schematic drawing of a CO_2 Trap. Each sorbent element consists of granular sorbent media sandwiched between two stainless steel screens packed into PVC grates; glass wool packing reduces dead space between trap elements and provides support to the screens. Trap elements are fit into a PVC cylinder (trap body) and connected to 4-inch diameter in-ground receivers using a PVC coupler. Components are sealed together with rubber O-rings. The bottom sorbent element captures CO_2 efflux from the soil; the top sorbent element intercepts atmospheric CO_2.

As a modification of the Flux Chamber method, measurement of CO_2 efflux using soda-lime has been studied in the agriculture and forestry fields over more than three decades (Edwards, 1982; Pongracic et al., 1997; Keith and Wong, 2006). Zimbron et al., 2011, add the novel elements of unrestricted advective flow-through, and top and bottom trap elements. The bottom element captures CO_2 released from the soil surface while the top of the trap unit is open to the atmosphere. The novel open-top design addresses interferences due to concentration and/or pressure build up effects in sealed chambers that were identified by Dane et al., 2002. An upper trap element captures CO_2 driven into the trap, either due to diffusion or during periods when atmospheric pressure is greater than local soil gas pressure (Zimbron et al., 2011). The traps contain sufficient adsorbent to allow deployment for periods of two to four weeks. Extended deployment provides an integral time-averaged value. This overcomes the limitations of collecting instantaneous flux values in transient systems.

Field deployment of CO_2 Traps initially involves placement of an in-ground receiver consisting of 0.31 m of a 0.10 m internal diameter PVC pipe. The receiver pipe is installed to approximately 0.2 m below grade. The hollow center is re-packed with site soil to mimic natural soil conditions. Receivers are installed at least one day prior to deployment of the CO_2 Traps. This allows the soil to recover from installation disturbance. A PVC cap with an approximately 0.03 m hole drilled in the center is placed on top of the CO_2 Traps during deployment. This feature allows free advective air flow through the CO_2 Trap, while providing an approximately 94% reduction in cross-sectional area for diffusive flux of atmospheric CO_2 to the top trap. Reducing diffusive

flux to the top trap is important to ensure that that top sorbent element does not saturate and allow cross contamination of the lower element with atmospheric CO_2. Vented protective PVC covers are placed over the CO_2 Traps during deployment for protection from weather and for increased visibility.

3.3.3 CO_2 Trap Laboratory Analytical Methods

CO_2 Traps are typically deployed for a period of 10 – 20 days. Upon completion of a field deployment period, CO_2 Traps are returned to the lab and disassembled to recover the sorbent media. Prior to analysis, the sampled media is vacuum dried in a room temperature desiccator and homogenized. Total carbonate content of homogenized portions of dried samples is determined by gravimetric analysis (Bauer et al., 1972). This involves acidification of the sample in a system open to the atmosphere and measurement of weight loss. Samples are analyzed in triplicate. The final result is the average of replicate measurements reported as CO_2 content as a percent of sorbent mass (CO_2/sorbent). Typical variations in triplicate analyses are on the order of ± 10 – 15%. Generally, the variation in replicate analyses decreases as the concentration of sorbed CO_2 increases. The bottom trap elements are used to calculate soil CO_2 fluxes. The top trap elements are analyzed as a quality control measure to evaluate the potential for cross-contamination of the bottom traps by atmospheric CO_2. CO_2 fluxes are generally not calculated for these elements. Trip blank samples are analyzed with each round of field samples, to correct for CO_2 present in the sorbent media prior to deployment and sorbed during sample handling.

CO_2 fluxes are calculated by dividing the sorbed CO_2 mass by the constant cross-sectional area of the trap (8.1×10^{-3} m^2) and the known period that the trap was deployed. Total CO_2 fluxes (J_{CO2_Total}) are reported in units of micromoles per square meter per second ($\mu mol/m^2/sec$). This is consistent with soil science literature. Conversion of measured CO_2 fluxes to estimated natural LNAPL loss rates is discussed in Section 3.3.6.

3.3.4 Groundwater Temperature Measurement

For decades, it has been recognized that temperature can influence rates of petroleum biodegradation (Atlas, 1975; Dibble and Bartha, 1979; Zhou and Crawford, 1995; Zeman, 2012). With this in mind, measuring site temperature at wells collocated with CO_2 Traps became a key aspect of the CO_2 Trap field studies. Thermal monitoring methods evolved over the course of several rounds of field sampling. The following presents methods employed over the course of this study.

Initially, single well temperature measurements were collected at a site using a pair of HOBO Pendant® loggers (Onset Computer Corporation, Cape Cod, Massachusetts) sealed in glass bottles to protect the loggers from contact with LNAPL. The purpose was to monitor seasonal changes in site ground water temperature. The loggers were suspended by steel fishing wire from a 0.1 m long PVC float to measure temperature near the oil-water interface. An upper logger was attached directly to the bottom of the float. A lower logger was suspended approximately 0.2 m beneath the upper logger.

Over the course of several seasonal deployments, it became clear that collecting single well temperature data was insufficient. A new method of rapidly measuring in-well groundwater temperature through the smear zone was developed. Temperature profiles were measured during simultaneously with well gauging using an approximately 9 m long Teflon® coated Type K thermocouple wire. The sensing end of the thermocouple wire was spot welded and sealed in a glass tip using epoxy resin. For field measurements, the tip of the thermocouple wire was attached to the end of an oil-water interface probe using cable ties. The thermocouple wire was attached to an electronic thermometer with a precision of 0.1 °C. The thermocouple system was tested in the laboratory using several water baths and an alcohol filled glass thermometer. In the field, the thermocouple/interface probe setup was lowered into the monitoring wells until a fluid was encountered. Temperature readings were collected every 0.152 m beginning at the first encountered fluid in the well.

Temperature profiling yielded important insights. The time required to profile large number of wells at most of the surveyed sites made large scale repeated thermal profiling inefficient. Over several rounds of sampling, the procedure evolved to a simple screening pass with the interface probe/thermocouple system through the oil-water interface to check for the maximum encountered temperature. Due to site access issues and the evolution of thermal monitoring techniques, thermal data are only available for a subset of the sample locations at sites A, B, and C.

3.3.5 Correction for Naturally Occurring CO_2

Primary sources of CO_2 efflux at grade include natural soil respiration and degradation of petroleum hydrocarbons. Establishing the CO_2 flux contribution due to natural soil respiration is critical to accurately estimating natural losses of LNAPL. Background subtraction and carbon isotope analysis can be used to estimate the relative CO_2 contributions from LNAPL degradation and natural soil respiration (Sihota et al., 2011; Sihota and Mayer, 2012).

Background subtraction (Sihota et al., 2011), is based on the principle that total CO_2 flux (J_{CO2_Total}) at LNAPL sites is the summation of the fluxes due to petroleum degradation (J_{CO2_LNAPL}) and natural soil respiration ($J_{CO2\_Background}$):

Equation 3.1. $J_{CO2\_Total} = J_{CO2\_LNAPL} + J_{CO2\_Background}$

or

Equation 3.2 $J_{CO2\_LNAPL} = J_{CO2\_Total} - J_{CO2\_Background}$

Using this method, CO_2 efflux measurements are collected at grade over the LNAPL body (LNAPL areas) and over areas presumed to be unaffected by LNAPL (background areas). It has been shown that background subtraction can be effective at identifying regions of large natural LNAPL loss rates, and effectively estimating the loss rates (Sihota et al., 2011; Sihota and Mayer, 2012).

This method is by far the simplest avenue for generating natural loss rate estimates from measured CO_2 fluxes. However, the background subtraction method is

not appropriate at all sites. Spatial variability of background CO_2 effluxes at some sites leads to significant uncertainty in the calculated LNAPL loss values. Additionally, some sites have shown LNAPL area CO_2 effluxes of similar order of magnitude to background area CO_2 fluxes. This leads to ambiguity as to whether or not natural losses of LNAPL are occurring. The problem is that natural losses of LNAPL may be occurring at rates that are undetectable using the background subtraction method. This phenomena has been studied at a site in Bemidji Minnesota (Sihota and Mayer, 2012). Finally, selecting appropriate background sample locations at many active or recently decommissioned industrial facilities can be challenging.

The second method used to separate CO_2 contribution from soil respiration and natural losses of LNAPL is stable carbon (^{12}C and ^{13}C) and radiocarbon (^{14}C) isotope analysis (Sihota and Mayer, 2012). Carbon isotopes analyses of groundwater and soil gas have previously been used to evaluate natural attenuation at hydrocarbon and chlorinated solvent sites (Suchomel et al., 1990; Aggarwal and Hinchee, 1991; Conrad et al., 1997; Coffin et al., 2008). Carbon isotope analysis has also been used to study weathering of petroleum reservoirs (Stahl, 1980) and to differentiate anthropogenic and natural sources of atmospheric CO, CO_2 and CH_4 (Klouda and Connolly, 1995; Levin et al., 1995; Avery Jr et al., 2006).

Utilization of these isotopic methods, especially ^{14}C can yield more precise LNAPL loss rate estimates and can help identify zones where small losses of LNAPL are generating CO_2 fluxes near background levels. The cost of ^{14}C analysis places

practical limits on the number of samples that can be analyzed. The technique for applying isotopic analysis to CO_2 Traps was developed late in field studies described herein.

One LNAPL sample and 2 background samples from one round at Site A were analyzed for ^{14}C and $\delta^{13}C$. The sample was from the core of the LNAPL body and had the largest measured CO_2 flux for that sample round. Calculated LNAPL loss rates using a radiocarbon correction agreed well with those calculated using the background subtraction method for that sample. Similar results have been reported by others (Sihota and Mayer, 2012), suggesting that the background subtraction method is adequate for calculating LNAPL loss rates where biodegradation related CO_2 fluxes are large relative to natural soil respiration. Because of cost involved and timing of the method development for isotopic analysis of CO_2 Traps, all samples discussed in this paper were analyzed using the background correction method.

3.3.6 Natural LNAPL Loss Rate Calculations

Stoichiometric production of CO_2 from LNAPL (based on J_{CO2_LNAPL}) can be transformed into a volumetric LNAPL loss (gallons/acre/yr) based on the density and molecular weight of the LNAPL. Estimates of natural losses of LNAPL reported in this paper are based on benzene (C_6H_6) as the characteristic stoichiometric composition of LNAPL, and an assumed LNAPL density of 0.8 g/ml. These assumptions result in a conversion factor of 550 (gal/acre/year) per 1 ($\mu mol/m^2/sec$).

Data analysis and reporting for these field studies was based on multi-step process. First, the raw CO_2 laboratory data (g CO_2 / g sorbent) for each sample were compared to the theoretical sorption capacity (30% by weight). Since it is not possible to determine when a trap element saturated in the field, samples that exceed sorption capacity provide a minimum value for CO_2 flux for that location (i.e. actual flux value is greater than or equal to measured flux). Secondly, replicates of each sample were compared to replicates of the travel blank using the 95% confidence interval (95% CI) from a two sample T-test on the difference of means. Samples whose 95% CI on the difference from the travel blank included a value less than or equal to 0 were identified as a non-detect and the data were not analyzed further.

Finally, replicates of each LNAPL area sample (except non-detects) were compared to replicates of all site background samples using the 95% CI from a two sample T-test. Samples whose 95% CI of the difference from average background included values less than or equal to 0 were identified as not significantly greater than background. A value of ns was reported for these locations. The mean difference in CO_2 flux and the 95% confidence limits of CO_2 flux were converted to units of (gal/acre/yr) and reported as the natural LNAPL loss rate. LNAPL loss rate results were rounded to 2 significant figures.

3.4 Results

3.4.1 CO_2 Fluxes and Natural Losses of LNAPL at Six Sites

Results of a single round of sampling at 117 CO_2 Trap locations at the six field sites are shown on Table 3.1. These values correspond to the size of the gray circles shown on Figure 3.2. CO_2 fluxes are reported as the average and standard deviation of replicate laboratory analytical analyses. LNAPL loss rates were calculated using the background correction method as described above. No background location could be established for Site F. Additionally, the sampling at Site F was performed before the carbon isotope adjustment technique was developed for the CO_2 Traps. The calculated LNAPL loss rates from Site F (23 samples) are presented on Table 3.1 with a dagger symbol to identify them as uncorrected. These samples will not be analyzed or discussed further in this paper.

Sample results reported in Table 3.1 are summarized as follows. There were 19 background samples across 5 sites. Background CO_2 fluxes ranged from 0.7 to 9.0 $\mu mol/m^2/sec$, with a mean of 3.6 $\mu mol/m^2/sec$. LNAPL area CO_2 fluxes at 75 LNAPL sample locations (not including Site F) ranged from 0.7 to 36 $\mu mol/m^2/sec$ with a mean of 7.0 $\mu mol/m^2/sec$. Twenty eight LNAPL samples did not significantly exceed background CO_2 fluxes. CO_2 fluxes of the reduced set which exceed local background values ranged from 3.3 to 36 $\mu mol/m^2/sec$ with a mean of 9.5 $\mu mol/m^2/sec$. Calculated background subtracted LNAPL loss rates for the 47 LNAPL area samples range from 660 – 18,000 gal/acre/yr with a mean of 3,800 gal/acre/yr.

Table 3.1. CO_2 Trap Results for Six Field Sites.

Site	Location	Class	Deployed	Recovered	CO_2 flux ($\mu mol/m^2/sec$)		Loss Rate (gal/acre/yr)		GW Temp (° C)	Comments
					Avg	Stdev	Avg	95% CI		
A	1	BG	9/30/11	11/10/11	1.7	0.3	- -	- -	16.8	
A	2	BG	9/29/11	11/10/11	3.6	0.9	- -	- -	16.2	
A	3	BG	9/29/11	11/10/11	1.9	0.5	- -	- -	- -	
A	4	LNAPL	9/30/11	11/10/11	17	1.1	**8,100**	**6,900 - 9,300**	20.3	Triplicate Location
A	5	LNAPL	9/30/11	11/10/11	24	0.1	**12,000**	**11,000 - 12,000**	20.3	Triplicate Location
A	6	LNAPL	9/30/11	11/10/11	22	0.3	**11,000**	**10,000 - 11,000**	20.3	Triplicate Location
A	7	LNAPL	9/29/11	11/10/11	6.4	0.4	**2,200**	**1,700 - 2,700**	17.6	LNAPL to total depth
A	8	LNAPL	9/29/11	11/10/11	5.0	0.5	**1,400**	**880 - 2,000**	18.6	
A	9	LNAPL	9/29/11	11/10/11	3.9	0.1	**800**	**350 - 1,300**	16.8	
A	10	LNAPL	9/29/11	11/10/11	5.8	0.4	**1,900**	**1,300 - 2,400**	16.5	
A	11	LNAPL	9/29/11	11/10/11	8.3	0.1	**3,200**	**2,800 - 3,700**	14.9	
A	12	LNAPL	9/29/11	11/10/11	1.6	0.2	ns	ns	15.7	
A	13	LNAPL	9/29/11	11/10/11	1.1	0.2	ns	ns	16.4	
A	14	LNAPL	9/29/11	11/10/11	5.1	0.4	**1,500**	**950 - 2,100**	14.8	
A	15	LNAPL	9/29/11	11/10/11	1.5	0.4	ns	ns	16.5	
A	16	LNAPL	9/29/11	11/10/11	11	0.4	**4,700**	**4,200 - 5,200**	20.0	
A	17	LNAPL	9/29/11	11/10/11	1.5	0.1	ns	ns	17.9	
A	18	LNAPL	9/29/11	11/10/11	4.6	0.2	**1,200**	**730 - 1,700**	16.6	
A	19	LNAPL	9/29/11	11/10/11	4.8	0.6	**1,300**	**610 - 2,000**	15.6	
A	20	LNAPL	9/29/11	11/10/11	6.6	0.3	**2,300**	**1,800 - 2,800**	17.7	
A	21	LNAPL	9/29/11	11/10/11	8.4	0.1	**3,300**	**2,800 - 3,700**	13.6	
A	22	LNAPL	9/29/11	11/10/11	2.1	0.1	ns	ns	- -	
A	23	LNAPL	9/29/11	11/10/11	5.8	0.2	**1,900**	**1,400 - 2,300**	17.6	
B	1	BG	11/10/11	11/29/11	2.4	1.0	- -	- -	18.1	
B	2	BG	11/10/11	11/29/11	1.9	0.5	- -	- -	17.6	
B	3	LNAPL	11/10/11	11/29/11	4.2	0.8	**1,100**	**150 - 2,100**	20.9	
B	4	LNAPL	11/10/11	11/29/11	3.4	0.5	**660**	**120 - 1,200**	20.8	
B	5	LNAPL	11/10/11	11/29/11	6.2	1.0	**2,200**	**1,100 - 3,400**	21.7	
B	6	LNAPL	11/10/11	11/29/11	8.5	1.3	**3,500**	**1,600 - 5,400**	17.6	
B	7	LNAPL	11/10/11	11/29/11	5.8	0.9	**2,000**	**940 - 3,100**	20.3	
B	8	LNAPL	11/10/11	11/29/11	6.8	0.9	**2,500**	**1,500 - 3,600**	20.8	
B	9	LNAPL	11/10/11	11/29/11	7.2	0.1	**2,800**	**2,400 - 3,200**	20.6	
B	10	LNAPL	11/10/11	11/29/11	0.69	0.4	ns	ns	- -	
C	1	BG	3/28/12	4/11/12	2.2	0.1	- -	- -	25.9	Triplicate 1
C	2	BG	3/28/12	4/11/12	3.4	0.4	- -	- -	25.9	Triplicate 1
C	3	BG	3/28/12	4/11/12	3.4	0.1	- -	- -	25.9	Triplicate 1
C	4	BG	3/28/12	4/11/12	5.6	0.4	- -	- -	26.9	
C	5	BG	3/28/12	4/11/12	1.6	0.1	- -	- -	- -	
C	6	LNAPL	3/28/12	4/11/12	2.1	0.4	ns	ns	28.3	
C	7	LNAPL	3/28/12	4/11/12	2.3	0.1	ns	ns	25.7	
C	8	LNAPL	3/28/12	4/11/12	6.9	0.7	**2,000**	**1,300 - 2,700**	- -	
C	9	LNAPL	3/28/12	4/11/12	5.8	0.6	**1,300**	**630 - 2,000**	- -	
C	10	LNAPL	3/28/12	4/11/12	3.5	0.3	ns	ns	- -	
C	11	LNAPL	3/28/12	4/11/12	5.9	0.2	**1,400**	**940 - 1,900**	- -	
C	12	LNAPL	3/28/12	4/11/12	2.4	0.5	ns	ns	- -	
C	13	LNAPL	3/28/12	4/11/12	6.6	0.9	**1,800**	**820 - 2,800**	27.0	Triplicate 2
C	14	LNAPL	3/28/12	4/11/12	30	2.1	**14,000**	**11,000 - 17,000**	27.0	Triplicate 2
C	15	LNAPL	3/28/12	4/11/12	21	1.1	**9,500**	**8,200 - 11,000**	27.0	Triplicate 2
C	16	LNAPL	3/28/12	4/11/12	29	1.1	**14,000**	**13,000 - 16,000**	28.9	
C	17	LNAPL	3/28/12	4/11/12	1.9	0.5	ns	ns	26.6	
C	18	LNAPL	3/28/12	4/11/12	36	0.4	**18,000**	**17,000 - 18,000**	- -	
C	19	LNAPL	3/28/12	4/11/12	16	0.7	**7,200**	**6,400 - 7,900**	26.9	
C	20	LNAPL	3/28/12	4/11/12	3.8	0.3	ns	ns	- -	
D	1	BG	8/5/10	8/10/10	1.4	0.9	- -	- -	- -	
D	2	BG	8/5/10	8/10/10	6.5	0.5	- -	- -	- -	Not used for BG correction
D	3	LNAPL	8/5/10	8/10/10	6.2	0.3	**2,600**	**1,800 - 3,400**	- -	
D	4	LNAPL	8/5/10	9/20/10	5.0	0.2	**1,900**	**1,100 - 2,700**	- -	
D	5	LNAPL	8/5/10	8/10/10	3.5	0.6	**1,200**	**370 - 1,900**	- -	
D	6	LNAPL	8/5/10	8/10/10	4.7	0.3	**1,800**	**950 - 2,600**	- -	
D	7	LNAPL	8/5/10	8/10/10	7.4	0.5	**3,300**	**2,500 - 4,000**	- -	
D	8	LNAPL	8/5/10	8/10/10	3.3	0.5	**1,000**	**190 - 1,800**	- -	Transect Area
D	9	LNAPL	8/5/10	8/10/10	1.9	0.6	ns	ns	- -	Transect Area
D	10	LNAPL	8/5/10	8/10/10	1.2	0.6	ns	ns	- -	Transect Area
D	11	LNAPL	8/5/10	8/10/10	2.1	0.8	ns	ns	- -	Transect Area
D	12	LNAPL	8/5/10	8/10/10	5.2	1.2	**2,100**	**1,100 - 3,000**	- -	Transect Area
D	13	LNAPL	8/5/10	8/10/10	3.6	1.0	**1,200**	**330 - 2,000**	- -	Transect Area
D	14	LNAPL	8/5/10	8/10/10	5.7	0.6	**2,300**	**1,600 - 3,100**	- -	
D	15	LNAPL	8/5/10	8/10/10	4.7	0.3	**1,700**	**920 - 2,400**	- -	
D	16	LNAPL	8/5/10	8/10/10	2.3	0.2	ns	ns	- -	
D	17	LNAPL	8/5/10	8/10/10	14	0.8	**6,900**	**6,000 - 7,700**	- -	
E	1	BG	8/15/11	8/25/11	4.4	1.0	- -	- -	- -	Triplicate 1
E	2	BG	8/15/11	8/25/11	2.1	1.6	- -	- -	- -	Triplicate 1
E	3	BG	8/15/11	8/25/11	4.6	1.0	- -	- -	- -	Triplicate 1
E	4	BG	8/15/11	8/25/11	9.0	1.8	- -	- -	- -	
E	5	BG	8/15/11	8/25/11	0.74	0.6	- -	- -	- -	
E	6	BG	8/15/11	8/25/11	3.6	0.5	- -	- -	- -	
E	7	BG	8/15/11	8/25/11	8.3	0.6	- -	- -	- -	
E	8	LNAPL	8/16/11	8/25/11	5.2	2.2	ns	ns	- -	
E	9	LNAPL	8/18/11	8/25/11	7.1	2.9	ns	ns	- -	Duplicate 1
E	10	LNAPL	8/18/11	8/25/11	7.2	0.8	**1,400**	**590 - 2,200**	- -	Duplicate 1
E	11	LNAPL	8/15/11	8/25/11	2.0	1.0	ns	ns	- -	
E	12	LNAPL	8/15/11	8/25/11	12	4.3	**4,000**	**130 - 7,900**	- -	

Site	Location	Class	Deployed	Recovered	CO_2 flux ($\mu mol/m^2/sec$)		Loss Rate (gal/acre/yr)		GW Temp (° C)	Comments
					Avg	Stdev	Avg	95% CI		
E	13	LNAPL	8/15/11	8/25/11	4.4	0.4	ns	ns	- -	
E	14	LNAPL	8/15/11	8/25/11	5.0	1.3	ns	ns	- -	
E	15	LNAPL	8/15/11	8/25/11	3.5	1.3	ns	ns	- -	
E	16	LNAPL	8/15/11	8/25/11	6.8	0.5	**1,100**	**430 - 1,900**	- -	
E	17	LNAPL	8/15/11	8/25/11	4.6	0.5	ns	ns	- -	
E	18	LNAPL	8/15/11	8/25/11	5.5	1.8	ns	ns	- -	
E	19	LNAPL	8/15/11	8/25/11	4.2	0.7	ns	ns	- -	
E	20	LNAPL	8/15/11	8/25/11	12.0	1.1	**4,000**	**3,100 - 5,000**	- -	
E	21	LNAPL	8/16/11	8/25/11	1.3	0.7	ns	ns	- -	
E	22	LNAPL	8/16/11	8/25/11	4.8	0.6	ns	ns	- -	
E	23	LNAPL	8/16/11	8/25/11	2.7	0.6	ns	ns	- -	
E	24	LNAPL	8/16/11	8/25/11	8.2	1.4	**2,000**	**750 - 3,100**	- -	
F	1	LNAPL	6/22/11	7/12/11	2.3	0.1	**1,300†**	- -	- -	Triplicate Location
F	2	LNAPL	6/22/11	7/12/11	3.4	0.1	**1,800†**	- -	- -	Triplicate Location
F	3	LNAPL	6/22/11	7/12/11	1.4	0.1	**790†**	- -	- -	Triplicate Location
F	4	LNAPL	6/22/11	7/12/11	6.4	0.2	**3,500†**	- -		
F	5	LNAPL	6/22/11	7/12/11	2.4	0.4	**1,300†**	- -	- -	
F	6	LNAPL	6/22/11	7/12/11	3.5	0.1	**1,900†**	- -	14.1	
F	7	LNAPL	6/22/11	7/12/11	33	1.4	**18,000†**	- -	- -	
F	8	LNAPL	6/22/11	7/12/11	11	0.1	**5,800†**	- -	- -	High Resolution Area
F	9	LNAPL	6/22/11	7/12/11	0.92	0.1	**500†**	- -	- -	High Resolution Area
F	10	LNAPL	6/22/11	7/12/11	0.82	0.1	**450†**	- -	- -	High Resolution Area
F	11	LNAPL	6/22/11	7/12/11	1.4	0.2	**760†**	- -	- -	High Resolution Area
F	12	LNAPL	6/22/11	7/12/11	1.4	0.0	**780†**	- -	- -	High Resolution Area
F	13	LNAPL	6/22/11	7/12/11	3.2	0.2	**1,700†**	- -	- -	High Resolution Area
F	14	LNAPL	6/22/11	7/12/11	12	0.2	**6,600†**	- -	- -	High Resolution Area
F	15	LNAPL	6/22/11	7/12/11	5.7	0.2	**3,200†**	- -	- -	High Resolution Area
F	16	LNAPL	6/22/11	7/12/11	13	0.3	**7,400†**	- -	- -	High Resolution Area
F	17	LNAPL	6/22/11	7/12/11	34	1.3	**19,000†**	- -	- -	
F	18	LNAPL	6/22/11	7/12/11	1.3	0.2	**690†**	- -	- -	
F	19	LNAPL	6/22/11	7/12/11	3.3	0.7	**1,800†**	- -	- -	
F	20	LNAPL	6/22/11	7/12/11	1.3	0.3	**710†**	- -	- -	
F	21	LNAPL	6/22/11	7/12/11	3.6	0.4	**2,000†**	- -	- -	
F	22	LNAPL	6/22/11	7/12/11	1.3	0.5	**700†**	- -	- -	
F	23	LNAPL	6/22/11	7/12/11	2.3	0.4	**1,200†**	- -	- -	

Notes:
† - No background location available and ^{14}C analysis not performed. Loss rates have not been corrected for natural CO_2 flux.
- - No data.
Avg - Average (mean) of replicate CO_2 trap laboratory analyses.
BG - Background CO_2 Trap location.
Calc - Calculated LNAPL loss rate based on background CO_2 flux subtraction method.
gal/acre/yr - Gallons LNAPL per acre per year.
LNAPL- LNAPL loss rate measurement CO_2 Trap location.
$\mu mol/m^2/sec$ - 10^{-6} moles CO_2 per square meter per second.
ns - CO_2 flux not significantly greater than background based on 95% confidence interval. No LNAPL loss calculated.
Stdev - Standard deviation of replicate CO_2 trap laboratory analyses.
95% CI - 95% Confidence interval of the calculated LNAPL loss rate. Calculated as described in the text.

Natural losses for all rounds of sampling are summarized on Figure 3.4. The figure shows box and whisker plots of all samples that exceeded background CO_2 fluxes for Sites A-E and non-corrected equivalent natural loss rates for Site F. The data include 3 rounds of sampling at Site A and 4 rounds of sampling at Site D. Background subtracted loss rates for Sites A-E range from 400 – 18,000 gal/acre/yr with an average of 3,500 gal/acre/yr. Loss rates at Sites A, B, D, and E show similarity across a range of hydrogeologic and LNAPL conditions. Loss rates at Site C (located in Hawaii) show a notably larger average loss rate, and a greater range of losses compared to the other sites.

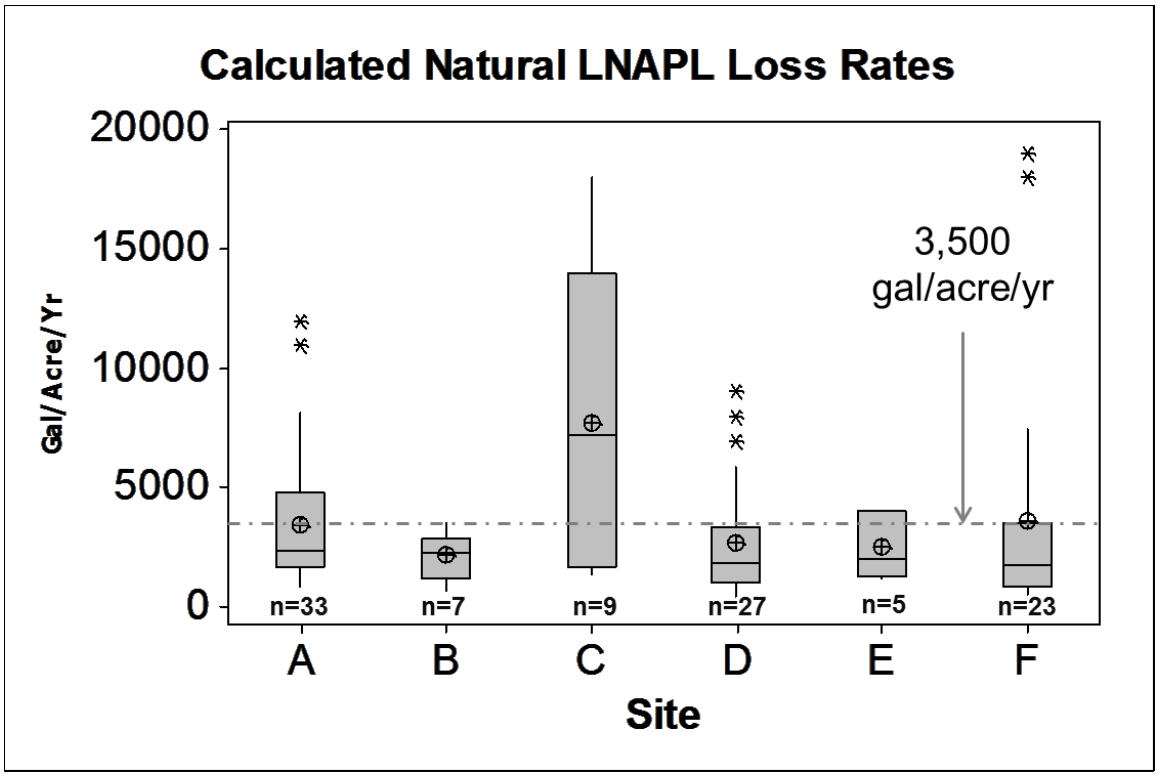

Figure 3.4. LNAPL loss rates (gal/acre/yr) for 6 field sites. Reported loss rates for Sites A-E are background subtracted. Reported loss rates for Site F have not been corrected for naturally occurring CO_2. Boxes and whiskers show interquartile range. Horizontal lines within boxes show median value. Cross hairs show mean value. Asterisks show outliers. "n" values represent total number of samples considered. The dashed line represents the average natural LNAPL loss rate for all samples. Data include 3 rounds from Site A and 4 rounds from Site D.

3.4.2 Detailed Analysis of Site A

The following sections provide an analysis of observed trends for three rounds of CO_2 flux data collected at Site A between May 17, 2011 and May 4, 2012. First, background corrected LNAPL loss rates are compared to in-well LNAPL thickness, smear zone thickness, depth to smear zone, maximum in-well groundwater temperature, and LNAPL type. Next seasonal trends for 3 rounds of sampling are presented. Finally, a comparison of spatial temperature trends between two seasons is presented.

3.4.2.1 Comparison of Site Characteristics

Background subtracted LNAPL loss rates for each of the three sampling events were compared to selected site characteristics. Only samples that significantly exceeded background values were considered. Results are shown on Figure 3.5. In-well LNAPL thickness and groundwater temperature data were collected as described in the methods section. Depth to smear zone and smear zone thickness data were collected from cone penetrometer test (CPT) and LIF logs. LNAPL type description was provided by the site environmental consultant and reflects their classification system. The charts show background subtracted LNAPL loss rates. The data points on the first 4 charts show individual sample results. The vertical error bars on these charts show the 95% confidence interval on the difference of CO_2 flux from background. The magnitude of the bars on the 5th chart (LNAPL type) shows mean LNAPL loss rate for each LNAPL type with the vertical error bars showing standard deviation.

Figure 3.5 indicates that LNAPL loss rates are largely independent of smear zone thickness, depth to smear zone, and LNAPL type. No relationship is apparent between in-well LNAPL thickness and calculated loss rate either. At first glance, there doesn't appear to be a correlation between maximum in-well groundwater temperature and calculated loss rate. However, it should be noted that there is a significant increase in the calculated loss rate at approximately 20°C. This is noteworthy because previous studies suggest that biodegradation of petroleum compounds should increase around 20°C (Atlas, 1975; Dibble and Bartha, 1979; Zhou and Crawford, 1995; Zeman, 2012). Temperature vs. LNAPL loss trends are discussed further in the next two sections.

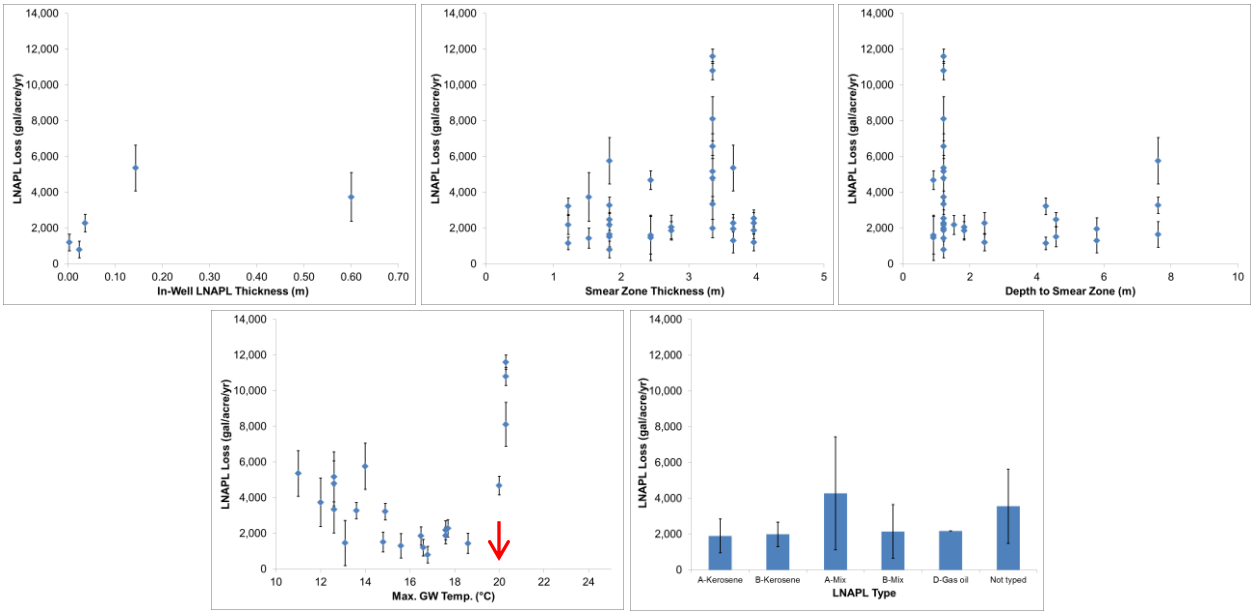

Figure 3.5. Comparison of background subtracted LNAPL loss rates to selected site characteristics. Only samples that exceeded background were used in the comparison. From top left, In-well LNAPL thickness (m), smear zone thickness (m), depth to smear zone (m), maximum in-well groundwater temperature (°C), LNAPL Type. The red arrow on the temperature chart shows the 20 °C line, above which biological activity is expected to increase significantly. Error bars on the first 4 charts are 95% confidence interval of calculated loss rate. Error bars on the last chart are standard deviation of average LNAPL loss for each LNAPL type.

3.4.2.2 Seasonal Trends

Figure 3.6 shows results of 3 rounds of sampling performed at Site A between May 17, 2011 and May 4, 2012. When the seasonal data were plotted, several apparent seasonal trend groupings emerged. These are shown on Figure 3.6 as Group I through Group IV. Group I consists of LNAPL locations where samples exceeded background CO_2 flux values during each of the seasonal sampling events. Group II and Group III are composed of sampling locations that only exceeded background CO_2 flux values during certain sampling events. These two categories have been further divided into samples that show an apparent upward trend over the three sampling rounds (Group II) and samples that show little to no change over the three sampling rounds

(Group III). Group IV represents samples that did not exceed background CO_2 flux values during any sampling event.

Results are plotted on Figure 3.6 as raw CO_2 flux on the primary vertical axis vs. date. The gray lines show average and standard deviation of background CO_2 fluxes for each sampling event. The secondary y axis shows equivalent LNAPL loss rate. These values have not been background subtracted. Sample locations 4, 5, and 6 are located approximately 2 m from each other in a triangular pattern. Comparing the measured CO_2 fluxes of these three locations also provides insight into local variability of the measured CO_2 fluxes. The large standard deviation of the background samples in May 2012 illustrates variability in background readings. This highlights a primary source of uncertainty in LNAPL loss rates calculated using the background subtraction method.

As can be seen on Figure 3.6, Group I generally contains the largest measured CO_2 fluxes. This group is likely minimally affected by the choice to use a background subtraction method for analysis. Group II and Group III consist of measured CO_2 fluxes that in some cases are not significantly different from background fluxes. It is possible that samples in this group are collecting CO_2 from natural losses of LNAPL, but at rates that are indistinguishable from background. Note: this is speculative as it is impossible to distinguish the source of the CO_2 without additional data (e.g. carbon isotope data).

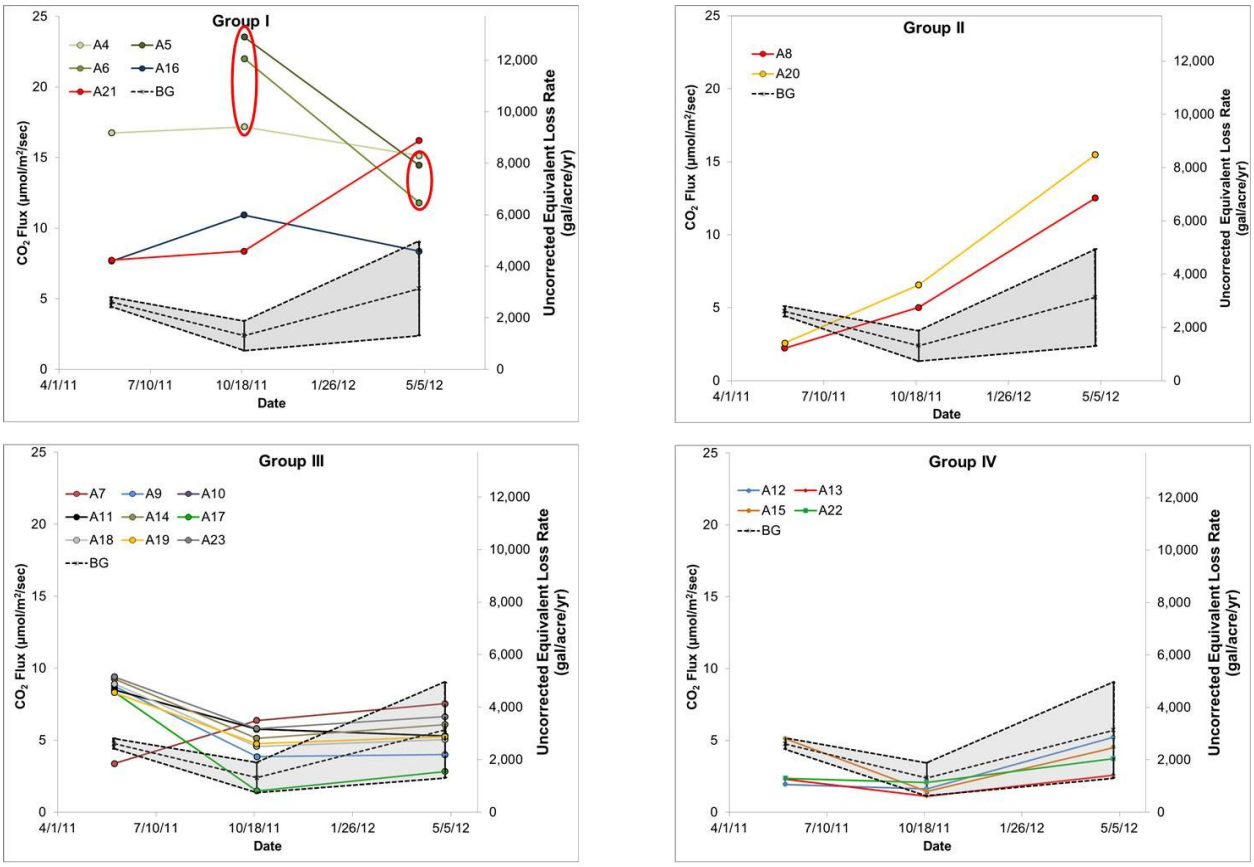

Figure 3.6. Seasonal variability of CO_2 flux at Site A. Group I exceeds background CO_2 flux in spring and fall. Group II and Group III fluxes sometimes exceed background CO_2 flux. Group II shows an apparent increasing trend. Group III shows variable trend near background CO_2 flux values. Group IV does not exceed background CO_2 flux values during any of the three sampling events. The red ovals on the Group I plot highlight the triplicate area where 3 traps are collocated in a triangular pattern with 2 m spacing.

Figure 3.7 shows the sample locations plotted by category on a site map to evaluate spatial trends. The figure suggests that the observed temporal trends also have spatial relevance. A similar pattern was observed in the spatially distributed groundwater temperature readings from two sample rounds as discussed in the next section.

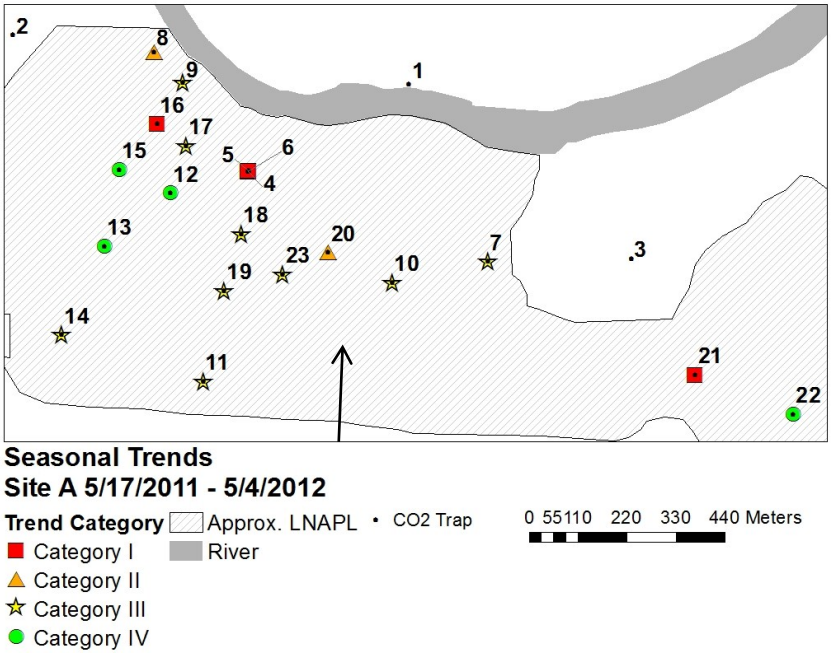

Figure 3.7. Spatial distribution of seasonal trends identified in Figure 3.6. Numbers match CO_2 Trap sampling locations in Table 3.1. The arrow shows general groundwater flow direction.

3.4.2.3 Groundwater Temperature Analysis

Figure 3.8 shows maximum in-well groundwater temperature readings from September 29, 2011, and May 3, 2012 plotted on a site map. Spatial patterns of temperature show an increase in temperature in the direction of groundwater flow, towards the core of the LNAPL body. This is appears to be the result of heat generated by biodegradation of LNAPL constituents. In September 2011, groundwater temperatures near sample locations 4, 5, and 6 were approximately 6 °C warmer than at the locations near the upgradient edge of the LNAPL body. A similar pattern of groundwater temperatures (only colder) can be seen in May 2012. The pattern of groundwater temperatures shown on Figure 3.8, are similar to the pattern of seasonal trend groupings shown on Figure 3.7.

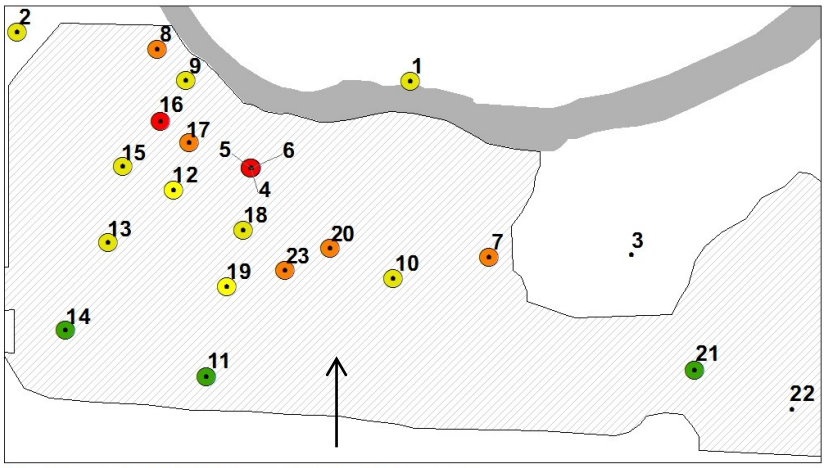

Maximum In-Well Groundwater Temperature
(Degree Celcius)
Site A 9/29/2011

210 105 0 210 Meters

13.6 - 14.9
16.9 - 18.6
• CO2 Trap
15.0 - 15.7
18.7 - 20.3
Approx. LNAPL
15.8 - 16.8
River

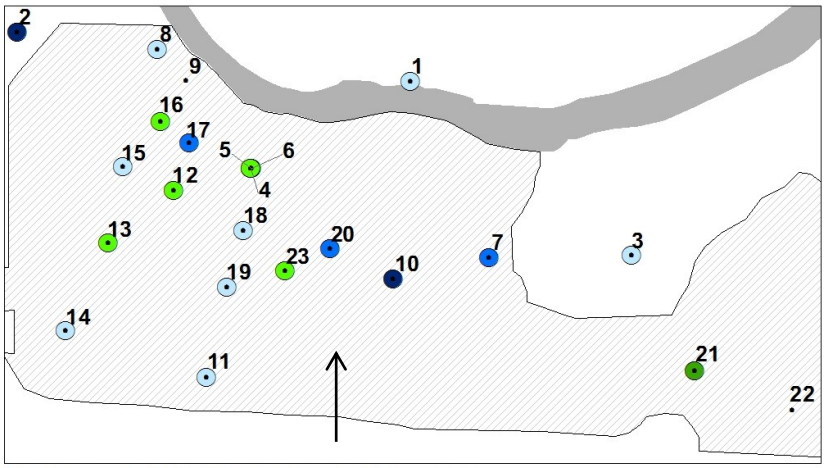

Maximum In-Well Groundwater Temperature
(Degree Celcius)
Site A 5/3/2012

210 105 0 210 Meters

9.9 - 10.0
12.4 - 13.5
• CO2 Trap
10.1 - 11.0
13.6 - 14.9
Approx. LNAPL
11.1 - 12.3
River

Figure 3.8. Spatial distribution of maximum in-well groundwater temperature. Late September 2011 (upper) and early May 2012 (lower). Numbers represent CO_2 Trap sampling locations in Table 3.1. Colored circles represent temperature as denoted on the figures. Note the coldest temperature range in September matches the warmest temperature range in May. Also note the similarity in the spatial patterns between well temperatures in September and May, as well as the similarity of these patterns with the patterns on Figure 3.7. Numbers match CO_2 Trap sampling location in Table 3.1. The arrows show general groundwater flow direction.

With this observation in mind, a reduced data set consisting of the Group I, II, and III calculated LNAPL loss rates were plotted against temperature on Figure 3.9. Values that were not significantly different from background CO_2 fluxes are plotted along the horizontal axis. It should be noted that because site-wide groundwater temperature measurements were only collected in September 2011 and May 2012, these data do not include calculated loss rates from May 2011.

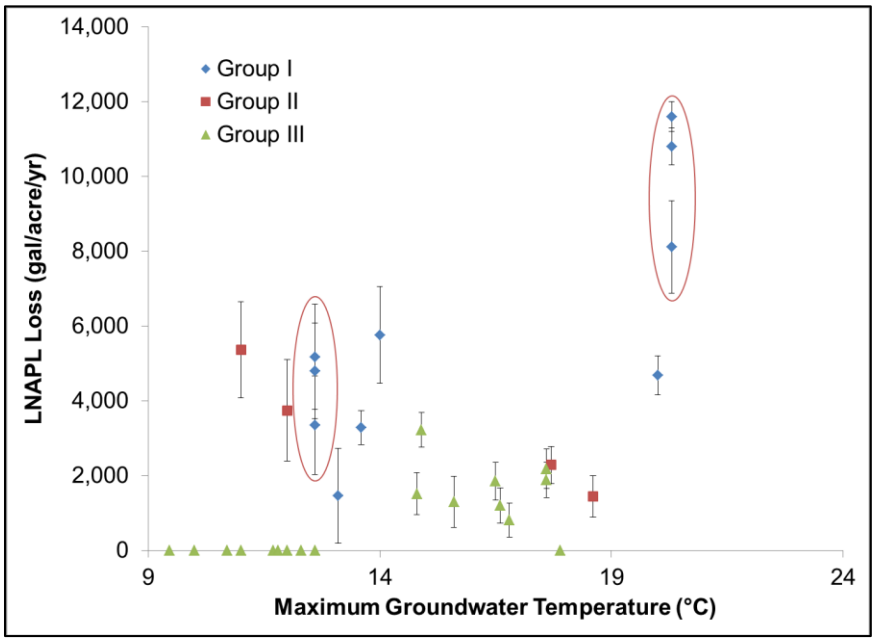

Figure 3.9. Background subtracted LNAPL loss rate vs. temperature by seasonal trend category. Vertical error bars are 95% confidence interval of background subtracted LNAPL loss rate. The red ovals highlight the triplicate locations.

While no clear relationship was apparent between temperature and loss rate when the bulk site data was plotted (Figure 3.5), the data as plotted on Figure 3.9 suggests that trends can be identified when greater care is taken in interpreting the data. Group I samples show a distinct increase in calculated LNAPL loss rate with increased groundwater temperature. Group II samples show an inverted trend. The

reason for this is not known. Most notably, Group III samples show an apparent trend of capturing significant CO_2 relative to background CO_2 flux at groundwater temperatures greater than 14°C.

These observations suggest that seasonal groundwater temperature fluctuations can help explain observed seasonal fluctuations in calculated LNAPL loss rates. This suggests that groundwater temperatures have a consequential influence on natural LNAPL loss rates. This observation forms a foundation for the hypothesis that maintaining groundwater temperature in optimal ranges (i.e. 20°C at the study site) could dramatically enhance natural losses of LNAPL.

3.5 Conclusions

CO_2 fluxes were measured at 117 locations at six LNAPL sites. Natural losses of LNAPL calculated using the background correction method ranged from 660 – 18,000 gal/acre/yr with a mean of 3,800 gal/acre/yr. An analysis of the influence of site and LNAPL characteristics was performed at one of the six sites. Results indicate that natural losses of LNAPL are largely independent of in-well LNAPL thickness, depth to smear zone, smear zone thickness, or LNAPL type. However, temperature related seasonal variations in CO_2 flux and associated natural losses of LNAPL were observed. These observations form a foundation for the hypothesis that maintaining groundwater temperature in optimal ranges could dramatically enhance natural losses of LNAPL. Additional research has been proposed to study the relationship between smear zone temperature and natural losses of LNAPL.

The studies showed that the background subtraction method can yield sufficient results at sites where a suitable background location can be found, if the rate of CO_2 generation associated with natural losses of LNAPL is significantly greater than the rate of natural soil CO_2 generation and if the variability of background CO_2 fluxes is relatively small. If background CO_2 fluxes are large (or are widely variable), or LNAPL loss rates are small, it may be difficult to distinguish CO_2 generated by LNAPL loss from naturally occurring CO_2. At some sites, background locations may not be available. When possible, isotopic data should be collected to support calculations using the background subtraction method. While further research will undoubtedly result in additional insights and revised methodologies, the results described herein support the hypothesis that CO_2 Traps are an effective tool for estimating natural losses of LNAPL.

3.6 Recognition

Funding for the field studies described herein was provided by Chevron, Suncor Energy, and Union Pacific Railroad. Field data was collected with support from CH2M HILL, AECOM, Stantec Inc., Trihydro Corporation, and URS Corporation. The authors would also like to recognize the hard work and long hours of CSU laboratory staff Gary Dick (lab technician) and undergraduate students Sonja Koldewyn, Sarah Breidt, Rebecca Bradley, Adam Byrne, Calista Campbell, and Ellen Daugherty for support during trap construction and analysis.

4 CONCLUSIONS

Subsurface LNAPL bodies are a legacy of past practices at petroleum manufacturing, distribution, and storage facilities. Because traditional LNAPL remedies are often costly and have limited effectiveness (ITRC, 2009a), developing an effective understanding of natural LNAPL loss rates is an important step in establishing LNAPL management strategies. Natural LNAPL loss rates can be used to demonstrate LNAPL stability, to form a basis for initiating or discontinuing hydraulic recovery, to estimate longevity of LNAPL bodies, and as a benchmark to compare relative effectiveness of different remedial alternatives (ITRC, 2009b). Further, an understanding of underlying processes gained through field studies can guide development of new, more sustainable, LNAPL remediation technologies.

In recent years, researchers have used various methods to study natural losses of LNAPL. These include aqueous geochemistry (Johnson et al., 2006; Lundegard and Johnson, 2006; ITRC, 2009b); soil gas profiles (Amos et al., 2005; Johnson et al., 2006; Lundegard and Johnson, 2006; ITRC, 2009b); efflux of biodegradation related soil gases (e.g. CO_2) at grade (Sihota et al., 2011); and direct measurements of LNAPL fluxes (Mahler et al., 2011; Mahler et al., 2012; Smith et al., 2012). Each of these methods has advantages and limitations. Building off work by others, a new technology (CO_2 Traps) was developed to address limitations of current methods.

The first manuscript presented in this thesis discussed CO_2 Trap design features, laboratory testing of the CO_2 Traps, and an application at a single field site. Closed

system column testing showed that the selected sorbent media is capable of quantitatively recovering CO_2. This testing also verified that the sorption capacity of the media (~30% CO_2 by mass) was in the range indicated by the manufacturer. This information is useful when planning maximum field deployment times, and as a means of quality checking field sampling results. Open system column testing showed that CO_2 Traps, as designed, are capable of quantitatively measuring CO_2 flux through the surface in open systems.

Results of a single round of CO_2 Trap deployment at a field site showed that the CO_2 Traps could distinguish zones of elevated CO_2 flux over the LNAPL body, relative to naturally occurring CO_2 flux at background locations. Background subtracted LNAPL loss rates ranging from 800 to 12,000 gal/acre/yr were calculated using CO_2 Trap data. Carbon isotope analysis was performed on one travel blank sample, two background samples, and one LNAPL area sample. Radiocarbon (^{14}C) results provided a means to account for naturally occurring CO_2 flux. Results of the ^{14}C correction agreed well with the background subtraction method for that location. The location selected for carbon isotope analysis had the largest measured CO_2 flux. This supports the understanding that background subtraction can be an effective means of calculating natural LNAPL loss rate at locations with large degradation related CO_2 fluxes. Finally, stable carbon isotope analysis performed on a CO_2 Trap sample and on samples of LNAPL collected near the CO_2 Trap location provided further evidence of the source of the CO_2. The stable carbon isotope signature of the CO_2 from over the LNAPL zone was similar to the

signature of the LNAPL and was slightly more depleted in ^{13}C, which is consistent with fractionation occurring during biodegradation.

The second manuscript presented in this thesis discussed measurement of CO_2 fluxes at 117 locations at six LNAPL sites. Natural LNAPL loss rates were calculated using the background correction method. Calculated background corrected LNAPL loss rates for ranged from 660 – 18,000 gal/acre/yr with a mean of 3,800 gal/acre/yr. A detailed analysis of the influence of site and LNAPL characteristics on calculated LNAPL loss rates was performed for one of the six sites. Results of the analysis showed no significant influence of in-well LNAPL thickness, depth to smear zone, smear zone thickness, or LNAPL type on calculated loss rates. Significant seasonal variations in CO_2 flux and calculated LNAPL loss rates were observed. Grouping sample locations by apparent seasonal trends and plotted spatially provided further insight.

Spatial distributions suggested that the site may be characterized by zones of natural loss activity. In some areas (Category I, Figures 3.6 and 3.7), rates of CO_2 production exceeded background CO_2 fluxes throughout the year, but vary seasonally in intensity with temperature. In contrast, some areas (Categories II and III, Figures 3.6 and 3.6), only produced CO_2 at rates in excess of background CO_2 fluxes during certain warm periods. Furthermore, some areas (Category IV, Figures 3.6 and 3.7) did not produce CO_2 at rates in excess of background CO_2 fluxes during any season. These observations generally agree with groundwater temperatures measured across the oil-water interface in wells adjacent to the CO_2 Trap locations. Since biological activity is

strongly influenced by groundwater temperatures (Atlas, 1975; Dibble and Bartha, 1979; Zhou and Crawford, 1995; Zeman, 2012), the relationship between measured losses and temperature is not surprising. Further exploration of the link between temperature and LNAPL loss rate should be undertaken.

An observation can be made about the LNAPL locations that did not produce CO_2 in excess of background CO_2 fluxes during any round. When plotted spatially, these locations form a cluster within the core of the LNAPL body. This cluster is located near several previous in-site remediation pilot tests. It is possible that this area represents a region where the majority of the LNAPL has attenuated. Without further investigation, this is speculative. A follow-on investigation of soil, LNAPL, and groundwater characteristics targeted to address each of the identified groupings may yield a more complete interpretation.

While further work will undoubtedly result in additional insights and revised methodologies, the results described herein support the hypothesis that CO_2 Traps are an effective tool for estimating natural losses of LNAPL. Additionally, application of CO_2 Traps at six field sites has yielded important insights that may help with development and monitoring of new innovative LNAPL remediation technologies, including thermally enhanced LNAPL attenuation. Additional discussion of future work is provided in the next section.

5 FUTURE WORK

The CO_2 Traps described in this thesis have been developed as a tool to support monitoring of natural LNAPL loss rates. Data collected at 6 LNAPL field sites indicates that natural LNAPL loss rates are large (100s – 10,000s gal/acre/yr). More importantly, through these applications, insights into local variability and site conditions affecting LNAPL loss rates were gained. These insights may support development of new sustainable LNAPL mitigation strategies. CO_2 Traps will be one tool used to monitor the effectiveness of these efforts. This section discusses ongoing and future work to refine CO_2 Trap field methods and introduces upcoming projects that will use CO_2 Traps as monitoring tools.

5.1 Accounting for Naturally Occurring CO_2 Fluxes

CO_2 fluxes associated with soil respiration need to be considered when calculating natural LNAPL loss rates using CO_2 Traps. Failing to account for natural soil respiration can lead to overestimating natural losses of LNAPL. The background subtraction method is effective if three conditions are met: 1) appropriate background locations are available at a site (i.e. similar vegetation, soil type, soil moisture, surface covering); 2) the CO_2 generated from natural losses is significantly larger than the natural (background) CO_2 production rate; and 3) variability of background CO_2 flux rates is small relative to the magnitude of natural losses of LNAPL. If any of these conditions are not met, the background subtraction method will not be effective. Additionally, the background subtraction method can only detect large losses. It is

entirely possible that small natural loss rates are occurring at rates that cannot be distinguished from the background CO_2 flux.

Following Sihota et al., 2011; Sihota and Mayer, 2012, carbon isotope analysis provides a promising alternative to background subtraction as a method for estimating losses of LNAPL. This method is especially promising at sites that do not meet the previously discussed criteria. This is an especially important tool where small natural loss rates occur, or where no suitable background location can be established. Carbon isotope data should be collected whenever possible. These data are critical for sites that do not meet background subtraction criteria. Additionally, these data can be used as a means of validating background subtraction methods at sites that meet the criteria.

5.2 Local Variability and Pre-Screening

Location replicate samples have been collected at five field sites (A, C, D, E, F) by placing multiple CO_2 Traps within 1 to 3 m of each other. Results show both small and large local variations of results. This suggests that a solution to addressing local variability may not be as simple as up-scaling the cross-sectional area of the CO_2 Traps.

New methods of rapidly pre-screening field sites are being developed. The proposed methods would use an electronic CO_2 concentration detector to make rapid real time measurements of CO_2 concentration at grade over an entire site. The results would be plotted spatially to screen for CO_2 “hot spots” and for areas of widely variable CO_2 flux. This pre-screening would allow for more strategic targeted deployment of CO_2

Traps in order to optimize the number of traps deployed. More traps can be deployed in areas of greater apparent variability in CO_2 concentration. Additionally, this pre-screening could also be used to evaluate background areas and variability of background areas before deploying CO_2 Traps so that need for carbon isotope analysis could be established early on in a project. Research into pre-screening technology and relationship to measured CO_2 fluxes should be advanced in order to develop more effective field deployment techniques.

5.3 Traps for Monitoring Flux of Other Gases

The design of the CO_2 Traps consists of multiple flow-through compartments filled with a sorbent media. The initial design was developed and tested for measuring CO_2, as the final end product of hydrocarbon mineralization. However, other gases of interest may exit at grade over subsurface releases. One significant assumption of the CO_2 Trap method is that any CH_4 generated during petroleum degradation is converted to CO_2 in the vadose zone. If unconverted CH_4 escapes at grade, LNAPL loss rates will be underestimated. While this would still be conservative from a remediation planning standpoint, it is desirable to achieve the most accurate estimate possible.

Studies are currently looking at ways to modify the CO_2 Trap design to estimate CH_4 fluxes at grade. Additionally, studies are underway to modify the traps to estimate any fluxes of volatile organic compounds (VOCs). These modifications would allow a more thorough carbon mass balance at the soil-atmosphere interface. Additionally, the

ability to measure VOC efflux at grade has important implications for environmental monitoring.

5.4 Thermal Monitoring and STELA

Analysis of seasonal variations in calculated natural LNAPL loss rates combined with measured groundwater temperatures across an LNAPL body led to the conclusion that groundwater temperature has a significant influence on natural loss rates. Field data suggests that natural loss rates can increase significantly at groundwater temperatures above approximately 20°C. This observation is consistent with recent laboratory studies (Zeman, 2012), and with historical studies (Atlas, 1975; Dibble and Bartha, 1979; Zhou and Crawford, 1995). With this in mind, new work has begun to develop Sustainable Thermally Enhanced LNAPL Attenuation (STELA) technology. The concept of the STELA program is that modest heating of groundwater near an LNAPL smear zone can help increase biological degradation of LNAPL with a minimal energy input. This technology may lead to an exciting new frontier in LNAPL management strategies. Ongoing work to develop and deploy this technology will use CO_2 Traps to monitor CO_2 fluxes and calculate LNAPL loss rates before, during, and after application of the STELA system. To further explore the influences of temperature and seasonality, it is important to collect groundwater thermal data concurrently with CO_2 Traps wherever possible.

6 REFERENCES

Aggarwal, P.K. and Hinchee, R.E., 1991. Monitoring in situ biodegradation of hydrocarbons by using stable carbon isotopes. Environmental Science & Technology, 25(6): 1178-1180.

Amos, R.T., Mayer, K.U., Bekins, B.A., Delin, G.N. and Williams, R.L., 2005. Use of dissolved and vapor-phase gases to investigate methanogenic degradation of petroleum hydrocarbon contamination in the subsurface. Water Resour. Res., 41(W02001).

Atlas, R.M., 1975. Effects of Temperature and Crude Oil Composition on Petroleum Biodegradation. Applied Microbiology, 30(3): 396-403.

Auer, L.H., Rosenberg, N.D., Birdsell, K.H. and Whitney, E.M., 1996. The effects of barometric pumping on contaminant transport. Journal of Contaminant Hydrology, 24(2): 145-166.

Avery Jr, G.B., Willey, J.D. and Kieber, R.J., 2006. Carbon isotopic characterization of dissolved organic carbon in rainwater: Terrestrial and marine influences. Atmospheric Environment, 40(39): 7539-7545.

Bauer, H.P., Beckett, P.H.T. and Bie, S.W., 1972. A rapid gravimetric method for estimating calcium carbonate in soils. Plant and Soil, 37(3): 689-690.

Bremer, D.J. and Ham, J.M., 2002. Measurement and Modeling of Soil CO_2 Flux in a Temperate Grassland Under Mowed and Burned Regimes. Ecological Applications, 12(5): 1318-1328.

Coffin, R.B. et al., 2008. Radiocarbon and Stable Carbon Isotope Analysis to Confirm Petroleum Natural Attenuation in the Vadose Zone. Environmental Forensics, 9(1): 75-84.

Conrad, M.E. et al., 1997. Combined 14C and δ13C Monitoring of in Situ Biodegradation of Petroleum Hydrocarbons. Environmental Science & Technology, 31(5): 1463-1469.

Craig, H., 1953. The geochemistry of the stable carbon isotopes. Geochimica et Cosmochimica Acta, 3(2–3): 53-92.

Dane, J.H., Topp, G.C., Campbell, G.S. and Soil Science Society of America., 2002. Methods of soil analysis. Part 4, Physical methods. Soil Science Society of America book series. Soil Science Society of America, Madison, Wis., xli, 1692 p. pp.

Dibble, J.T. and Bartha, R., 1979. Effect of environmental parameters on the biodegradation of oil sludge. Applied and Environmental Microbiology, 37(4): 729-739.

Dreimanis, A., 1962. Quantitative gasometric determination of calcite and dolomite by using Chittick apparatus. Journal of Sedimentary Research, 32(3): 520-529.

Edwards, N.T., 1982. The Use of Soda-Lime for Measuring Respiration Rates in Terrestrial Systems. Pedobiologia, 23(5): 321-330.

EPA, 2005. Cost and Performance Report for LNAPL Recovery: Multi-Phase Extraction and Dual-Pump Recovery of LNAPL at the BP Former Amoco Refinery, Sugar Creek, MO. EPA 542-R-05-016, U.S. Environmental Protection Agency.

Healy, R.W., Striegl, R.G., Russell, T.F., Hutchinson, G.L. and Livingston, G.P., 1996. Numerical Evaluation of Static-Chamber Measurements of Soil-Atmosphere Gas Exchange: Identification of Physical Processes. Soil Sci. Soc. Am. J., 60(3): 740-747.

ITRC, 2009a. Evaluating LNAPL Remedial Technologies for Achieving Project Goals. LNAPL-2., LNAPL-2. Interstate Technology & Regulatory Council, Washington, D.C.

ITRC, 2009b. Evaluating Natural Source Zone Depletion at Sites with LNAPL. LNAPL-1., LNAPL-1. Interstate Technology and Regulatory Council, Washington, D.C.

Jensen, L.S. et al., 1996. Soil Surface CO_2 Flux as an Index of Soil Respiration In Situ A Comparison of Two Chamber Methods. Soil Biology & Biochemistry, 28(10/11): 1297-1306.

Johnson, P., Lundegard, P. and Liu, Z., 2006. Source Zone Natural Attenuation at Petroleum Hydrocarbon Spill Sites-I: Site-Specific Assessment Approach. Groundwater Monitoring & Remediation, 26(4): 82-92.

Johnson, P.C., Bruce, C., Johnson, R.L. and Kemblowski, M.W., 1998. In Situ Measurement of Effective Vapor-Phase Porous Media Diffusion Coefficients. Environmental Science & Technology, 32(21): 3405-3409.

Keith, H. and Wong, S.C., 2006. Measurement of Soil CO_2 Efflux Using Soda Lime Absorption: Both Quantitative and Reliable. Soil Biology & Biochemistry, 38(1121-1131).

Klouda, G.A. and Connolly, M.V., 1995. Radiocarbon (14C) measurements to quantify sources of atmospheric carbon monoxide in urban air. Atmospheric Environment, 29(22): 3309-3318.

Levin, I., Graul, R. and Trivett, N.B.A., 1995. Long-term observations of atmospheric CO_2 and carbon isotopes at continental sites in Germany. Tellus B, 47(1-2): 23-34.

Lundegard, P.D. and Johnson, P.C., 2006. Source Zone Natural Attenuation at Petroleum Hydrocarbon Spill Sites-II: Application to a Former Oil Field. Groundwater Monitoring & Remediation, 26(4): 93-106.

Ma, J., Rixey, W.G., DeVaull, G.E., Stafford, B.P. and Alvarez, P.J.J., 2012. Methane Bioattenuation and Implications for Explosion Risk Reduction along the Groundwater to Soil Surface Pathway above a Plume of Dissolved Ethanol. Environmental Science & Technology, 46(11): 6013-6019.

Mahler, N., Sale, T. and Lyverse, M., 2012. A Mass Balance Approach to Resolving LNAPL Stability. Ground Water.

Mahler, N., Sale, T., Smith, T. and Lyverse, M., 2011. Use of Single-Well Tracer Dilution Tests to Evaluate LNAPL Flux at Seven Field Sites. Ground Water.

Massmann, J. and Farrier, D.F., 1992. Effects of atmospheric pressures on gas transport in the vadose zone. Water Resour. Res., 28(3): 777-791.

McCoy, K., Zimbron, J., Sale, T. and Lyverse, M., 2012. Measurement of Natural LNAPL Loss Rates Using CO_2 Traps.

Minitab, 2010. V16.2.2. Minitab Inc. State College, PA.

Molins, S., Mayer, K.U., Amos, R.T. and Bekins, B.A., 2010. Vadose zone attenuation of organic compounds at a crude oil spill site - Interactions between biogeochemical reactions and multicomponent gas transport. Journal of Contaminant Hydrology, 112: 15-29.

Pongracic, S., Kirschbaum, M.U.F. and Raison, R.J., 1997. Comparison of Soda Lime and Infrared Gas Analysis Techniques for In Situ Measurement of Forest Soil Respiration. Can. J. For. Res., 27: 1890-1895.

Sihota, N.J. and Mayer, K.U., 2012. Characterizing vadose zone hydrocarbon biodegradation using CO_2-effluxes, isotopes, and reactive transport modeling. Vadose Zone Journal.

Sihota, N.J., Singurindy, O. and Mayer, K.U., 2011. CO_2-Efflux Measurements for Evaluating Source Zone Natural Attenuation Rates in a Petroleum Hydrocarbon Contaminated Aquifer. Environmental Science and Technology, 45(2): 482-488.

Smith, T., Sale, T. and Lyverse, M., 2012. Measurement of LNAPL Flux Using Single-Well Intermittent Mixing Tracer Dilution Tests. Ground Water: no-no.

Stahl, W.J., 1980. Compositional changes and $_{13}C/_{12}C$ fractionations during the degradation of hydrocarbons by bacteria. Geochimica et Cosmochimica Acta, 44(11): 1903-1907.

Stuiver, M. and Polach, H.A., 1977. Discussion. Reporting of ^{14}C Data. Radiocarbon, 19(3): 355-363.

Suchomel, K.H., Kreamer, D.K. and Long, A., 1990. Production and transport of carbon dioxide in a contaminated vadose zone: a stable and radioactive carbon isotope study. Environmental Science & Technology, 24(12): 1824-1831.

Wyatt, D.E., Richers, D.M. and Pirkle, R.J., 1995. Barometric pumping effects on soil gas studies for geological and environmental characterization. Environmental Geology, 25(4): 243-250.

Zeman, N.R., 2012. Thermally Enhanced Bioremediation of Petroleum Hydrocarbons. M.S. Thesis, Colorado State University, Fort Collins, Colorado.

Zhou, E. and Crawford, R.L., 1995. Effects of oxygen, nitrogen, and temperature on gasoline biodegradation in soil. Biodegradation, 6(2): 127-140.

Zimbron, J., Sale, T. and Lyverse, M., 2011. Gas Flux Measurement Using Traps. US Patent 13/197,657. Submitted to US Patent Office August 3.

Appendix A LABORATORY DATA

Table A.1. Closed System Test Data

Test	Position	% CO_2 Injected (g/g)	Total Captured % CO_2 (g/g)	Stdev	CV	n	Bl Corrected % CO_2 (g/g)	Stdev	CV	n	% Rec	Comments
Bl 1	- -	- -	**1.3%**	0.1%	11%	7	- -	- -	- -	'- -	- -	
Bl 2	- -	- -	**2.2%**	- -	- -	- -	- -	- -	- -	- -	- -	single analytical run used all sample
1	Bo	0.9%	**2.2%**	- -	- -	- -	**0.84%**	0.041%	5%	2	**89%**	
	T		**1.1%**	- -	- -	- -	- -	- -	- -	1	- -	
2	Bo	1.8%	**3.7%**	- -	- -	- -	**2.4%**	0.32%	14%	3	**130%**	
	T		**2.5%**	- -	- -	- -	**1.1%**	2.0%	174%	3	- -	
3	Bo	3.5%	**5.9%**	- -	- -	- -	**4.6%**	0.52%	11%	3	**130%**	
	T		**1.7%**	- -	- -	- -	**0.35%**	0.76%	214%	3	- -	
4	Bo	7.0%	**10%**	- -	- -	- -	**9.1%**	0.71%	7.8%	3	**130%**	
	T		**1.5%**	- -	- -	- -	**0.18%**	0.35%	193%	3	- -	
5	Bo	16%	**16%**	- -	- -	- -	**15%**	1.4%	9.6%	3	**94%**	
	T		**1.8%**	- -	- -	- -	**0.51%**	0.66%	130%	3	- -	
6	Bo	26%	**25%**	- -	- -	- -	**23%**	- -	- -	1	**90%**	single analytical run used all sample, sorbent uses "blank 2"
	T		**1.9%**	- -	- -	- -	- -	- -	- -	1	- -	single analytical run used all sample, sorbent uses "blank 2"
7	Bo	60%	**32%**	- -	- -	- -	**31%**	1.4%	4.6%	2	**52%**	
	T		**18%**	- -	- -	- -	**16%**	0.47%	2.9%	3	- -	

Notes:
- - No data
% Rec - % recovery
Bl - blank sample
Bl Cor - blank corrected captured CO_2 concentration
Bo - bottom trap element
CV - coefficient of variation
n - number of analytical replicates
Stdev - standard deviation
T - top trap element

Table A.2. Open System Test Injected CO_2 Flux Rates.

Test	Characteristic	Value	stdev	CV	n
1	Flow Rate (ml/min)	873	12	1.4%	10
	Concentration (μmol/ml)	34	0.059	0.17%	51
	Injected CO_2 Flux (μmol/m^2/sec)	**1,351**			
2	Flow Rate (ml/min)	694	13	1.9%	20
	Concentration (μmol/ml)	34	0.078	0.2%	52
	Injected CO_2 Flux (μmol/m^2/sec)	**1,048**			
3	Flow Rate (ml/min)	447	6.9	1.5%	17
	Concentration (μmol/ml)	34	0.13	0.37%	111
	Injected CO_2 Flux (μmol/m^2/sec)	**687**			
4	Flow Rate (ml/min)	244	1.6	0.66%	15
	Concentration (μmol/ml)	34	0.086	0.25%	194
	Injected CO_2 Flux (μmol/m^2/sec)	**374**			
5	Flow Rate (ml/min)	568	9.45	1.7%	19
	Concentration (μmol/ml)	34	0.11	0.32%	92
	Injected CO_2 Flux (μmol/m^2/sec)	**882**			
6	Flow Rate (ml/min)	676	13.26	2.0%	22
	Concentration (μmol/ml)	34	0.0854	0.25%	78
	Injected CO_2 Flux (μmol/m^2/sec)	**1,042**			
7	Flow Rate (ml/min)	348	4.55	1.3%	22
	Concentration (μmol/ml)	34	0.0479	0.14%	205
	Injected CO_2 Flux (μmol/m^2/sec)	**535**			

Notes:
Column cross sectional area is 0.369 m^2
CV - coefficient of variation
stdev - standard deviation
n - number of measurements

Table A.3. Open System Test CO_2 Trap Data.

Test	Location	Position	Total Measured % CO_2 (g/g)	Stdev	CV	n	Bl Cor % CO_2 (g/g)	Stdev	CV	n	Total Mass (gm)	Time (days)	Captured CO_2 Flux ($\mu mol/m^2/sec$)
1	Bl	Bo	**2.6%**	1.1%	41%		- -	- -	- -	- -	- -	- -	- -
1	A	Bo	**13%**	- -	- -	- -	10%	2.3%	23%	3	76.96	0.17	**1,448**
1	B	Bo	**9.7%**	- -	- -	- -	7.0%	0.96%	14%	3	76.66	0.17	**1,009**
1	C	Bo	**12%**	- -	- -	- -	9.0%	1.0%	11%	3	76.93	0.17	**1,297**
1	Bl	T	**2.3%**	0.98%	43%	3	- -	- -	- -	- -	- -	- -	- -
1	A	T	**1.9%**	0.085%	4.5%	3	- -	- -	- -	- -	- -	- -	- -
1	B	T	**2.0%**	0.094%	4.7%	3	- -	- -	- -	- -	- -	- -	- -
1	C	T	**2.7%**	0.65%	24%	3	- -	- -	- -	- -	- -	- -	- -
2	Bl	Bo	**2.4%**	0.45%	19%	6	- -	- -	- -	- -	- -	- -	
2	A	Bo	**6.7%**	- -	- -	- -	4.3%	0.20%	5%	3	77.20	0.18	**614**
2	B	Bo	**8.1%**	- -	- -	- -	5.7%	1.8%	31%	3	78.47	0.18	**819**
2	C	Bo	**7.6%**	- -	- -	- -	5.2%	1.8%	35%	3	77.28	0.18	**736**
2	Bl	T	**2.7%**	0.98%	36%	5	- -	- -	- -	- -	- -	- -	- -
2	B	T	**2.0%**	0.34%	17%	3	- -	- -	- -	- -	- -	- -	- -
2	C	T	**1.7%**	1.7%	104%	3	- -	- -	- -	- -	- -	- -	- -
3	Bl	Bo	**1.7%**	0.044%	2.6%	3	- -	- -	- -	- -	- -	- -	
3	A	Bo	**9.5%**	- -	- -	- -	7.8%	0.77%	10%	3	77.72	0.39	**512**
3	B	Bo	**9.2%**	- -	- -	- -	7.5%	0.43%	6%	3	77.61	0.39	**491**
3	C	Bo	**9.0%**	- -	- -	- -	7.3%	0.95%	13%	14	77.73	0.39	**476**
3	Bl	T	**1.8%**	0.13%	7.2%	3	- -	- -	- -	- -	- -	- -	- -
3	A	T	**1.1%**	0.11%	9.6%	3	- -	- -	- -	- -	- -	- -	- -
3	B	T	**3.2%**	2.5%	79%	3	- -	- -	- -	- -	- -	- -	- -
3	C	T	**1.9%**	0.63%	32%	3	- -	- -	- -	- -	- -	- -	- -
4	Bl	Bo	**1.4%**	0.13%	9.5%	3	- -	- -	- -	- -	- -	- -	
4	A	Bo	**9.9%**	- -	- -	- -	8.5%	0.70%	8%	3	78.59	0.67	**322**
4	B	Bo	**9.2%**	- -	- -	- -	7.8%	0.40%	5%	3	77.84	0.67	**294**
4	C	Bo	**8.6%**	- -	- -	- -	7.2%	0.49%	7%	3	77.84	0.67	**273**
4	Bl	T	**2.5%**	0.88%	36%	3	- -	- -	- -	- -	- -	- -	- -
4	A	T	**2.0%**	0.26%	13%	3	- -	- -	- -	- -	- -	- -	- -
4	B	T	**3.5%**	1.2%	35%	3	- -	- -	- -	- -	- -	- -	- -
4	C	T	**2.5%**	0.35%	14%	3	- -	- -	- -	- -	- -	- -	- -
5	Bl	Bo	**1.6%**	0.31%	19%	3	- -	- -	- -	- -	- -	- -	- -
5	A	Bo	**8.5%**	- -	- -	- -	6.8%	0.17%	3%	3	78.26	0.31	**555**
5	B	Bo	**8.1%**	- -	- -	- -	6.5%	0.42%	7%	3	77.95	0.31	**521**
5	C	Bo	**8.8%**	- -	- -	- -	7.1%	0.37%	5%	3	78.45	0.31	**580**
5	Bl	T	**0.9%**	0.15%	16%	2	- -	- -	- -	- -	- -	- -	- -
5	A	T	**1.6%**	0.28%	17%	2	- -	- -	- -	- -	- -	- -	- -
5	B	T	**1.9%**	0.35%	18%	3	- -	- -	- -	- -	- -	- -	- -
5	C	T	**2.7%**	1.1%	40%	3	- -	- -	- -	- -	- -	- -	- -

Test	Location	Position	Total Measured % CO_2 (g/g)	Stdev	CV	n	Bl Cor % CO_2 (g/g)	Stdev	CV	n	Total Mass (gm)	Time (days)	Captured CO_2 Flux ($\mu mol/m^2/sec$)
6	Bl	Bo	**1.6%**	0.033%	2.0%	2	- -	- -	- -	- -	- -	- -	- -
6	A	Bo	**9.7%**	- -	- -	- -	8.1%	0.66%	8%	3	76.23	0.27	**752**
6	B	Bo	**8.9%**	- -	- -	- -	7.3%	0.78%	11%	3	76.23	0.27	**671**
6	C	Bo	**9.2%**	- -	- -	- -	7.6%	0.36%	5%	3	76.23	0.27	**702**
6	Bl	T	**1.8%**	0.44%	25%	3	- -	- -	- -	- -	- -	- -	- -
6	A	T	**1.2%**	0.15%	12%	3	- -	- -	- -	- -	- -	- -	- -
6	B	T	**1.3%**	0.11%	8.6%	3	- -	- -	- -	- -	- -	- -	- -
6	C	T	**1.7%**	0.35%	20%	3	- -	- -	- -	- -	- -	- -	- -
7	Bl	Bo	**1.5%**	0.18%	12%	3	- -	- -	- -	- -	- -	- -	- -
7	A	Bo	**12%**	0.98%	8.2%	3	10.4%	0.98%	9%	3	78.80	0.71	**375**
7	B	Bo	**11%**	0.73%	6.4%	3	9.9%	0.73%	7%	3	78.24	0.71	**354**
7	C	Bo	**11%**	0.46%	4.0%	3	9.9%	0.46%	5%	3	78.56	0.71	**355**

Notes:
Trap cross sectional area is 8.1×10^{-3} m^2
No data for Test 7 top elements, or Test 2 top element A
- - No data
Bl - blank sample
Bl Cor - blank corrected captured CO_2
Bo - bottom trap element
CV - coefficient of variation
n - number of analytical replicates
Stdev - standard deviation
T - top trap element

Table A.4. Open System Test Soil Moisture Data.

Tray	Pan Mass (kg)	Wet Soil + Pan (kg)	Dry Soil + Pan (kg)	Water (g)	Soil (g)	water content (g/g)	Vol solid[1] (cm^3)	Vol Water[2] (cm^3)	Porosity[3]				
									0.25 Saturation	0.30 Saturation	0.35 Saturation	0.40 Saturation	0.45 Saturation
1	1.508	4.726	4.698	28.00	3,190	**0.88%**	1,204	28	**7%**	**5%**	**4%**	**3%**	**3%**
2	2.044	5.320	5.224	96.00	3,180	**3.0%**	1,200	96	**24%**	**19%**	**15%**	**12%**	**10%**
3	1.900	5.064	4.988	76.00	3,088	**2.5%**	1,165	76	**20%**	**15%**	**12%**	**10%**	**8%**
4	2.042	5.118	5.072	46.00	3,030	**1.5%**	1,143	46	**12%**	**9%**	**7%**	**6%**	**5%**
								Avg	**16%**	**12%**	**10%**	**8%**	**6%**
								Stdev	**8%**	**6%**	**5%**	**4%**	**3%**

Notes:

1 - Assumes solid density of 2.65 g/cm^3

2 - Assumes water density of 1 g/cm^3

3 - In-situ porosity not measured, range of porosities assumed for saturation calculations

Avg - average

Stdev - standard deviation

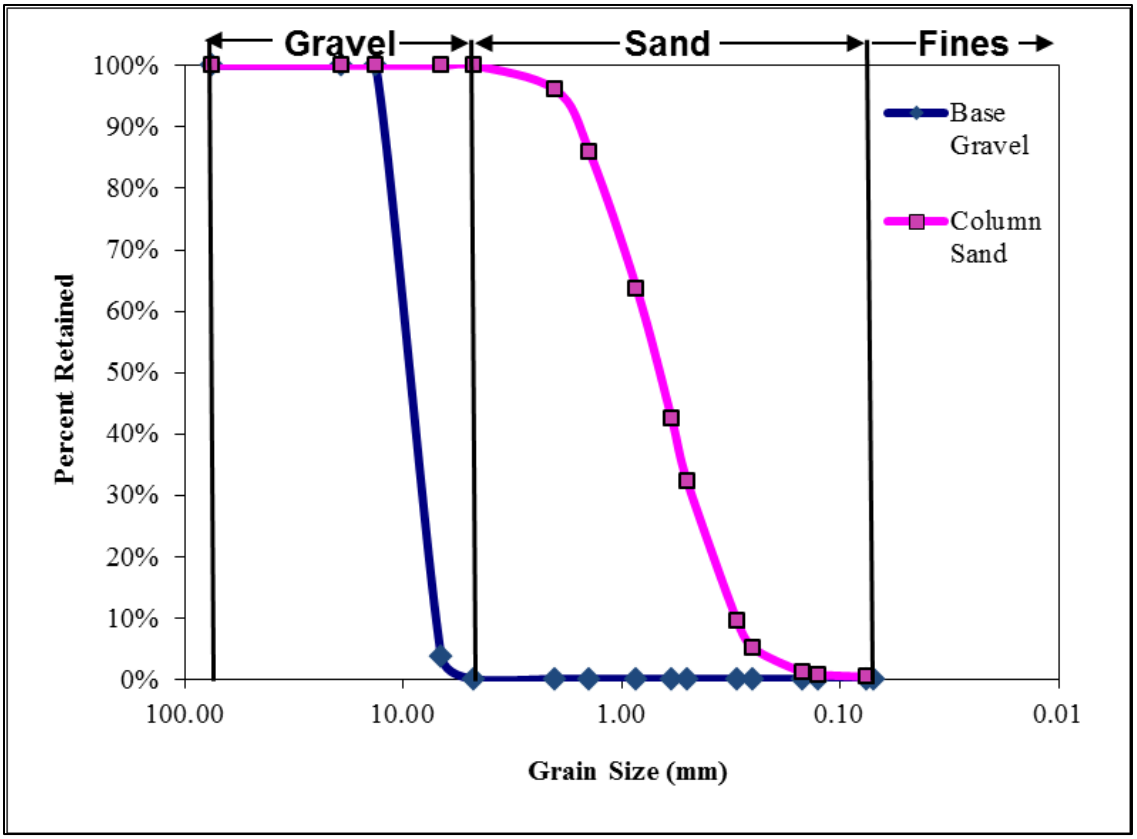

Figure A.1. Grain size chart for large column fill.

Appendix B FIELD DATA

Table B.1. CO_2 Trap Field Data and Site Characteristics.

Site	Loc	Class	Deployed	Recovered	CO_2 flux ($\mu mol/m^2/sec$)		Loss Rate (gal/acre/yr)		Depth to LNAPL (m btoc)	Depth to Water (m btoc)	LNAPL Thickness (m)	GW Temp (° C)	LNAPL Type	Depth to Smear Zone (m bgs)	Smear Zone Thickness (m)	Comments
					Avg	Stdev	Avg	95% CI								
A	1	BG	- -	- -	- -	- -	- -	- -	- -	- -	- -	- -	- -	- -	- -	Installed R2
A	2	BG	5/17/11	6/8/11	4.5	0.3	- -	- -	- -	- -	- -	- -	- -	- -	- -	
A	3	BG	5/17/11	6/8/11	5.0	0.5	- -	- -	- -	- -	- -	- -	- -	- -	- -	
A	4	LNAPL	5/17/11	6/8/11	17	0.8	**6,600**	**5,900 - 7,300**	- -	- -	- -	- -	A-Mix	1.2	3.4	
A	5	LNAPL	- -	- -	- -	- -	- -	- -	- -	- -	- -	- -	A-Mix	- -	- -	Installed R2
A	6	LNAPL	- -	- -	- -	- -	- -	- -	- -	- -	- -	- -	A-Mix	- -	- -	Installed R2
A	7	LNAPL	5/17/11	6/8/11	3.4	0.1	ns	ns	- -	- -	- -	9.5	D-Gas oil	1.5	1.2	
A	8	LNAPL	5/17/11	6/8/11	2.2	0.1	ns	ns	- -	- -	- -	- -	A-Mix	1.2	1.5	
A	9	LNAPL	5/17/11	6/8/11	8.8	0.2	**2,200**	**1,900 - 2,500**	- -	- -	- -	- -	B-Mix	1.2	1.8	
A	10	LNAPL	5/17/11	6/8/11	8.5	0.6	**2,100**	**1,400 - 2,700**	- -	- -	- -	- -	A-Mix	1.8	2.7	
A	11	LNAPL	5/18/11	6/8/11	6.9	0.3	**1,200**	**800 - 1,500**	- -	- -	- -	- -	A-Kerosene	4.3	1.2	
A	12	LNAPL	5/17/11	6/8/11	1.9	1.0	ns	ns	- -	- -	- -	- -	- -	2.7	3.0	
A	13	LNAPL	5/17/11	6/8/11	2.3	0.3	ns	ns	- -	- -	- -	- -	- -	3.4	3.4	
A	14	LNAPL	5/17/11	6/8/11	9.3	0.3	**2,500**	**2,100 - 2,900**	- -	- -	- -	- -	B-Kerosene	4.6	1.8	
A	15	LNAPL	5/17/11	6/8/11	5.1	0.3	ns	ns	- -	- -	- -	- -	- -	2.4	2.7	
A	16	LNAPL	5/17/11	6/8/11	7.7	0.7	**1,600**	**540 - 2,700**	- -	- -	- -	- -	B-Mix	0.9	2.4	
A	17	LNAPL	5/17/11	6/8/11	8.4	0.5	**2,000**	**1,500 - 2,500**	- -	- -	- -	- -	- -	1.2	3.4	
A	18	LNAPL	5/17/11	6/8/11	8.9	0.5	**2,300**	**1,700 - 2,900**	- -	- -	- -	- -	A-Mix	2.4	4.0	
A	19	LNAPL	5/17/11	6/8/11	8.3	0.5	**2,000**	**1,300 - 2,600**	- -	- -	- -	- -	A-Kerosene	5.8	3.7	
A	20	LNAPL	5/17/11	6/8/11	2.6	0.4	ns	ns	- -	- -	- -	- -	A-mix	1.2	3.7	
A	21	LNAPL	5/17/11	6/8/11	7.7	0.6	**1,600**	**920 - 2,400**	- -	- -	- -	- -	Not typed	7.6	1.8	
A	22	LNAPL	5/17/11	6/8/11	2.4	0.1	ns	ns	- -	- -	- -	- -	- -	9.4	1.8	
A	23	LNAPL	5/17/11	6/8/11	9.4	0.4	**2,600**	**2,100 - 3,000**	- -	- -	- -	- -	A-Mix	1.2	4.0	
A	1	BG	9/30/11	11/10/11	1.7	0.3	- -	- -	- -	3.62	- -	16.8	- -	- -	- -	
A	2	BG	9/29/11	11/10/11	3.6	0.9	- -	- -	- -	3.66	- -	16.2	- -	- -	- -	
A	3	BG	9/29/11	11/10/11	1.9	0.5	- -	- -	- -	- -	- -	- -	- -	- -	- -	
A	4	LNAPL	9/30/11	11/10/11	17	1.1	**8,100**	**6,900 - 9,300**	- -	2.66	- -	20.3	A-Mix	1.2	3.4	Triplicate Location
A	5	LNAPL	9/30/11	11/10/11	24	0.1	**12,000**	**11,000 - 12,000**	- -	2.66	- -	20.3	A-Mix	1.2	3.4	Triplicate Location
A	6	LNAPL	9/30/11	11/10/11	22	0.3	**11,000**	**10,000 - 11,000**	- -	2.66	- -	20.3	A-Mix	1.2	3.4	Triplicate Location
A	7	LNAPL	9/29/11	11/10/11	6.4	0.4	**2,200**	**1,700 - 2,700**	3.59	- -	> 3.99	17.6	D-Gas oil	1.5	1.2	LNAPL to total depth
A	8	LNAPL	9/29/11	11/10/11	5.0	0.5	**1,400**	**880 - 2,000**		2.99	- -	18.6	A-Mix	1.2	1.5	
A	9	LNAPL	9/29/11	11/10/11	3.9	0.1	**800**	**350 - 1,300**	3.49	3.52	0.02	16.8	B-Mix	1.2	1.8	
A	10	LNAPL	9/29/11	11/10/11	5.8	0.4	**1,900**	**1,300 - 2,400**	- -	4.24	- -	16.5	A-Mix	1.8	2.7	
A	11	LNAPL	9/29/11	11/10/11	8.3	0.1	**3,200**	**2,800 - 3,700**	- -	5.33	- -	14.9	A-Kerosene	4.3	1.2	
A	12	LNAPL	9/29/11	11/10/11	1.6	0.2	ns	ns	4.73	4.74	0.01	15.7	- -	2.7	3.0	
A	13	LNAPL	9/29/11	11/10/11	1.1	0.2	ns	ns	- -	5.68	- -	16.4	- -	3.4	3.4	
A	14	LNAPL	9/29/11	11/10/11	5.1	0.4	**1,500**	**950 - 2,100**	- -	5.23	- -	14.8	B-Kerosene	4.6	1.8	
A	15	LNAPL	9/29/11	11/10/11	1.5	0.4	ns	ns	- -	5.33	- -	16.5	- -	2.4	2.7	
A	16	LNAPL	9/29/11	11/10/11	11	0.4	**4,700**	**4,200 - 5,200**	- -	2.55	- -	20.0	B-Mix	0.9	2.4	
A	17	LNAPL	9/29/11	11/10/11	1.5	0.1	ns	ns	- -	3.57	- -	17.9	- -	1.2	3.4	
A	18	LNAPL	9/29/11	11/10/11	4.6	0.2	**1,200**	**730 - 1,700**	5.13	5.13	0.003	16.6	A-Mix	2.4	4.0	
A	19	LNAPL	9/29/11	11/10/11	4.8	0.6	**1,300**	**610 - 2,000**	- -	5.27	- -	15.6	A-Kerosene	5.8	3.7	
A	20	LNAPL	9/29/11	11/10/11	6.6	0.3	**2,300**	**1,800 - 2,800**	4.13	4.17	0.04	17.7	A-mix	1.2	3.7	
A	21	LNAPL	9/29/11	11/10/11	8.4	0.1	**3,300**	**2,800 - 3,700**	- -	8.57	- -	13.6	Not typed	7.6	1.8	
A	22	LNAPL	9/29/11	11/10/11	2.1	0.1	ns	ns	- -	- -	- -	- -	- -	9.4	1.8	

Site	Loc	Class	Deployed	Recovered	CO_2 flux ($\mu mol/m^2/sec$)		Loss Rate (gal/acre/yr)		Depth to LNAPL (m btoc)	Depth to Water (m btoc)	LNAPL Thickness (m)	GW Temp (° C)	LNAPL Type	Depth to Smear Zone (m bgs)	Smear Zone Thickness (m)	Comments
					Avg	Stdev	Avg	95% CI								
A	23	LNAPL	9/29/11	11/10/11	5.8	0.2	**1,900**	**1,400 - 2,300**	- -	4.57	- -	17.6	A-Mix	1.2	4.0	
A	1	BG	4/23/12	5/4/12	1.9	1.6	- -	- -	- -	4.02	- -	12.0	- -	- -	- -	
A	2	BG	4/23/12	5/4/12	8.0	0.5	- -	- -	- -	4.10	- -	9.9	- -	- -	- -	
A	3	BG	4/23/12	5/4/12	7.2	0.7	- -	- -	- -	2.90	- -	12.0	- -	- -	- -	
A	4	LNAPL	4/23/12	5/4/12	15	0.9	**5,200**	**3,800 - 6,600**	- -	3.12	- -	12.6	A-Mix	1.2	3.4	Triplicate Location
A	5	LNAPL	4/23/12	5/4/12	14	0.1	**4,800**	**3,500 - 6,100**	- -	3.12	- -	12.6	A-Mix	1.2	3.4	Triplicate Location
A	6	LNAPL	4/23/12	5/4/12	12	0.6	**3,300**	**2,000 - 4,700**	- -	3.12	- -	12.6	A-Mix	1.2	3.4	Triplicate Location
A	7	LNAPL	4/23/12	5/4/12	7.5	1.4	ns	ns	3.69	3.98	0.30	11.0	D-Gas oil	1.5	1.2	
A	8	LNAPL	4/23/12	5/4/12	13	0.8	**3,700**	**2,400 - 5,100**	3.29	3.89	0.60	12.0	A-Mix	1.2	1.5	
A	9	LNAPL	4/23/12	5/4/12	4.0	0.2	ns	ns	- -		- -	- -	B-Mix	1.2	1.8	
A	10	LNAPL	4/23/12	5/4/12	5.3	0.3	ns	ns	- -	4.74	- -	10.0	A-Mix	1.8	2.7	
A	11	LNAPL	4/23/12	5/4/12	3.8	0.1	ns	ns	- -	5.86	- -	11.7	A-Kerosene	4.3	1.2	
A	12	LNAPL	4/23/12	5/4/12	5.2	3.2	ns	ns	5.20	5.42	0.22	12.4	- -	2.7	3.0	
A	13	LNAPL	4/23/12	5/4/12	2.6	1.2	ns	ns	6.20	6.33	0.14	12.9	- -	3.4	3.4	
A	14	LNAPL	4/23/12	5/4/12	6.1	0.4	ns	ns	- -	5.80	- -	11.8	B-Kerosene	4.6	1.8	
A	15	LNAPL	4/23/12	5/4/12	4.5	1.5	ns	ns	5.79	5.94	0.15	12.2	- -	2.4	2.7	
A	16	LNAPL	4/23/12	5/4/12	8.4	0.1	**1,500**	**190 - 2,700**	- -	2.95	- -	13.1	B-Mix	0.9	2.4	
A	17	LNAPL	4/23/12	5/4/12	2.8	0.5	ns	ns	3.69	3.78	0.09	10.7	- -	1.2	3.4	
A	18	LNAPL	4/23/12	5/4/12	5.1	0.3	ns	ns	5.62	5.65	0.03	12.3	A-Mix	2.4	4.0	
A	19	LNAPL	4/23/12	5/4/12	5.2	0.5	ns	ns	5.79	5.79	0.01	12.0	A-Kerosene	5.8	3.7	
A	20	LNAPL	4/23/12	5/4/12	15	0.3	**5,400**	**4,100 - 6,600**	4.63	4.78	0.14	11.0	A-mix	1.2	3.7	
A	21	LNAPL	4/23/12	5/4/12	16	0.4	**5,800**	**4,500 - 7,100**	- -	9.05	- -	14.0	Not typed	7.6	1.8	
A	22	LNAPL	4/23/12	5/4/12	3.7	0.2	ns	ns	- -	- -	- -	- -	- -	9.4	1.8	
A	23	LNAPL	4/23/12	5/4/12	6.6	0.3	ns	ns	5.07	5.23	0.16	12.6	A-Mix	1.2	4.0	
B	1	BG	11/10/11	11/29/11	2.4	1.0	- -	- -	- -	3.75	- -	18.1	- -	- -	- -	
B	2	BG	11/10/11	11/29/11	1.9	0.5	- -	- -	- -	4.59	- -	17.6	- -	- -	- -	
B	3	LNAPL	11/10/11	11/29/11	4.2	0.8	**1,100**	**150 - 2,100**	2.91	3.18	0.27	20.9	RR Diesel	- -	- -	
B	4	LNAPL	11/10/11	11/29/11	3.4	0.5	**660**	**120 - 1,200**	3.36	3.63	0.27	20.8	RR Diesel	- -	- -	
B	5	LNAPL	11/10/11	11/29/11	6.2	1.0	**2,200**	**1,100 - 3,400**	3.11	3.29	0.18	21.7	RR Diesel	- -	- -	
B	6	LNAPL	11/10/11	11/29/11	8.5	1.3	**3,500**	**1,600 - 5,400**	- -	4.33	- -	17.6	RR Diesel	- -	- -	
B	7	LNAPL	11/10/11	11/29/11	5.8	0.9	**2,000**	**940 - 3,100**	3.65	3.92	0.27	20.3	RR Diesel	- -	- -	
B	8	LNAPL	11/10/11	11/29/11	6.8	0.9	**2,500**	**1,500 - 3,600**	3.41	3.72	0.31	20.8	RR Diesel	- -	- -	
B	9	LNAPL	11/10/11	11/29/11	7.2	0.1	**2,800**	**2,400 - 3,200**	4.97	4.98	0.01	20.6	RR Diesel	- -	- -	
B	10	LNAPL	11/10/11	11/29/11	0.69	0.4	ns	ns	- -	- -	- -	- -	RR Diesel	- -	- -	
C	1	BG	3/28/12	4/11/12	2.2	0.1	- -	- -	- -	5.90	- -	25.9	- -	- -	- -	Triplicate 1
C	2	BG	3/28/12	4/11/12	3.4	0.4	- -	- -	- -	5.90	- -	25.9	- -	- -	- -	Triplicate 1
C	3	BG	3/28/12	4/11/12	3.4	0.1	- -	- -	- -	5.90	- -	25.9	- -	- -	- -	Triplicate 1
C	4	BG	3/28/12	4/11/12	5.6	0.4	- -	- -	- -	2.46	- -	26.9	- -	- -	- -	
C	5	BG	3/28/12	4/11/12	1.6	0.1	- -	- -	- -	- -	- -	- -	- -	- -	- -	
C	6	LNAPL	3/28/12	4/11/12	2.1	0.4	ns	ns	5.76	5.82	0.06	28.3	- -	- -	- -	
C	7	LNAPL	3/28/12	4/11/12	2.3	0.1	ns	ns	- -	3.45	- -	25.7	- -	- -	- -	
C	8	LNAPL	3/28/12	4/11/12	6.9	0.7	**2,000**	**1,300 - 2,700**	- -	- -	- -	- -	- -	- -	- -	
C	9	LNAPL	3/28/12	4/11/12	5.8	0.6	**1,300**	**630 - 2,000**	- -	- -	- -	- -	- -	- -	- -	
C	10	LNAPL	3/28/12	4/11/12	3.5	0.3	ns	ns	- -	- -	- -	- -	- -	- -	- -	
C	11	LNAPL	3/28/12	4/11/12	5.9	0.2	**1,400**	**940 - 1,900**	- -	- -	- -	- -	- -	- -	- -	
C	12	LNAPL	3/28/12	4/11/12	2.4	0.5	ns	ns	- -	- -	- -	- -	- -	- -	- -	
C	13	LNAPL	3/28/12	4/11/12	6.6	0.9	**1,800**	**820 - 2,800**	3.31	3.36	0.05	27.0	- -	- -	- -	Triplicate 2
C	14	LNAPL	3/28/12	4/11/12	30	2.1	**14,000**	**11,000 - 17,000**	3.31	3.36	0.05	27.0	- -	- -	- -	Triplicate 2
C	15	LNAPL	3/28/12	4/11/12	21	1.1	**9,500**	**8,200 - 11,000**	3.31	3.36	0.05	27.0	- -	- -	- -	Triplicate 2
C	16	LNAPL	3/28/12	4/11/12	29	1.1	**14,000**	**13,000 - 16,000**	- -	2.77	- -	28.9	- -	- -	- -	
C	17	LNAPL	3/28/12	4/11/12	1.9	0.5	ns	ns	- -	2.30	- -	26.6	- -	- -	- -	
C	18	LNAPL	3/28/12	4/11/12	36	0.4	**18,000**	**17,000 - 18,000**	- -	- -	- -	- -	- -	- -	- -	
C	19	LNAPL	3/28/12	4/11/12	16	0.7	**7,200**	**6,400 - 7,900**	- -	2.99	- -	26.9	- -	- -	- -	
C	20	LNAPL	3/28/12	4/11/12	3.8	0.3	ns	ns	- -	- -	- -	- -	- -	- -	- -	

Site	Loc	Class	Deployed	Recovered	CO_2 flux ($\mu mol/m^2/sec$)		Loss Rate (gal/acre/yr)		Depth to LNAPL (m btoc)	Depth to Water (m btoc)	LNAPL Thickness (m)	GW Temp (° C)	LNAPL Type	Depth to Smear Zone (m bgs)	Smear Zone Thickness (m)	Comments
					Avg	Stdev	Avg	95% CI								
D	1	BG	8/5/10	8/10/10	1.4	0.9	- -	- -	- -	- -	- -	- -	- -	- -	- -	
D	2	BG	8/5/10	8/10/10	6.5	0.5	- -	- -	- -	- -	- -	- -	- -	- -	- -	Not used for BG correction
D	3	LNAPL	8/5/10	8/10/10	6.2	0.3	**2,600**	**1,800 - 3,400**	- -	- -	- -	- -	- -	- -	- -	
D	4	LNAPL	8/5/10	9/20/10	5.0	0.2	**1,900**	**1,100 - 2,700**	- -	- -	- -	- -	- -	- -	- -	
D	5	LNAPL	8/5/10	8/10/10	3.5	0.6	**1,200**	**370 - 1,900**	- -	- -	- -	- -	- -	- -	- -	
D	6	LNAPL	8/5/10	8/10/10	4.7	0.3	**1,800**	**950 - 2,600**	- -	- -	- -	- -	- -	- -	- -	
D	7	LNAPL	8/5/10	8/10/10	7.4	0.5	**3,300**	**2,500 - 4,000**	- -	- -	- -	- -	- -	- -	- -	
D	8	LNAPL	8/5/10	8/10/10	3.3	0.5	**1,000**	**190 - 1,800**	- -	- -	- -	- -	- -	- -	- -	Transect Area
D	9	LNAPL	8/5/10	8/10/10	1.9	0.6	ns	ns	- -	- -	- -	- -	- -	- -	- -	Transect Area
D	10	LNAPL	8/5/10	8/10/10	1.2	0.6	ns	ns	- -	- -	- -	- -	- -	- -	- -	Transect Area
D	11	LNAPL	8/5/10	8/10/10	2.1	0.8	ns	ns	- -	- -	- -	- -	- -	- -	- -	Transect Area
D	12	LNAPL	8/5/10	8/10/10	5.2	1.2	**2,100**	**1,100 - 3,000**	- -	- -	- -	- -	- -	- -	- -	Transect Area
D	13	LNAPL	8/5/10	8/10/10	3.6	1.0	**1,200**	**330 - 2,000**	- -	- -	- -	- -	- -	- -	- -	Transect Area
D	14	LNAPL	8/5/10	8/10/10	5.7	0.6	**2,300**	**1,600 - 3,100**	- -	- -	- -	- -	- -	- -	- -	
D	15	LNAPL	8/5/10	8/10/10	4.7	0.3	**1,700**	**920 - 2,400**	- -	- -	- -	- -	- -	- -	- -	
D	16	LNAPL	8/5/10	8/10/10	2.3	0.2	ns	ns	- -	- -	- -	- -	- -	- -	- -	
D	17	LNAPL	8/5/10	8/10/10	14	0.8	**6,900**	**6,000 - 7,700**	- -	- -	- -	- -	- -	- -	- -	
D	1	BG	12/3/10	12/17/10	0.82	0.1	- -	- -	- -	- -	- -	- -	- -	- -	- -	
D	2	BG	12/3/10	12/17/10	0.58	0.3	- -	- -	- -	- -	- -	- -	- -	- -	- -	
D	3	LNAPL	12/3/10	12/17/10	4.7	1.1	ns	ns	- -	- -	- -	- -	- -	- -	- -	
D	4	LNAPL	- -	- -	- -	- -	- -	- -	- -	- -	- -	- -	- -	- -	- -	Destroyed after R1
D	5	LNAPL	12/3/10	12/17/10	8.3	1.0	**4,200**	**ns - 9,400**	- -	- -	- -	- -	- -	- -	- -	
D	6	LNAPL	12/3/10	12/17/10	0.24	0.1	ns	ns	- -	- -	- -	- -	- -	- -	- -	
D	7	LNAPL	12/3/10	12/17/10	1.4	0.1	**400**	**240 - 550**	- -	- -	- -	- -	- -	- -	- -	
D	8	LNAPL	- -	- -	- -	- -	- -	- -	- -	- -	- -	- -	- -	- -	- -	Transect Area, Location inaccessible
D	9	LNAPL	- -	- -	- -	- -	- -	- -	- -	- -	- -	- -	- -	- -	- -	Transect Area, Location inaccessible
D	10	LNAPL	- -	- -	- -	- -	- -	- -	- -	- -	- -	- -	- -	- -	- -	Transect Area, Location inaccessible
D	11	LNAPL	12/3/10	12/17/10	0.33	0.4	ns	ns	- -	- -	- -	- -	- -	- -	- -	Transect Area
D	12	LNAPL	12/3/10	12/17/10	1.7	0.6	ns	ns	- -	- -	- -	- -	- -	- -	- -	Transect Area
D	13	LNAPL	12/3/10	12/17/10	0.12	0.0	ns	ns	- -	- -	- -	- -	- -	- -	- -	Transect Area
D	14	LNAPL	12/3/10	12/17/10	0.57	0.1	ns	ns	- -	- -	- -	- -	- -	- -	- -	
D	15	LNAPL	12/3/10	12/17/10	1.7	0.3	**550**	**220 - 880**	- -	- -	- -	- -	- -	- -	- -	
D	16	LNAPL	12/3/10	12/17/10	0.56	0.1	ns	ns	- -	- -	- -	- -	- -	- -	- -	
D	17	LNAPL	12/3/10	12/17/10	2.0	0.4	**720**	**120 - 1,300**	- -	- -	- -	- -	- -	- -	- -	
D	1	BG	3/10/11	3/24/11	0.20	0.0	- -	- -	- -	- -	- -	- -	- -	- -	- -	
D	2	BG	3/10/11	3/24/11	0.95	0.7	- -	- -	- -	- -	- -	- -	- -	- -	- -	
D	3	LNAPL	3/10/11	3/24/11	2.5	0.3	**1,000**	**640 - 1,400**	- -	- -	- -	- -	- -	- -	- -	
D	4	LNAPL	- -	- -	- -	- -	- -	- -	- -	- -	- -	- -	- -	- -	- -	Destroyed after R1
D	5	LNAPL	- -	- -	- -	- -	- -	- -	- -	- -	- -	- -	- -	- -	- -	Location inaccessible
D	6	LNAPL	3/10/11	3/24/11	0.28	0.6	ns	ns	- -	- -	- -	- -	- -	- -	- -	
D	7	LNAPL	3/10/11	3/24/11	0.33	0.2	ns	ns	- -	- -	- -	- -	- -	- -	- -	
D	8	LNAPL	- -	- -	- -	- -	- -	- -	- -	- -	- -	- -	- -	- -	- -	Location inaccessible
D	9	LNAPL	- -	- -	- -	- -	- -	- -	- -	- -	- -	- -	- -	- -	- -	Location inaccessible
D	10	LNAPL	- -	- -	- -	- -	- -	- -	- -	- -	- -	- -	- -	- -	- -	Location inaccessible
D	11	LNAPL	- -	- -	- -	- -	- -	- -	- -	- -	- -	- -	- -	- -	- -	Location inaccessible
D	12	LNAPL	- -	- -	- -	- -	- -	- -	- -	- -	- -	- -	- -	- -	- -	Location inaccessible
D	13	LNAPL	- -	- -	- -	- -	- -	- -	- -	- -	- -	- -	- -	- -	- -	Location inaccessible
D	14	LNAPL	3/10/11	3/24/11	1.7	0.1	**640**	**290 - 990**	- -	- -	- -	- -	- -	- -	- -	
D	15	LNAPL	3/10/11	3/24/11	0.80	0.1	ns	ns	- -	- -	- -	- -	- -	- -	- -	
D	16	LNAPL	- -	- -	- -	- -	- -	- -	- -	- -	- -	- -	- -	- -	- -	
D	17	LNAPL	3/10/11	3/24/11	3.1	0.0	**1,400**	**1,000 - 1,700**	- -	- -	- -	- -	- -	- -	- -	

Site	Loc	Class	Deployed	Recovered	CO_2 flux ($\mu mol/m^2/sec$)		Loss Rate (gal/acre/yr)		Depth to LNAPL (m btoc)	Depth to Water (m btoc)	LNAPL Thickness (m)	GW Temp (° C)	LNAPL Type	Depth to Smear Zone (m bgs)	Smear Zone Thickness (m)	Comments
					Avg	Stdev	Avg	95% CI								
D	1	BG	7/26/11	8/8/11	18	5.6	- -	- -	- -	- -	- -	- -	- -	- -	- -	Not used for BG correction
D	2	BG	7/26/11	8/8/11	2.3	0.1	- -	- -	- -	- -	- -	- -	- -	- -	- -	Location inaccessible
D	3	LNAPL	7/26/11	8/8/11	11	1.8	**4,500**	**3,700 - 5,400**	- -	- -	- -	- -	- -	- -	- -	
D	4	LNAPL	- -	- -	- -	- -	- -	- -	- -	- -	- -	- -	- -	- -	- -	Destroyed after R1
D	5	LNAPL	- -	- -	- -	- -	- -	- -	- -	- -	- -	- -	- -	- -	- -	Location inaccessible
D	6	LNAPL	7/26/11	8/8/11	3.4	0.4	**650**	**52 - 1,300**	- -	- -	- -	- -	- -	- -	- -	
D	7	LNAPL	7/26/11	8/8/11	5.4	1.1	**1,700**	**1,200 - 2,200**	- -	- -	- -	- -	- -	- -	- -	
D	8	LNAPL	7/26/11	8/8/11	3.6	0.6	ns	ns	- -	- -	- -	- -	- -	- -	- -	Transect Area
D	9	LNAPL	- -	- -	- -	- -	- -	- -	- -	- -	- -	- -	- -	- -	- -	Transect Area, Location inaccessible
D	10	LNAPL	- -	- -	- -	- -	- -	- -	- -	- -	- -	- -	- -	- -	- -	Transect Area, Location inaccessible
D	11	LNAPL	7/26/11	8/8/11	4.5	0.6	**1,200**	**430 - 2,000**	- -	- -	- -	- -	- -	- -	- -	Transect Area
D	12	LNAPL	7/26/11	8/8/11	5.8	0.4	**2,000**	**1,400 - 2,500**	- -	- -	- -	- -	- -	- -	- -	Transect Area
D	13	LNAPL	7/26/11	8/8/11	13	0.9	**5,800**	**4,500 - 7,000**	- -	- -	- -	- -	- -	- -	- -	Transect Area
D	14	LNAPL	7/26/11	8/8/11	7.4	1.0	**2,800**	**2,000 - 3,700**	- -	- -	- -	- -	- -	- -	- -	
D	15	LNAPL	7/26/11	8/8/11	17	2.5	**7,900**	**6,100 - 9,600**	- -	- -	- -	- -	- -	- -	- -	
D	16	LNAPL	7/26/11	8/8/11	1.4	0.7	ns	ns	- -	- -	- -	- -	- -	- -	- -	
D	17	LNAPL	7/26/11	8/8/11	19	2.5	**9,000**	**5,700 - 12,000**	- -	- -	- -	- -	- -	- -	- -	
E	1	BG	8/15/11	8/25/11	4.4	1.0	- -	- -	- -	- -	- -	- -	- -	- -	- -	Triplicate 1
E	2	BG	8/15/11	8/25/11	2.1	1.6	- -	- -	- -	- -	- -	- -	- -	- -	- -	Triplicate 1
E	3	BG	8/15/11	8/25/11	4.6	1.0	- -	- -	- -	- -	- -	- -	- -	- -	- -	Triplicate 1
E	4	BG	8/15/11	8/25/11	9.0	1.8	- -	- -	- -	- -	- -	- -	- -	- -	- -	
E	5	BG	8/15/11	8/25/11	0.74	0.6	- -	- -	- -	- -	- -	- -	- -	- -	- -	
E	6	BG	8/15/11	8/25/11	3.6	0.5	- -	- -	- -	- -	- -	- -	- -	- -	- -	
E	7	BG	8/15/11	8/25/11	8.3	0.6	- -	- -	- -	- -	- -	- -	- -	- -	- -	
E	8	LNAPL	8/16/11	8/25/11	5.2	2.2	ns	ns	- -	- -	- -	- -	- -	- -	- -	
E	9	LNAPL	8/18/11	8/25/11	7.1	2.9	ns	ns	- -	- -	- -	- -	- -	- -	- -	Duplicate 1
E	10	LNAPL	8/18/11	8/25/11	7.2	0.8	**1,400**	**590 - 2,200**	- -	- -	- -	- -	- -	- -	- -	Duplicate 1
E	11	LNAPL	8/15/11	8/25/11	2.0	1.0	ns	ns	- -	- -	- -	- -	- -	- -	- -	
E	12	LNAPL	8/15/11	8/25/11	12	4.3	**4,000**	**130 - 7,900**	- -	- -	- -	- -	- -	- -	- -	
E	13	LNAPL	8/15/11	8/25/11	4.4	0.4	ns	ns	- -	- -	- -	- -	- -	- -	- -	
E	14	LNAPL	8/15/11	8/25/11	5.0	1.3	ns	ns	- -	- -	- -	- -	- -	- -	- -	
E	15	LNAPL	8/15/11	8/25/11	3.5	1.3	ns	ns	- -	- -	- -	- -	- -	- -	- -	
E	16	LNAPL	8/15/11	8/25/11	6.8	0.5	**1,100**	**430 - 1,900**	- -	- -	- -	- -	- -	- -	- -	
E	17	LNAPL	8/15/11	8/25/11	4.6	0.5	ns	ns	- -	- -	- -	- -	- -	- -	- -	
E	18	LNAPL	8/15/11	8/25/11	5.5	1.8	ns	ns	- -	- -	- -	- -	- -	- -	- -	
E	19	LNAPL	8/15/11	8/25/11	4.2	0.7	ns	ns	- -	- -	- -	- -	- -	- -	- -	
E	20	LNAPL	8/15/11	8/25/11	12.0	1.1	**4,000**	**3,100 - 5,000**	- -	- -	- -	- -	- -	- -	- -	
E	21	LNAPL	8/16/11	8/25/11	1.3	0.7	ns	ns	- -	- -	- -	- -	- -	- -	- -	
E	22	LNAPL	8/16/11	8/25/11	4.8	0.6	ns	ns	- -	- -	- -	- -	- -	- -	- -	
E	23	LNAPL	8/16/11	8/25/11	2.7	0.6	ns	ns	- -	- -	- -	- -	- -	- -	- -	
E	24	LNAPL	8/16/11	8/25/11	8.2	1.4	**2,000**	**750 - 3,100**	- -	- -	- -	- -	- -	- -	- -	

Site	Loc	Class	Deployed	Recovered	CO_2 flux ($\mu mol/m^2/sec$)		Loss Rate (gal/acre/yr)		Depth to LNAPL (m btoc)	Depth to Water (m btoc)	LNAPL Thickness (m)	GW Temp (° C)	LNAPL Type	Depth to Smear Zone (m bgs)	Smear Zone Thickness (m)	Comments
					Avg	Stdev	Avg	95% CI								
F	1	LNAPL	6/22/11	7/12/11	2.3	0.1	**1,300†**	- -	- -	- -	- -	- -	- -	- -	- -	Triplicate Location
F	2	LNAPL	6/22/11	7/12/11	3.4	0.1	**1,800†**	- -	- -	- -	- -	- -	- -	- -	- -	Triplicate Location
F	3	LNAPL	6/22/11	7/12/11	1.4	0.1	**790†**	- -	- -	- -	- -	- -	- -	- -	- -	Triplicate Location
F	4	LNAPL	6/22/11	7/12/11	6.4	0.2	**3,500†**	- -	- -	8.35	- -		Gasoline	- -	- -	
F	5	LNAPL	6/22/11	7/12/11	2.4	0.4	**1,300†**	- -	- -	- -	- -	- -	- -	- -	- -	
F	6	LNAPL	6/22/11	7/12/11	3.5	0.1	**1,900†**	- -	- -	7.17	0.04	14.1	Gasoline	- -	- -	
F	7	LNAPL	6/22/11	7/12/11	33	1.4	**18,000†**	- -	- -	8.45	0.42	- -	Gasoline	- -	- -	
F	8	LNAPL	6/22/11	7/12/11	11	0.1	**5,800†**	- -	- -	- -	- -	- -	Gasoline	- -	- -	High Resolution Area
F	9	LNAPL	6/22/11	7/12/11	0.92	0.1	**500†**	- -	- -	- -	- -	- -	Gasoline	- -	- -	High Resolution Area
F	10	LNAPL	6/22/11	7/12/11	0.82	0.1	**450†**	- -	- -	- -	- -	- -	Gasoline	- -	- -	High Resolution Area
F	11	LNAPL	6/22/11	7/12/11	1.4	0.2	**760†**	- -	- -	- -	- -	- -	Gasoline	- -	- -	High Resolution Area
F	12	LNAPL	6/22/11	7/12/11	1.4	0.0	**780†**	- -	- -	- -	- -	- -	Gasoline	- -	- -	High Resolution Area
F	13	LNAPL	6/22/11	7/12/11	3.2	0.2	**1,700†**	- -	- -	- -	- -	- -	Gasoline	- -	- -	High Resolution Area
F	14	LNAPL	6/22/11	7/12/11	12	0.2	**6,600†**	- -	- -	- -	- -	- -	Gasoline	- -	- -	High Resolution Area
F	15	LNAPL	6/22/11	7/12/11	5.7	0.2	**3,200†**	- -	- -	- -	- -	- -	Gasoline	- -	- -	High Resolution Area
F	16	LNAPL	6/22/11	7/12/11	13	0.3	**7,400†**	- -	- -	- -	- -	- -	Gasoline	- -	- -	High Resolution Area
F	17	LNAPL	6/22/11	7/12/11	34	1.3	**19,000†**	- -	- -	- -	- -	- -	- -	- -	- -	
F	18	LNAPL	6/22/11	7/12/11	1.3	0.2	**690†**	- -	- -	- -	- -	- -	- -	- -	- -	
F	19	LNAPL	6/22/11	7/12/11	3.3	0.7	**1,800†**	- -	- -	- -	- -	- -	- -	- -	- -	
F	20	LNAPL	6/22/11	7/12/11	1.3	0.3	**710†**	- -	- -	- -	- -	- -	- -	- -	- -	
F	21	LNAPL	6/22/11	7/12/11	3.6	0.4	**2,000†**	- -	- -	- -	- -	- -	- -	- -	- -	
F	22	LNAPL	6/22/11	7/12/11	1.3	0.5	**700†**	- -	- -	- -	- -	- -	- -	- -	- -	
F	23	LNAPL	6/22/11	7/12/11	2.3	0.4	**1,200†**	- -	- -	- -	- -	- -	- -	- -	- -	

Notes:
All samples corrected for naturally occurring CO2 flux using background subtraction method unless otherwise noted
95% CI - 95 percent confidence interval on difference between location and average of background locations, calculation includes laboratory replicates
°C - degrees celcius
† - sample not corrected for naturally occuring CO_2 flux
Avg - mean based on replicate laboratory analyses
BG - background (natural soil respiration) CO_2 flux location
bgs - below ground surface
btoc - below top of casing
gal/acre/yr - gallons per acre per year
LNAPL - LNAPL CO2 flux location
Loc - location
$\mu mol/m^2/sec$ - micromoles (10^{-6} mol) per square meter per second
m - meters
ns - not significantly different from background based on 95% CI of two sample T-Test
Stdev - standard deviation based on replicate laboratory analyses
SZ - smear zone

Table B.2. CO_2 Trap Carbon Isotope Data and Fossil Fuel Calculations.

a) Carbon Isotope Data

Site	Class	Location	$\delta^{13}C$ (‰)	Fm_{sample}		^{14}C Age (yr)		ff_{sample}
				value	stdev	value	stdev	
A	TB	TB	-13.4	73%	0.1%	2,550	15	37%
A	BG	2	-21.9	96%	0.2%	340	15	17%
A	BG	1	-20.8	94%	0.2%	470	15	18%
A	LNAPL	6	-30.1	13%	0.1%	16,630	70	89%

b) Fossil Fuel Fractions

Site	Class	Location	Raw % CO_2 (g/g)	Total Trap mass (g)	Total CO_2 sorbed (g)	ff CO_2 (g)
A	TB	TB	1.9%	69.00	1.3	0.47
A	BG	2	6.7%	69.83	4.7	0.77
A	BG	1	3.2%	65.89	2.1	0.38
A	LNAPL	6	34%	81.45	27.8	25

c) Fossil Fuel Fraction CO_2 Fluxes and Natural LNAPL Loss Rates

Site	Class	Location	Deployed	Recovered	Days in Field	Total CO_2 Flux ($\mu mol/m^2/sec$)	ff CO_2 Flux ($\mu mol/m^2/sec$)	ff LNAPL Loss (gal/acre/yr)
A	TB	TB	- -	- -	- -	- -	- -	- -
A	BG	2	9/30/15	11/11/15	42	3.6	0.60	330
A	BG	1	10/1/15	11/11/15	41	1.7	0.30	170
A	LNAPL	6	10/1/15	11/11/15	41	22	20	11,000

Notes:
All samples are bottom trap elements
Trap cross sectional area for flux is $8.1 \times 10^{-3} m^2$
‰ - parts per mil (1/1000)
BG - background sample location
$\delta^{13}C$ - delta carbon 13
ff - fossil fuel fraction
LNAPL - LNAPL area sample
TB - travel blank sample

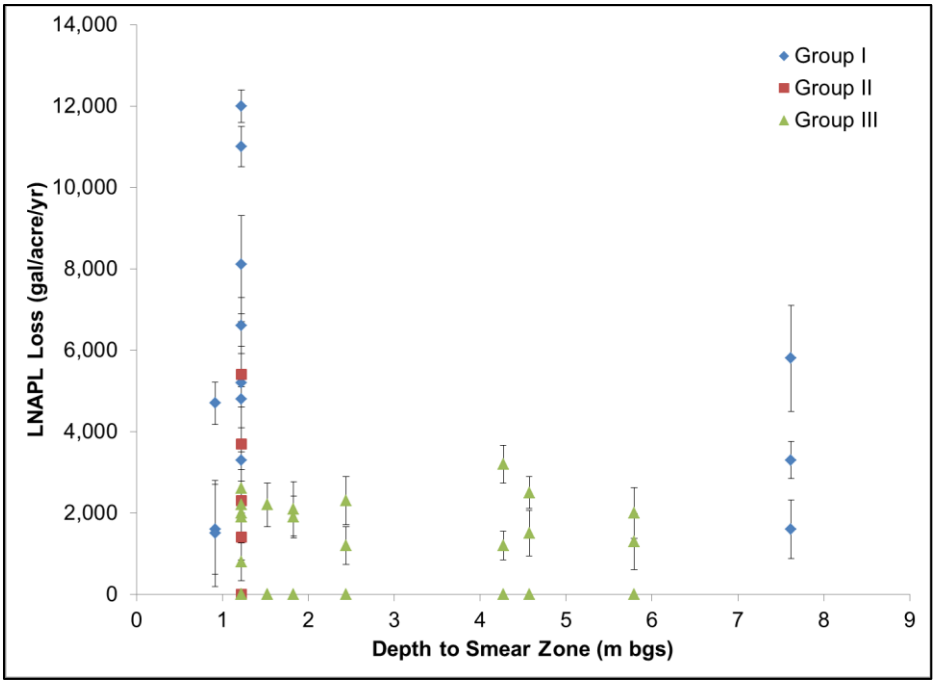

Figure B.1. LNAPL loss vs. depth to smear zone organized by group.

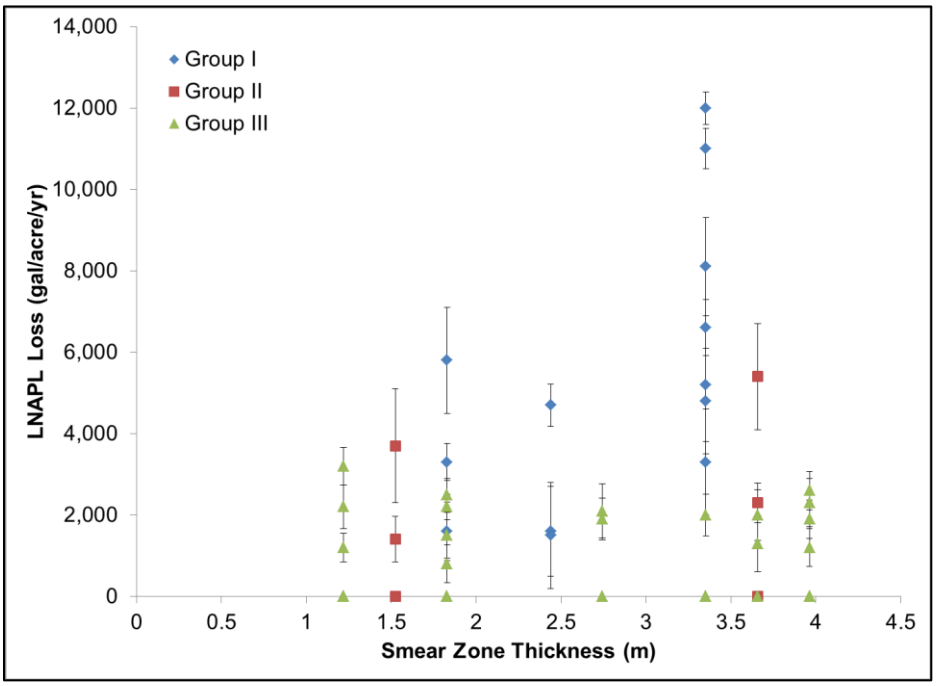

Figure B.2. LNAPL loss vs. smear zone thickness organized by group.

Appendix C SAMPLE CALCULATIONS

The following sample calculations are based on data from Site A Location 6 (9/30/11 – 11/10/11), unless otherwise noted.

CO_2 Flux

Sample calculations are based on the data presented in Table D.1.

Table C.1. Raw CO_2 Trap Results for CO_2 Flux Sample Calculation.

Class	Location	Tested Sample (g)	Measured CO_2 (g)	Raw $\%CO_2$ (g/g)	Avg Raw $\%CO_2$ (g/g)	Total Trap Mass (g)	Days Deployed	Area (m^2)
TB	- -	4.36	0.06	1.4%		69.50	- -	- -
TB	- -	4.60	0.10	2.2%		69.50	- -	- -
TB	- -	4.42	0.09	2.0%	1.9%	69.50	- -	- -
LNAPL	6	5.47	1.95	36%		81.45	41.0	8.1E-03
LNAPL	6	5.63	2.06	37%		81.45	41.0	8.1E-03
LNAPL	6	5.05	1.81	36%	- -	81.45	41.0	8.1E-03

$$CO_2 flux = \frac{Blank\ Subtracted\ \%CO_2 * Total\ Trap\ Mass}{Trap\ Area * Deployment\ Time}$$

Where:

Blank Subtracted $\%CO_2$ = difference between a laboratory sample replicate and the average of travel blank laboratory replicates (%)

Trap Mass = total dry mass of the sorbent element (g)

Trap Area = $8.1x10^{-3}m^2$

Deployment time = time (days) between deployment and recovery of CO_2 Trap

$$CO_2 flux = \frac{(.36 - 0.019) * 81.45g * \frac{1mol}{44.01g} * \frac{1{,}000{,}000\mu mol}{1mol}}{8.1x10^{-3}m^2 * 41.0day * \frac{24hr}{1day} * \frac{60min}{1hr} * \frac{60sec}{1min}} = 22\frac{\mu mol}{m^2 * sec}$$

Background Subtracted LNAPL Loss Rate and 95% Confidence Interval (CI). Background subtracted CO_2 flux rates and 95% confidence intervals were calculated using Minitab® statistical software (Minitab, 2010). Background subtracted CO_2 flux rates (μmol/m^2/sec) were converted to natural LNAPL loss (gal/acre/yr) rates using the correction factor of 550 (gal/acre/yr) per 1 (μmol/m^2/sec). Sample calculations are shown for the data presented in Table D.2. Calculated values have been rounded to 2 significant figures.

Table C.2. Raw CO_2 Trap Laboratory Replicate Data for 95% CI of Background Subtracted LNAPL Loss Rate.

Class	Location	CO_2 Flux (μmol/m^2/sec)	Average	Var	Stdev	n
BG	1	1.3				
BG	1	1.8				
BG	1	1.9				
BG	2	2.6				
BG	2	4.3				
BG	2	3.9				
BG	3	1.3				
BG	3	2.4				
BG	3	1.9	**2.4**	**1.1**	**1.1**	**9**
LNAPL	6	22				
LNAPL	6	22				
LNAPL	6	22	**22**	**0.10**	**0.32**	**3**

Background Subtracted Natural LNAPL Loss Rate:

$$\text{BG Sub. LNAPL Loss} = \left(22\,\frac{\mu\text{mol}}{\text{m}^2*\text{sec}} - 2.4\,\frac{\mu\text{mol}}{\text{m}^2*\text{sec}}\right) * 550\,\frac{\frac{\text{gal}}{\text{acre}*\text{yr}}}{\frac{\mu\text{mol}}{\text{m}^2*\text{sec}}} =$$

$$10{,}780\,\frac{\text{gal}}{\text{acre}*\text{yr}} \xrightarrow{\text{Round}} 11{,}000\,\frac{\text{gal}}{\text{acre}*\text{yr}}$$

Where:

BG Sub. LNAPL Loss is the background subtracted LNAPL loss rate

95% Confidence Interval for Background Subtracted Natural LNAPL Loss Rate:

95% confidence intervals s were calculated by the minitab software (Minitab, 2010). A (1-α)*100% confidence interval is calculated as follows.

$$\mathrm{CI} = \mathrm{BG\ Sub.\ LNAPL\ Loss} \pm \left(t_{\frac{\alpha}{2}} * S\right) * 550$$

Where:

$$\mathrm{S} = \sqrt{\frac{\mathrm{Stdev}_{\mathrm{LNAPL}}^2}{\mathrm{n}_{\mathrm{LNAPL}}} + \frac{\mathrm{Stdev}_{\mathrm{BG}}^2}{\mathrm{n}_{\mathrm{BG}}}}$$

$\mathbf{t_{\alpha/2}}$ = the 2-sided t value for a (1-α)*100% confidence interval (generated by the software) with DF degrees of freedom (rounded down to nearest whole number):

$$\mathrm{DF} = \frac{(\mathrm{Var}_{\mathrm{LNAPL}} + \mathrm{Var}_{\mathrm{BG}})^2}{\frac{\mathrm{Var}_{\mathrm{LNAPL}}{}^2}{\mathrm{n}_{\mathrm{LNAPL}} - 1} + \frac{\mathrm{Var}_{\mathrm{BG}}{}^2}{\mathrm{n}_{\mathrm{BG}} - 1}}$$

$\mathbf{Stdev_{LNAPL}}$ = the standard deviation of laboratory replicate CO_2 fluxes for an LNAPL sample

$\mathbf{Stdev_{BG}}$ = the standard deviation of laboratory replicate CO_2 fluxes for all background locations

$\mathbf{n_{LNAPL}}$ = the number of laboratory replicate analyses for the LNAPL location

$\mathbf{n_{BG}}$ = the number of laboratory replicate analyses for all background locations

$\mathbf{Var_{LNAPL}}$ = the variance of laboratory replicate CO_2 fluxes for an LNAPL sample

$\mathbf{Var_{BG}}$ = the variance of laboratory replicate CO_2 fluxes for all background locations

Using data from Table D.1:

$$S = \sqrt{\frac{0.32\frac{\mu mol}{m^2 * sec}^2}{3} + \frac{1.1\frac{\mu mol}{m^2 * sec}^2}{9}} = 0.41\frac{\mu mol}{m^2 * sec}$$

$$DF = \frac{(0.10 + 1.1)^2}{\frac{0.1^2}{3-1} + \frac{1.1^2}{9-1}} = 9$$

Using $t_{\alpha/2}$ = 2.262 (generated by the minitab software package) for α/2 = 0.025 and DF=9:

$$CI = 10{,}780\frac{\text{gal}}{\text{acre} * \text{yr}} \pm \left(2.262 * 0.41\frac{\mu mol}{m^2 * sec}\right) * 550\frac{\frac{gal}{acre * yr}}{\frac{\mu mol}{m^2 * sec}} = 10{,}780 \pm 510\frac{\text{gal}}{\text{acre} * \text{yr}}$$

$$CI = 10{,}270 - 11{,}290\frac{\text{gal}}{\text{acre} * \text{yr}} \xrightarrow{\text{Round}} 10{,}000 - 11{,}000\frac{\text{gal}}{\text{acre} * \text{yr}}$$

Fossil Fuel Fraction

Fossil fuel fraction calculations performed for Site A Location 6 using data presented in Table C.2a.

$$\mathbf{Fm}_{sample} = (\boldsymbol{ff}_{sample})\,(\boldsymbol{Fm}_{ff}) + (\mathbf{1} - \boldsymbol{ff}_{sample})(\boldsymbol{Fm}_{atm})$$

Where:

Fm_{sample} = Fraction modern carbon in sample

Fm_{ff} = Fraction modern carbon in fossil fuel (assumed to be 0)

Fm_{atm} = Fraction modern carbon in atmosphere at time of analysis (1.15 Avery Jr et al., 2006)

$$0.13 = (\boldsymbol{ff}_{sample})\,(0) + (\mathbf{1} - \boldsymbol{ff}_{sample})(1.15) \rightarrow \boldsymbol{ff}_{sample} = 1 - \frac{0.13}{1.15} = 0.89 = 89\%$$

Table C.3. Molar Masses for LNAPL Loss Calculation Comparison.

Molar Mass		
C	H	g/mol
6	6	78.11
7	8	92.14
8	10	106.17
4	10	58.12
10	22	142.28
22	46	310.60
44	90	619.19

Table C.4. Sample Calculations of LNAPL Loss Rate for Different LNAPL Compositions.

Class	Location	CO_2 Flux ($\mu mol/m^2/s$)	Ring Hydrocarbons			Chain Hydrocarbons				min BG Corrected Loss (gal/acre/yr)	max BG Corrected Loss (gal/acre/yr)	avg BG Corrected Loss (gal/acre/yr)	stdev	CV
			BG Subtract Loss C_6H_6 (gal/acre/yr)	BG subtract Loss C_7H_8 (gal/acre/yr)	BG Subtract Loss C_8H_{10} (gal/acre/yr)	BG Subtract Loss C_4H_{10} (gal/acre/yr)	BG Subtract Loss $C_{10}H_{22}$ (gal/acre/yr)	BG Subtract Loss $C_{22}H_{46}$ (gal/acre/yr)	BG Subtract Loss $C_{44}H_{90}$ (gal/acre/yr)					
BG	1	1.7	- -	- -	- -	- -	- -	- -	- -	- -	- -	- -	- -	- -
BG	2	3.6	- -	- -	- -	- -	- -	- -	- -	- -	- -	- -	- -	- -
BG	3	1.9	- -	- -	- -	- -	- -	- -	- -	- -	- -	- -	- -	- -
LNAPL	4	17	8,100	8,200	8,300	9,100	8,900	8,800	8,800	8,100	9,100	8,600	390	5%
LNAPL	5	24	12,000	12,000	12,000	13,000	13,000	13,000	13,000	12,000	13,000	13,000	530	4%
LNAPL	6	22	11,000	11,000	11,000	12,000	12,000	12,000	12,000	11,000	12,000	12,000	530	4%
LNAPL	7	6.4	2,200	2,200	2,200	2,400	2,400	2,400	2,400	2,200	2,400	2,300	110	5%
LNAPL	8	5.0	1,400	1,500	1,500	1,600	1,600	1,600	1,600	1,400	1,600	1,500	79	5%
LNAPL	9	3.9	800	810	820	900	880	870	870	800	900	850	39	5%
LNAPL	10	5.8	1,900	1,900	1,900	2,100	2,000	2,000	2,000	1,900	2,100	2,000	76	4%
LNAPL	11	8.3	3,200	3,300	3,300	3,600	3,500	3,500	3,500	3,200	3,600	3,400	150	4%
LNAPL	12	1.6	ns	ns	ns	ns	ns	ns	ns	ns	ns	ns	ns	ns
LNAPL	13	1.1	ns	ns	ns	ns	ns	ns	ns	ns	ns	ns	ns	ns
LNAPL	14	5.1	1,500	1,500	1,500	1,700	1,600	1,600	1,600	1,500	1,700	1,600	76	5%
LNAPL	15	1.5	ns	ns	ns	ns	ns	ns	ns	ns	ns	ns	ns	ns
LNAPL	16	11	4,700	4,700	4,800	5,200	5,100	5,100	5,100	4,700	5,200	5,000	210	4%
LNAPL	17	1.5	ns	ns	ns	ns	ns	ns	ns	ns	ns	ns	ns	ns
LNAPL	18	4.6	1,200	1,200	1,200	1,300	1,300	1,300	1,300	1,200	1,300	1,300	53	4%
LNAPL	19	4.8	1,300	1,300	1,300	1,500	1,400	1,400	1,400	1,300	1,500	1,400	76	5%
LNAPL	20	6.6	2,300	2,300	2,300	2,500	2,500	2,500	2,500	2,300	2,500	2,400	110	5%
LNAPL	21	8.4	3,300	3,300	3,300	3,700	3,600	3,600	3,500	3,300	3,700	3,500	170	5%
LNAPL	22	2.1	ns	ns	ns	ns	ns	ns	ns	ns	ns	ns	ns	ns
LNAPL	23	5.8	1,900	1,900	1,900	2,100	2,100	2,000	2,000	1,900	2,100	2,000	90	5%
		min	800	810	820	900	880	870	870					
		max	12,000	12,000	12,000	13,000	13,000	13,000	13,000					
		avg	3,800	3,800	3,800	4,200	4,100	4,100	4,100					

Notes:
All calculations assume a fluid density of 0.8 g/ml
avg - average
BG - background area
CV - coefficient of variation
LNAPL - LNAPL area
min - minimum
max - maximum
stdev - standard deviation

Appendix D CO_2 TRAP DEPLOYMENT TIME CHARTS

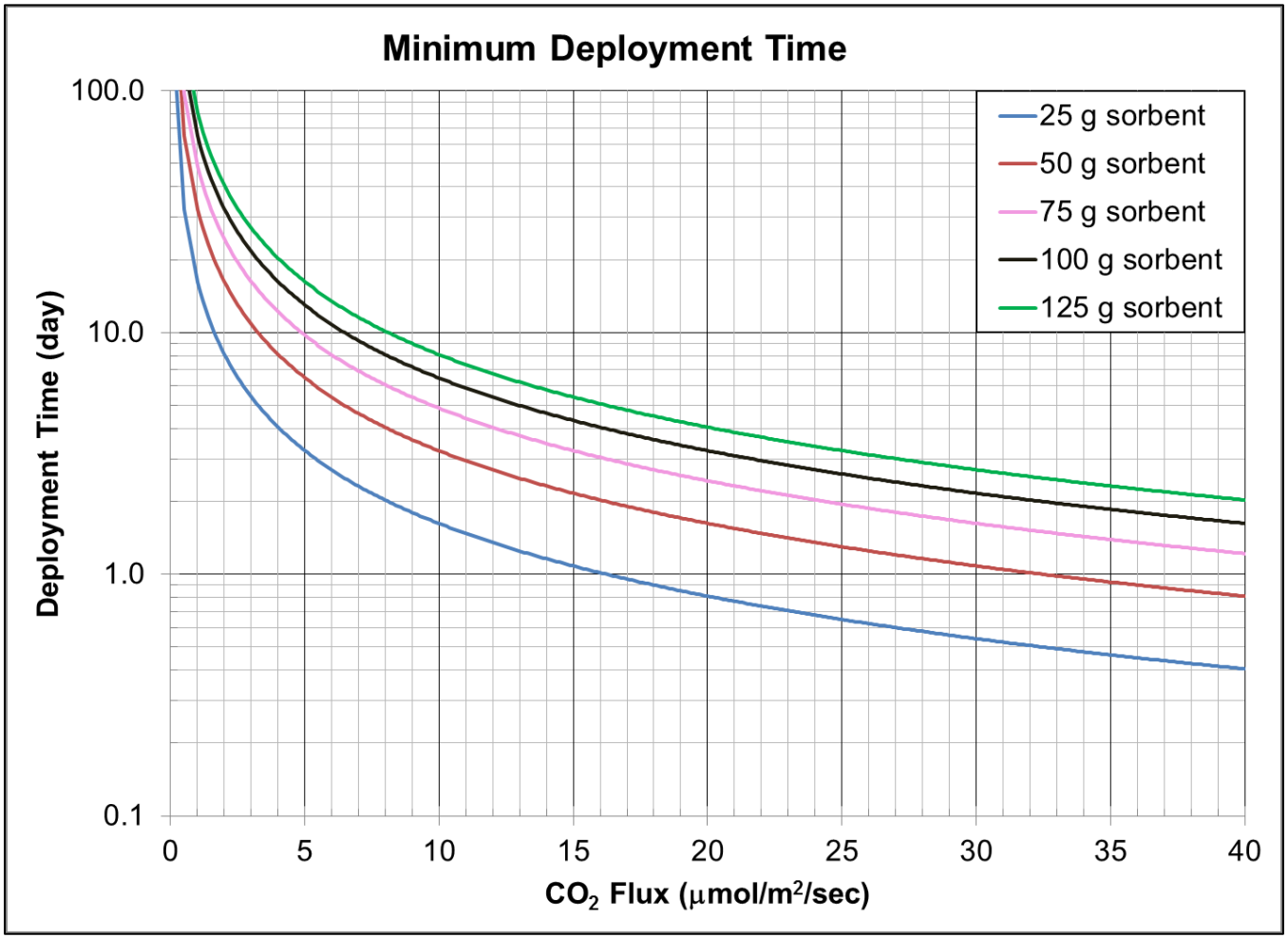

Figure D.1. Minimum deployment time. Time required to reach detection limit (assumed 2% by mass) for a range of sorbent masses. Calculation ignores any pre-existing CO_2 in the trap.

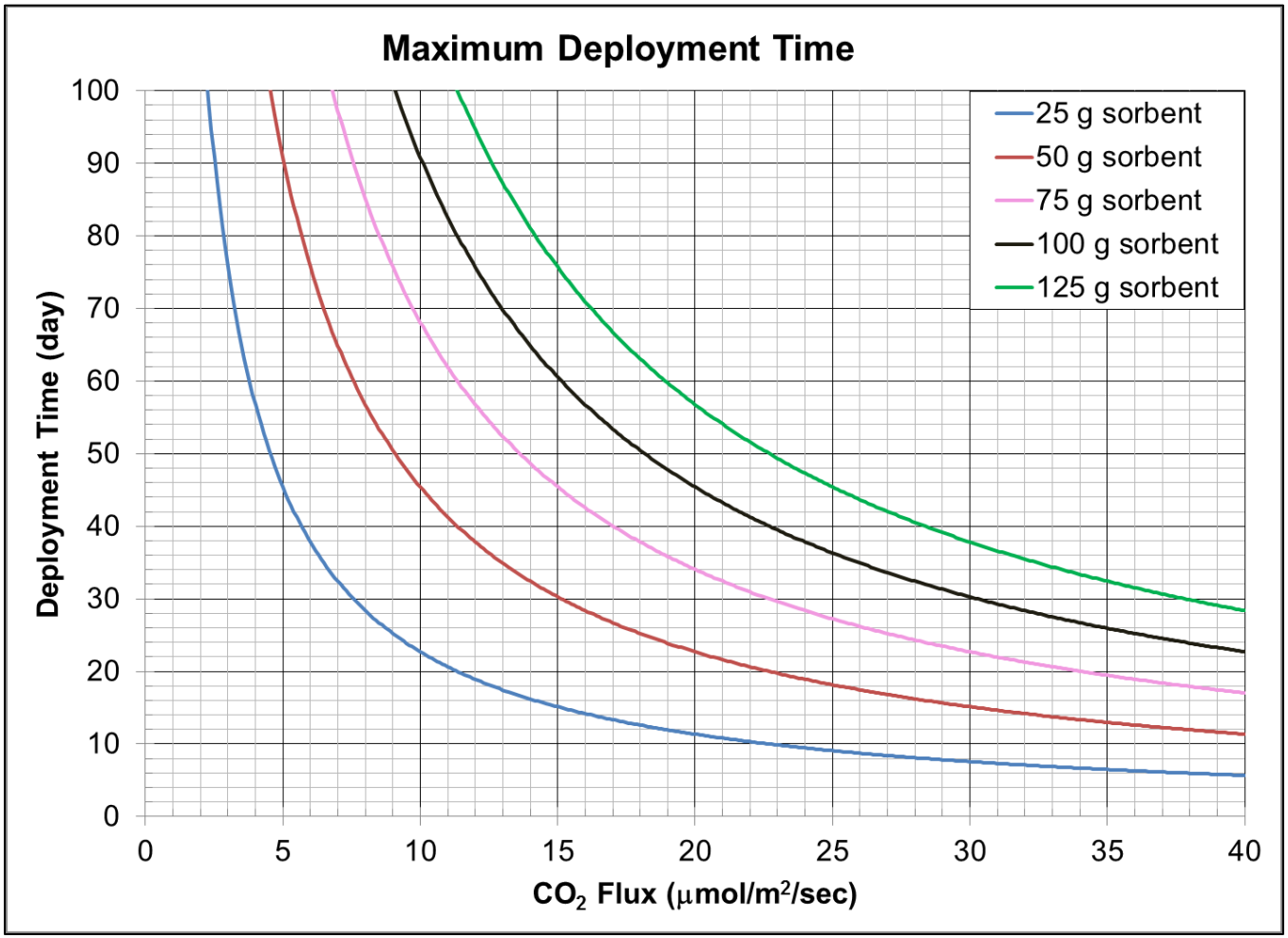

Figure D.2. Maximum deployment time. Time required to reach saturation (28% sorbed CO_2 by mass) for a range of sorbent masses. Calculation assumes 2% pre-existing CO_2 in trap (bringing total sorbed CO_2 to 30%)

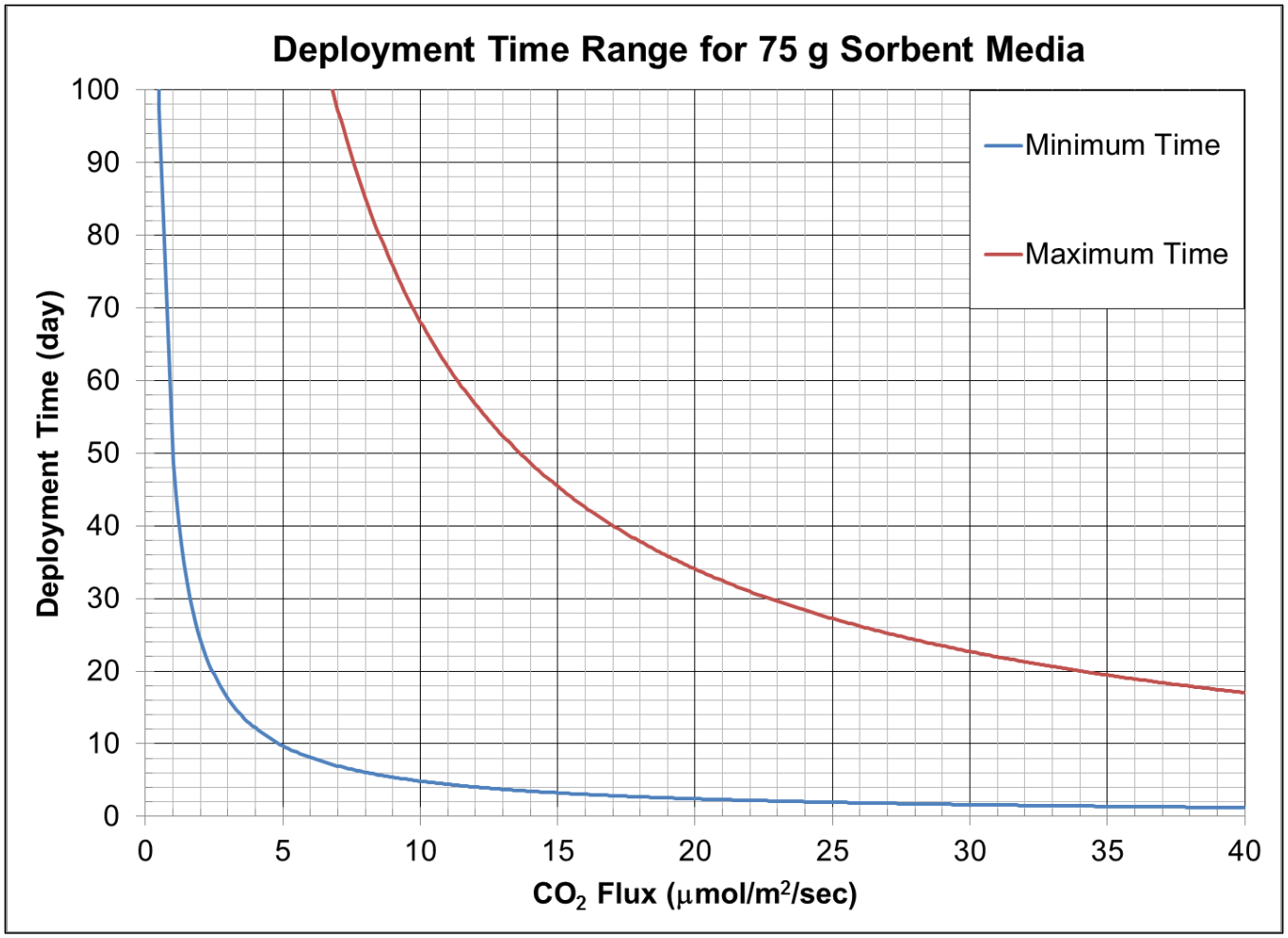

Figure D.3. Deployment time range for 75 g sorbent media. Calculation assumes a minimum of 2% additional sorbed CO_2 required for detection. Calculation assumes a maximum of 28% additional CO_2 can be sorbed.

Appendix E CO_2 TRAP DEPLOYMENT PROTOCOL

Standard Operating Procedure "CO_2 Trap Deployment and Replacement Protocol".

Colorado State University, Center for Contaminant Hydrology.
Generated by: Julio Zimbron and Kevin McCoy
Last modified: August 17, 2012.

The following document has been prepared to summarize protocols for deployment of CO_2 traps in support of studies to evaluate rates of natural attenuation of light non-aqueous phase liquid hydrocarbons (LNAPL). The document includes a list of tools required for deploying the traps. Material Safety Data Sheets (MSDSs) for the sorbent media in the traps, and the lubricant to be used on the receiver ends are available upon request.

Caution should be used when handling traps as they are filled with caustic CO_2 sorbent media. The sorbent media is contained within the traps and should not pose a direct contact hazard as long as the traps are not damaged and are handled with care. Personal protective equipment selection for handling the media is defined in the MSDSs. As a minimum, CSU uses nitrile gloves beneath leather work gloves and safety glasses when handling the fully assembled traps.

Please contact Julio Zimbron at CSU with any questions or comments regarding sampling procedures.

Julio Zimbron (970) 491-0626 (Office)
(970) 219-2401 (Mobile)

Equipment List

1) Replacement protocol (this document), MSDS sheets for SodaSorb™ and lubricant gel.
2) Site maps.
3) CO_2 trap shipment and installation log – will be shipped with traps from CSU.
4) Appropriate PPE (not provided, to be determined by site contractor).
5) CO_2 trap receivers (Figure 1) – to be permanently installed at the site.
6) CO_2 trap housings (Figure 1).
7) CO_2 Traps (Figure 2) – Will be shipped to the Site by CSU.
8) White plastic field cap (Figure 2) – These should remain onsite between sampling rounds.
9) Flathead screwdriver, or nut driver tool (Not provided) to remove ring clamp from top rubber shipping cap.
10) Temperature Loggers (optional).

Figure E.1. CO_2 Trap housing and in-ground receiver. Note the green housing identification label on the trap housing (left). CO_2 Trap in-ground receiver as it appears when housing is removed (Right).

Figure E.2. CO_2 Trap installation. CO_2 Trap (left), note that white plastic field cap has been installed. CO_2 trap installed on receiver (right), note white plastic field cap.

General Placement Guidelines

- CO_2 Trap sampling points should be located near existing groundwater wells. This is important for correlation of CO_2 fluxes to known geologic, hydrogeologic, and hydrocarbon distribution conditions.
- All CO_2 Trap sampling points should be located away from pavements or low permeability surface coverings of limited areal extent that may affect measurements.
- CO_2 Traps should not be deployed immediately after a rain or flood event, due to potential for transient effects of infiltrating water on near-surface gas transport.
- Clustered CO_2 Traps (where applicable) should be spaced approximately 2 meters apart in a triangular pattern.
- Surface vegetation should be cleared from directly beneath the proposed trap location prior to installation of the in-ground receiver.
- Background locations should be chosen where soils, vegetation, and general site conditions are similar to the LNAPL monitoring locations.
- Groundwater temperature and depth to groundwater should be measured at representative locations during each period of CO_2 trap deployment to facilitate correlation of CO_2 fluxes to site conditions.

In-ground Receiver Installation

1) Ensure that vegetation is removed from the CO_2 Trap installation location.

2) Dig a hole to approximately 7-inches below ground surface.

3) Place receiver in ground. Place end with brackets down. Keep receiver vertical in hole.

4) Backfill the annular AND internal space of the in-ground receiver back to original grade. Make sure receiver stays vertical. Compact soil with hand tools to achieve compaction as close as possible to pre-digging conditions.

CO_2 Trap Installation

A shipment and installation log will be shipped with the traps. The log should be filled out with the date and time that each trap is installed and removed for return.

- Field CO_2 Traps. These shall be deployed as determined during project planning.
- 1 Trip Blank will be included. **This trap should not be opened.** It will remain at the Site and be returned to CSU with the other traps after the sampling Period.

- **KEEP TRAPS UPRIGHT.**
- **Traps contain caustic material, use caution when handling.**
- **Keep traps as dry as possible.**

Procedure

1) Find the appropriate CO_2 Trap for the location (ref. site map). Remove field housing from receiver (Figure F.1).

2) Wipe the outside of the in-ground receiver (Figure F.1) with a towel to clean off any grit and dirt that could damage the o-rings. After wiping the receiver down, apply lubricant to the top outer edge of the receiver.

3) Use flat head screwdriver to remove ring clamp and rubber shipping cap from top of trap. Use caution when the top rubber cap is removed in case the top retaining screen comes loose.

4) Remove the PVC shipping base from the CO_2 Trap (it should slide directly out with relatively little force). This may be best accomplished by setting the unit upright on the ground, stepping on the small PVC lip, and pulling directly upward on the trap body.

5) Set aside rubber shipping cap and PVC shipping base as these will be needed for shipping the traps back to CSU.

6) Place CO_2 Trap onto receiver (Figure F.2). The CO_2 Trap should slide onto the receiver with relatively little force.

7) Place white plastic field cap on top of CO_2 Trap (Figure F.2).

8) Replace housing over trap and secure to receiver using thumbscrews.

Returning Traps to CSU

1) At end of monitoring period, reverse steps. Place a small amount of lubricant on the PVC shipping plug before inserting back into bottom of the trap. The shipping plug should slide in with relatively little effort. Note date and time removed from ground on the log. Place the log in dry cooler with traps.

2) Ship to CSU in dry coolers (Keep traps upright):

Colorado State University
Engineering Research Center
1320 Campus Delivery
Fort Collins, CO 80523
Attn: Julio Zimbron

(970) 491-0626

Pressure / Temperature Loggers

If feasible, depth to water, depth to LNAPL, and total well depth should be gauged in the well nearest each CO_2 Trap during each period of deployment. If practical, groundwater temperature and depth to water should also be recorded at representative locations using continuous data loggers during the entire period of study.

LIST OF ABBREVIATIONS

Term	Definition
°C	degrees celcius
^{12}C	carbon 12 isotope
^{13}C	carbon 13 isotope
^{14}C	carbon 14 (radiocarbon) isotope
6N HCl	6 normal hydrochloric acid
95% CI	95 percent confidence interval
A.C.S.	American Chemical Society
bgs	below ground surface
C_6H_6	benzene
$CaCO_3$	calcium carbonate
CH_4	methane
CO	carbon monoxide
CO_2	carbon dioxide
CPT	cone penetrometer test
CSU	Colorado State University
$\delta^{13}C$	delta carbon 13
ff_{sample}	fossil fuel carbon fraction in sample
Fm_{atm}	modern carbon fraction in the atmosphere
Fm_{ff}	modern carbon fraction in fossil fuel (assumed 0)
Fm_{sample}	modern carbon fraction in sample
g	grams
g/cm^3	grams per cubic centimeter
$g/m^2/day$	grams per square meter per day
g/ml	grams per milliliter
gal/acre/yr	gallons per acre per year
HCl	hydrochloric acid
INSTAAR	Institute of Arctic and Alpine Research
$J_{CO2\ Background}$	natural soil respiration related CO_2 flux
$J_{CO2\ LNAPL}$	LNAPL related CO_2 flux
$J_{CO2\ Total}$	total CO_2 flux
$kg/m^2/yr$	kilograms per square meter per year
LIF	laser induced fluorescence
LNAPL	light non-aqueous phase liquid
m	meter
m^2	square meters
$\mu mol/m^2/sec$	micromoles (10^{-6} moles) per square meter per second
$\mu mol/sec$	micromoles (10^{-6} moles) per second
Na_2CO_3	sodium carbonate
NBS	National Bureau of Standards
NREL	Natural Resources and Ecology Lab
O_2	oxygen
PVC	polyvinyl chloride
sec	second
stdev	standard deviation
UC Boulder	University of Colorado Bouler
VPDB	Vienna PeeDee Belemnite